Report
P-15-19
February 2017

FracMan Kinematic Stability Assessment of Tunnels in Forsmark Layout D2

Mark Cottrell
Rita Kamera
Jan Hermanson

SVENSK KÄRNBRÄNSLEHANTERING AB

SWEDISH NUCLEAR FUEL
AND WASTE MANAGEMENT CO

Box 250, SE-101 24 Stockholm
Phone +46 8 459 84 00
skb.se

SVENSK KÄRNBRÄNSLEHANTERING

ISSN 1651-4416
SKB P-15-19
ID 1529017
February 2017

FracMan Kinematic Stability Assessment of Tunnels in Forsmark Layout D2

Mark Cottrell, Rita Kamera, Jan Hermanson
Golder Associates

Short Abstract

This report provides the results of the investigations undertaken by Golder Associates on behalf of SKB concerning the kinematic stability of rock blocks formed by natural fractures surrounding a proposed Forsmark nuclear waste repository layout.

The primary objective of the investigations that have been carried out is to provide objective estimates to block size and fragmentation in the Forsmark D2 deposition tunnel layout based on models and rock mechanical parameters derived in the Forsmark GeoDFN, version 2.2. The primary objective has been met by initial examination of the available literature to form a detailed understanding of the spatial pattern of natural fractures existing in the repository area. Using the derived understanding of the natural fracturing, tunnel scale models of the fracture network description are assembled. The models are sized to fit a 100 metre length of deposition tunnel with approximately 10–15 metres of host rock each side of the tunnel profile also included.

Tunnel scale models have been systematically analysed to assess for formation of rock blocks around the tunnel, the block geometry in terms of size, shape and mass, as well as the block factor of safety conditions. In addition, areal fracture intensity measures have been assessed for tunnel crown, invert and sidewall locations. Extension of the tunnel scale models has been achieved through incorporation of a Monte Carlo based probabilistic approach. The probabilistic route permits the assessment of the range of answers from multiple DFN (Discrete Fracture Network) realisations. The results have allowed assessment of the likelihood of blocks of specific geometry and their associated risks in terms of instability.

Stability sensitivities including rock domain location, tunnel orientation, as well as friction conditions and pore fluid pressure conditions have been investigated. The presented investigations have shown that fracture frictional conditions as well as the pore pressure state are highly influential in terms of affecting block kinematic stability.

Detailed Summary

This report provides the results of the investigations undertaken by Golder Associates on behalf of SKB concerning the DFN (Discrete Fracture Network) based analysis of kinematic stability of rock blocks formed by natural fractures surrounding a proposed Forsmark nuclear waste repository layout.

The primary objective of the investigations that have been carried out is to provide objective estimates to block size and fragmentation in the Forsmark D2 deposition tunnel layout based on models and rock mechanical parameters derived in the Forsmark GeoDFN, version 2.2 mainly established in reports by SKB (2008, 2010), Fox et al. (2007) and Glamheden et al. (2007).

The overall workflow that has been used contains the following tasks:

- Data Analysis and Construction of DFN model.
- Identification of Potential Rock Blocks from Surface Traces.
- Search into Rock Volume to find *Fully Defined Rock Blocks.*
- Evaluate Basic Block Kinematics.
- Evaluate Advanced Block Kinematics by considering Earthquake, Water Pressure, Rockbolt and Anchoring Strategies Effects; and
- Block Limit Equilibrium Stability *(green if FOS > 1, red if FOS < 1).*

The focus of the report considers the development and assembly of the properties describing the spatial pattern of natural fractures in the repository space. Specific descriptions for the fracture orientation, size, and intensity are considered, as well as descriptions relating to the mechanical properties for shear based friction and normal compressibility (compliance).

It should be recognised however, that in all of the analyses undertaken the proper post-excavation in situ stress field has not be considered. Therefore, the fracture normal stress responsible for the fracture frictional strength is only induced by each block self-weight. This is expected to affect the results considerably, and should be more fully addressed in future investigations.

Examination of the available literature has identified that the TCM (Tectonic Continuum Model) fracture description should be used to describe the spatial pattern of natural fracturing presented in the Forsmark study area. Adoption of the TCM description is because it includes definition of fractures from the outcrop and borehole scale that are considered part of a larger population of brittle deformation features which also includes faults and minor deformation zones identified as geophysical and topographic lineaments. Alternative (open) fracture set descriptions from available hydraulic DFN descriptions have also been identified, as well as a case for sealed fracture descriptions using a combination of TCM/Open fracture set descriptions.

Two rock domains, FFM01 and FFM06, in the Forsmark area were identified by SKB (Vidstrand P 2015, personal communication) as being of principal interest. For these two rock domains the global fracture sets have been assessed in terms of the principal parameters required for the construction of DFN (Discrete Fracture Network) models. For each rock domain global fracture sets have been parameterised, corresponding to North-East (NE), North-South (NS), North-West (NW), and Sub Horizontal (SH) sets. Parameterisation relates specifically to primary fracture set descriptors of orientation, intensity and size.

In addition to the main fracture properties, specification of rock mechanical data relevant to the focus domains has also been undertaken. Examination of existing reporting has allowed basic population of mechanical properties for describing both the intact (non-fractured) material behaviour (Young's Modulus and Poisson Ratio), as well as the fracture mechanical properties including shear response (friction) and compliance (compressibility). Property sets describing the shear response for open and sealed fracture types are identified. Of these types, the use of the conservative open fracture properties is followed since these provide a lower bound estimate of the fracture shear strength.

Sections 2.1 to 2.5 provide assembly of all of the necessary parameters required for construction of the DFN kinematic stability models. The following Section 2.6 identifies the possible mix of model configurations, together with the available reference data, and a simple summary of the arguments for and against using the configuration. These configurations broadly relate to use of A) all, B) open, and C) open/sealed fracture descriptions respectively. Of these configurations, the following model cases have been selected for kinematic stability analysis:

Table S-1. Model Cases Selected for Analysis.

Fracture Set Id	Type	Orientation	Intensity	Size
FFM01 (All)	All fractures	TCM Model *	TCM Model *	Power law,r_0 TCM*
FFM06 (All)	All fractures	TCM Model *	TCM Model *	Power law,r_0 TCM*

* from Fox et al. (2007). TCM = Tectonic Continuum Model.

Deposition tunnel geometry embedded in the fracture models has been provided by SKB (Vidstrand P 2015, personal communication). In terms of model representation, the tunnel geometry is described using multiple planar sections where the planar sections are sized depending on the level of curvature present. Two tunnel orientations are identified as being important, the first at N233 (representing 233 degrees clockwise from North), and the second at N143 degrees (i.e. 143 degrees clockwise from North) respectively. Orientations of the tunnels is based on the repository design layout proposed by SKB, see Section 2.7.

DFN model generation and analysis approach and implementation form the main parts of Section 3. Here construction of the basic tunnel scale model is described, and optimisation of the model geometry in terms of sizing and validation is presented. The final model geometry is 25 × 100 × 25 metres, within which a 100 metre long tunnel section is centrally positioned. Close sizing of the DFN around the tunnel geometry allows a numerically efficient DFN model to be used whilst still ensuring the observed natural fracture characteristics are maintained. The sizing of the model was investigated and chosen to ensure that no edge effects are encountered in the block stability analyses. This was achieved by doing detailed comparisons of boundary effects between large and small sized fracture domains.

The kinematic stability analysis workflow is described in detail; this begins with a description of kinematic stability theory and is followed with description of the primary workflow steps and definition of force calculation terms included in the analysis as well as the shear yield function and factor of safety calculations. An important understanding is in the use of composite block output; here multiple adjacent blocks which are considered contiguous are output together as a single block entity. Required block statistics (block geometry, failure mode, and factor of safety) are based on the combined block geometry – the composite geometry.

Preliminary baseline assessment of the kinematic stability analysis has been undertaken ahead of later probabilistic based assessments. In these baseline analyses, single realisations have been performed for both FFM01 and FFM06 rock domains. In each of these configurations, both tunnel-fracture intersection as well as tunnel kinematic stability analysis has been completed.

- The baseline analyses for rock domain FFM01, the constructed model includes the global fracture sets identified as well as the conservative (open) frictional properties. The baseline analysis has investigated the fracture-tunnel intersection for crown, sidewall and invert locations. Analysis identified that crown and invert surfaces showed slightly higher levels of areal fracture intensity (P_{21}) compared to the sidewall positions. In terms of block stability, it is seen that over the 100 metre tunnel length approximately 200 blocks are formed, of which an average block weight of nearly 17 kg is seen, and a maximum block size of 457 kg is seen. In terms of block classification, of the 200 blocks, approximately 6 % (13) of the blocks are considered freefall, no blocks are considered kinematically unstable, and a significantly higher 94 % (197) are classified as being stable; and
- The baseline analyses for rock domain FFM06, the constructed model includes the global fracture sets identified as well as the conservative (open) frictional properties. The analysis identified

that crown and invert surfaces showed slightly lower levels of fracture intensity compared to the sidewall positions, this is the reverse of what is seen for FFM01. In terms of block stability, it is seen that over the 100 metre tunnel length approximately 450 blocks are formed, of which an average block weight of approximately 4 kg is realised, and a maximum block size of 412 kg is seen. In terms of block classification, of the 438 blocks, approximately 4 % (16) of the blocks are considered freefall, again no blocks are considered kinematically unstable, and a significantly high 96 % (422) are classified as being kinematically stable.

Continuing from the initial results of the baseline analyses, a probabilistic framework is developed in which multiple realisations are imported and automatically processed to assess the probabilistic based distributions relating to block geometry and block stability. The Monte Carlo realisation approach is implemented using the FracMan macro language facility, which upon execution creates the DFN model, excavates the tunnel void, tests for block stability, and finalises with the output of an ASCII text file detailing the results of all the block wedges identified and tested. The ASCII results files are then appended as each realisation analysis completes. The results are assembled in a tabular format, as histograms and cumulative based distributions of the primary variables (e.g. block geometry and Factor of Safety).

A number of different configurations have been assessed using the Monte Carlo realisation approach. For each configuration a number of realisations are required to provide a proper basis for estimating the range of responses, for these analyses typically 50 realisations have been used. A summary of the configurations that have been investigated through the probabilistic Monte Carlo approach is detailed below:

Table S-2. Probabilistic Analysis Configurations Investigated.

Case	Domain	Fracture Data				Tunnel Direction	Fracture Friction	Pore Level
		Type	Orienta-tion	Intensity	Size			
I	FFM01	TCM	TCM	TCM	TCM	N233	Open	0 MPa
II	FFM01	TCM	TCM	TCM	TCM	N143	Open	0 MPa
III	FFM06	TCM	TCM	TCM	TCM	N233	Open	0 MPa
IV	FFM06	TCM	TCM	TCM	TCM	N143	Open	0 MPa
V	FFM01	TCM	TCM	TCM	TCM	N233	Open	Hydro
VI	FFM06	TCM	TCM	TCM	TCM	N233	Open	Hydro
VII	FFM01	TCM	TCM	TCM	TCM	N233	Reduced	0 MPa

For each of the configurations listed in the above table, multiple realisations are performed and the results for each configuration are assembled independently. For each of the configurations assessed, detailed examination of the histogram and cumulative based distributions are provided, these include block count and factor of safety as well as block geometry (weight and volume).

The assembled output results show that:

- Models for domain FFM01 averages 250 blocks/100 metre run, average block weights are 20 kg, approximately 6 % of the formed blocks being freefall.
- Models for domain FFM06 averages 425 blocks/100 metre run, average block weights are 4 kg, approximately 5 % blocks freefall.
- In both FFM01 and FFM06 rock domains the percentage of unstable blocks is very low <1 %, typically only 1–2 blocks per 100 metre tunnel run seen.
- Tunnel orientation is seen to have little sensitivity in terms of block formation.
- Pore Pressure is a significant sensitivity to block kinematic stability. Increasing the pore pressure levels from zero to a uniform 5 MPa results in the number of unstable blocks increasing. Increasing the pore pressure indicates between 20–30 % of the blocks are unstable compared to dry case where <10 % are either unstable/freefall; and

- The simulations indicate that if the fracture friction properties are less then currently has been calibrated, then there is significant sensitivity and risk to increased levels of block instability.

In terms of future investigations, the following itemised points are considered for further investigation:

- Investigation of the sensitivity of bigger variations and assignment impacts of fracture surface friction properties, as well as impacts of variable pore pressure conditions.
- Investigation and consideration of other locations (e.g. deformation zones), depths, tunnel geometries and multi-tunnel intersection locations in the repository.
- Investigation of the impact of geomechanical upscaling in terms of how the intact rock material properties are degraded by the presence of natural fracturing.
- Investigation of the role of variable in situ stress and its inclusion into the kinematic stability models.
- Investigate the potential feasibility for using rockbolts or possibly shotcrete for block instability mitigation; and
- Investigate the potential for recursive block stability assessment with evolving cavity growth.

Contents

1 Introduction

This report provides the results of the investigations undertaken by Golder Associates on behalf of SKB concerning the DFN (Discrete Fractured Network) based analysis of kinematic stability of rock blocks formed by natural fractures surrounding a proposed Forsmark nuclear waste repository layout.

The objective of the investigations that have been carried out is to provide objective estimates to block size and fragmentation in the Forsmark D2 deposition tunnel layout based on models and rock mechanical parameters derived in the Forsmark GeoDFN, version 2.2 mainly established in reports by SKB (2008, 2010), Fox et al. (2007) and Glamheden et al. (2007).

The work considered in this report covers an initial analysis of appropriate DFN and rock mechanical parameters suitable for a block stability analysis and a preliminary assessments of kinematic stability.

The initial phase of work has focussed on the development of a series of Tasks which will permit integration of the available data and preliminary assessments of rock block stability and anchoring requirements. In achieving the identified goal, the following tasks have been undertaken:

- Task 1: GeoDFN Parameters & Model assessment; and
- Task 2: Probabilistic Assessment Rock Block Stability.

The overall workflow being used in the assessment of the Forsmark stability assessment is defined by:

- Assessing the appropriateness of available DFN models used in the SKB site investigations in Forsmark for block stability assessment.
- Construction of a chosen DFN model alternative.
- Identify Potential Rock Blocks from Surface Traces.
- Search into Rock Volume to find *Fully Defined Rock Blocks.*
- Evaluate Basic Block Kinematics.
- Evaluate Advanced Block Kinematics by considering Earthquake, Water Pressure, Rockbolt Anchoring Strategies and Effects; and
- Block Limit Equilibrium Stability *(green if FOS > 1, red if FOS < 1).*

2 Task 1: GeoDFN Parameters And Model Creation

Identification, mapping, modelling, and understanding of bedrock fractures at Forsmark are key components of the site description, since these directly help inform the repository safety assessment. Understanding existing natural fractures are important to both the design (available deposition volume, tunnelling, and excavation stability) and the long-term performance (groundwater and heat flow, radionuclide transport in the event that a canister is compromised, and the question of post-glacial seismic safety) of a spent nuclear fuel repository.

In the current reporting, particular interest is focussed on the kinematic stability of rock blocks formed around tunnel locations formed in the Forsmark FFM01 and FFM06 rock domains (Fox et al. 2007, SKB 2008, 2010).

To fully describe the properties of the natural fractures in the repository space, the following parameters must be appropriately defined:

- Fracture orientation.
- Fracture size (how large the fractures are).
- Fracture intensity (how many fractures there are, and how the number changes spatially).
- Fracture locations (i.e. spatial model).
- Fracture mineralogy (mineral infillings, host-rock alteration).
- Fracture hydraulic properties (transmissivity, hydraulic aperture); and
- Fracture mechanical properties (friction angle, cohesion, tensile strength, normal and tangential compliance, and dilation angle).

The following sections consider the data available for describing some of the key fracture attributes identified in the above itemised list.

2.1 GeoDFN Fracture Sets

Selected SKB reporting on developed DFN models (Fox et al. 2007, SKB 2008, 2010) has been examined to identify the primary geometrical fracture properties that should be included in the kinematic stability analyses undertaken. Several alternative models are available. Fox et al. (2007) has identified more than four alternative interpretations of the Forsmark rock mass that each have their distinct assumptions, strengths and limitations with regards to the derivation and potential usage of geometric properties of the fracture network.

The TCM (Tectonic Continuum Model) description, in which fractures at the outcrop and borehole scale are considered part of a larger population of brittle deformation features which also includes faults and minor deformation zones identified as geophysical and topographic lineaments. The fundamental basis of the tectonic continuum hypothesis is that fracture size and fracture intensity are coupled (one cannot change one without affecting the other), that fracture size is scale-invariant, and that it is consistent with the understanding of brittle deformation zones as intense clusters of connected smaller fractures. Specific details of the adopted TCM description can be found in the Fox et al. (2007) report. In discussion with SKB (Vidstrand P 2015, personal communication) it was agreed that the TCM alternative is the most appropriate model for the purpose of the block stability assessment as it considers all fractures at all scales. The TCM alternative has also been used in hydrogeological simulations (Follin 2008), and for the safety performance assessments (SKB 2010) undertaken to date.

Based on the TCM model alternative presented in Fox et al. (2007), Table 2-1 specifies the fracture set cases initially considered for potential kinematic stability assessment. It is seen in Table 2-1 that for each of the two fracture domains, FFM01 and FFM06, three configurations are initially identified, corresponding to cases of i) all fractures, ii) open fractures, and iii) sealed fractures respectively.

Table 2-1. Fracture Sets Considered in GeoDFN Model Parameters for Domains FFM01 and FFM06 from Fox et al. (2007) and SKB (2010).

Fracture Set Id	Type	Orientation	Intensity	Size
FFM01 (All)	All fractures	TCM	TCM	Power law, r_0 TCM
FFM01 (Open)	Open fractures	Hydro DFN	Raw data from boreholes	Power law, r_0 TCM
FFM01 (Open/Sealed)	Open/ Sealed	TCM (Sealed) Hydro DFN (Open)	TCM (sealed) Raw data from boreholes (open)	Power law, r_0 TCM
FFM06 (All)	All fractures	TCM	TCM	Power law, r_0 TCM
FFM06 (Open)	Open fractures	Hydro DFN	Raw data from boreholes	Power law, r_0 TCM
FFM06 (Open/Sealed)	Open/ Sealed	TCM (Sealed) Hydro DFN (Open)	TCM (sealed) Raw data from boreholes (open)	Power law, r_0 TCM

Based on the data identified in Table 2-1, the parameters used to describe the all fractures cases are considered in the following sections.

2.2 Domain FFM01: Fracture Sets

Parameters used for describing the spatial pattern of natural fractures in domain FFM01 are discussed in the following sections. The parameters described reflect those detailed in SKB (2010).

2.2.1 TCM Fracture Sets

Fracture sets have been classified into Global and Local sets in SKB (2010). In the current analyses only the Global fractures sets have been used, the smaller sized local fracture sets have not been included in the analyses. Local sets, as described by Fox et al. (2007), reflects local variations that may or may not occur in each domain.

Table 2-2. Global TCM Fracture Set Parameters for Domain FFM01.

Set	Orientation				Intensity	Size		
	Type [–]	Pole Trend [deg]	Pole Plunge [deg]	Conc. [–]	P_{32} [m²/m³]	r_0 [m]	Slope [–]	r_{max} [m]
NE	Fisher	314.90	1.30	20.94	1.733	0.659	3.02	564.20
NS	Fisher	270.10	5.30	21.34	1.292	0.059	2.78	564.20
NW	Fisher	230.10	4.60	15.70	0.948	0.594	2.85	564.20
SH	Fisher	0.80	87.30	17.42	0.624	0.816	2.85	564.20
EW	n/a	n/a	n/a	n/a	n/a	n/a	n/a	n/a

To be consistent with usage of the GeoDFN in the SKB (2010) report only the global fracture sets have been utilized in this study. The global fracture properties mirror the original listing of Table 6-34 in SKB (2010). Table 2-2 details the main properties of the global fracture sets of the TCM description used for domain FFM01.

Descriptions of the property types detailed in Table 2-2 are provided below:

- Distribution [–] is the type of statistical distribution used to fit the observed fracture orientation data. The Fisher type distribution relates to the Univariate Fisher description, and not the Elliptical Fisher distribution.
- Pole trend [degrees] refers to the direction of the mean fracture pole (normal) from North.
- Pole plunge [degrees] refers to the plunge of the mean fracture pole (normal).

- Conc. Is the Concentration parameter is used for the univariate Fisher distribution to describe its spread.
- P_{32} [m^2/m^3] represents the volumetric intensity of fractures in the size range $r_0 - r_{max}$.
- r_0 [metres] represents the mathematical minimum radius (the smallest fracture described by the power-law) is the min fracture radius for which the DFN model is valid.
- r_{max} [metres] represents the maximum truncated value of the size distribution, and is the max fracture radius for which the DFN model is valid; and
- No EW fracture set is identified in the TCM model description, but is identified in other fracture set and types.

Of the data defined in Table 2-2, it is seen there are four global fracture sets, corresponding to North-East (NE), North-South (NS), North-West (NW) and a Sub-Horizontal (SH) set. All four of these sets have fracture pole orientations that are stochastically described using separate Fisher based distributions.

The volumetric fracture intensities (P_{32}) for each of the four global sets are also prescribed in Table 2-2, here it is seen that the NE orientated set is the most intense in terms of intensity, this is closely followed by the NS orientated set, and then the NW orientated set. It is seen that the sub-horizontally aligned fracture set is weakest in terms of volumetric fracture intensity.

Figure 2-1 shows that the NW set is most likely the most important set for fracture with radii larger than 5 metres. In addition, the figure also demonstrates that the NS set is a half to one order of magnitude less intense than the other sets in any given size range, despite that the P_{32} being the second largest.

For this particular project it was decided, for testing purposes, to use a simplified assumption that the open fracture intensity in the HydroDFN can be seen as a proportion of the total intensity of the GeoDFN model. Whilst this assumption is not strictly correct as the min size truncation is different in the two DFN descriptions and thus the P_{32min}, it was considered a worth while simplification to test the block stability approach.

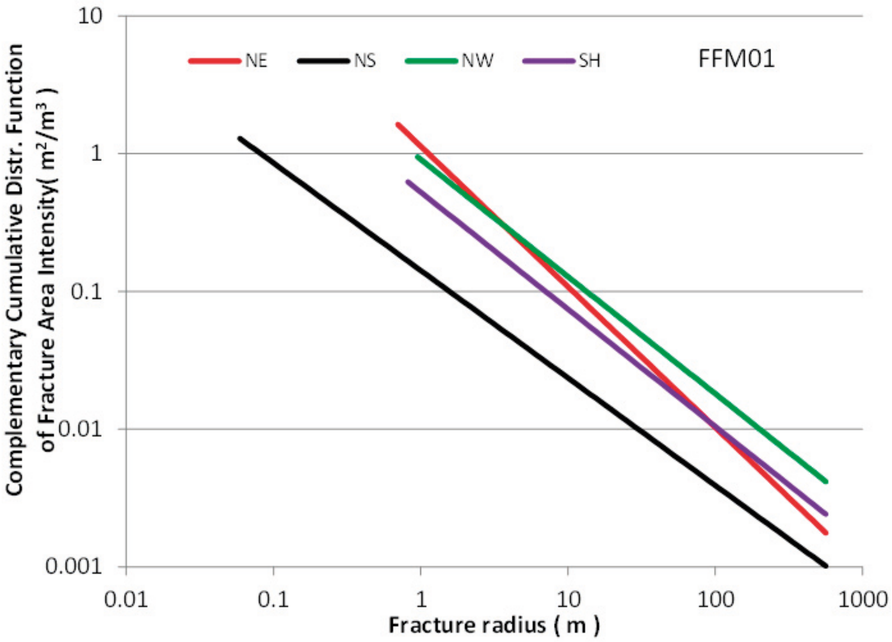

***Figure 2-1.** Complementary Cumulative Distribution Function of Fracture Intensity With Respect to Fracture Radius For Domain FFM01(Vidstrand P 2015, personal communication).*

2.2.2 Open Fracture Sets

Details about the derivation of the properties of the Open natural can be found in Follin (2008) and SKB (2010). The hydrogeological DFN parameters to be used for domain FFM01 are summarized in the Table 2-3. The properties of the fracture sets are presented for depths below 400 metres from the surface.

Table 2-3. Global Open Fracture Set Parameters for Domain FFM01 (Follin 2008, SKB 2010).

Set	Orientation				Intensity	Size (from All)		
	Type [–]	Pole Trend [deg]	Pole Plunge [deg]	Conc. [–]	P_{32} [m^2/m^3]	r_0 [m]	Slope [–]	r_{max} [m]
NE	Fisher	326.00	2.00	14.30	0.163	0.659	3.02	564.20
NS	Fisher	292.00	1.00	17.80	0.094	0.059	2.78	564.20
NW	Fisher	60.00	6.00	12.90	0.098	0.594	2.85	564.20
SH	Fisher	5.00	86.00	15.20	0.141	0.816	2.85	564.20
EW	Fisher	15.00	2.00	12.90	0.039	0.170	3.10	564.20

For the TCM case, geometrical properties of open fractures has been described in Follin (2008) and SKB (2010) and are shown in Table 2-3. They are in all aspects considered as being a sub-set of the "All" fracture population with identical spatial, orientation and size distributions. The difference is the significantly reduced fracture intensity for all fracture sets.

2.2.3 Sealed Fracture Sets

The rock mass at Forsmark is dominated by sealed fractures, while the open fractures are only a small sub-set of the total number of the fractures. The intensity (P_{32}) of the sealed fractures has been assumed equal to the difference between the fracture intensity of the TCM and Open (Hydro) fracture sets. The geometrical properties for the TCM case of the sealed fracture sets are detailed in Table 2-4.

Table 2-4. Sealed Fracture Set Parameters for Domain FFM01 from SKB (2010).

Fracture Set And Property	Intensity P_{32} [m^2/m^3]			Orientation	Size
	Open	TCM (Global)	Sealed(**)	Sealed	Sealed
NE	0.319	1.733	1.414	TCM All(global)	TCM All(global)
NS	0.073	1.292	1.219	TCM All(global)	TCM All(global)
NW	0.107	0.948	0.840	TCM All(local)	TCM All(local)
EW	0.088	n/a	0.00	TCM All(global)	TCM All(global)
HZ	0.543	0.624	0.081	TCM All(global)	TCM All(global)

** = P32(sealed) = P32(TCM) – P32(Open) is assumed as a simplified assumption.

Whilst it may not be strictly correct to compute the sealed fracture intensity from the difference in TCM and open fracture intensities, due to them corresponding to different size intervals, it is considered a worthwhile assumption for these initial investigations assessing block kinematic stability.

2.3 Domain FFM06 Fracture Sets

The parameters used for creation of the DFN fracture sets for rock domain FFM06 are outlined in the following subsections. These parameters are primarily extracted from the SKB (2010) report.

2.3.1 TCM Fracture Sets

The Global sets were selected used for the modelling of the domain FFM06 because of the same consideration as domain FFM01. Table 2-5 provides the parameter sets used for the TCM model of the FFM06 rock domain.

Table 2-5. Global TCM Fracture Set Parameters for Domain FFM06 from SKB (2010).

Set	Fracture Orientation				Intensity	Size		
	Distribution [–]	Pole Trend [deg]	Pole Plunge [deg]	Concentration [–]	P_{32} [m²/m³]	r_0 [m]	Slope [–]	r_{max} [m]
NE	Fisher	125.70	10.10	45.05	3.299	0.351	3.02	564.20
NS	Fisher	91.00	4.10	19.49	2.150	0.039	2.78	564.20
NW	Fisher	34.10	0.80	16.13	1.608	0.319	2.85	564.20
SH	Fisher	84.30	71.30	10.78	0.640	0.793	2.85	564.20

Similarly to seen in Figure 2-1 for rock domain FFM01, the following Figure 2-2 shows the complementary cumulative distribution function of fracture intensity with respect to fracture radius for domain FFM006.

This time, for domain FFM06 it is evident that that the NW fracture set is most likely the most important set for fracture with radii larger than approximately 70 metres. At sizes below this size it is evident that the NE fracture set (in red) is the most dominant. In addition, the figure again demonstrates that the NS set is again a half to one order of magnitude less intense than the other sets in any given size range, despite that the P_{32} being the second largest.

2.3.2 Open Fracture Sets

More information related to the open fracture properties can be found in Follin (2008) and SKB (2010, Table 6-75). The data used in the current work were taken for the depth set deeper than 400 metres from the surface. The hydrogeological DFN parameters to be used for domain FFM06 are summarized in the Table 2-6 below. The NE properties were used for the EW set since they are absent from the original TCM description.

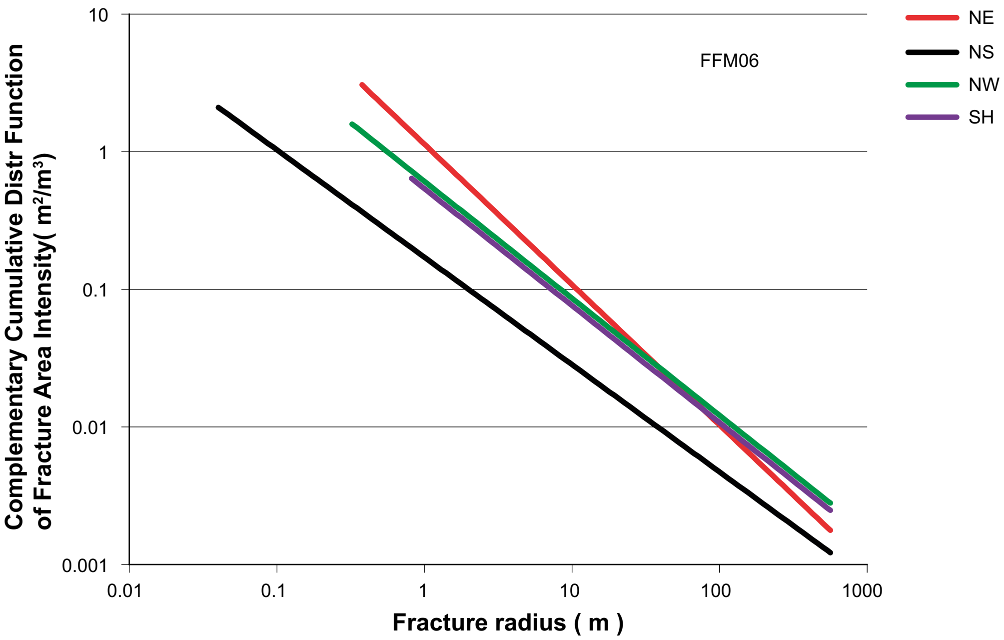

Figure 2-2. Complementary Cumulative Distribution Function of Fracture Intensity With Respect to Fracture Radius For Domain FFM006 (Vidstrand P 2015, personal communication).

Table 2-6. Global Open Fracture Set Parameters for Domain FFM06 from Follin (2008) and SKB (2010).

Set	Orientation				Intensity	Size (from TCM)		
	Distribution [–]	Pole Trend [deg]	Pole Plunge [deg]	Concentration [–]	P_{32} [m²/m³]	r_0 [m]	Slope [–]	r_{max} [m]
NE	Fisher	326.00	2.00	14.30	0.163	0.351	3.02	564.20
NS	Fisher	292.00	1.00	17.80	0.094	0.039	2.78	564.20
NW	Fisher	60.00	6.00	12.90	0.098	0.319	2.85	564.20
SH	Fisher	5.00	86.00	15.20	0.141	0.793	2.85	564.20
EW	Fisher	15.00	2.00	14.00	0.039	0.35(*)	3.02(*)	564.20

*Assumed fracture size parameters for EW set are copied directly from the NE fracture set.

2.3.3 Sealed Fracture Sets

In the domain FFM06, the intensity (P_{32}) of the sealed fractures was considered equal to the intensity difference of the all and open fracture sets. The data was evaluated for depth greater than 400 metres from the surface, detailed in SKB (2010, Table 6-75). The derived sealed fractures intensity properties are shown in Table 2-7.

Table 2-7. Sealed Fracture Set Parameters for Domain FFM06 from SKB (2010).

Set	Fracture Intensity P_{32} [m²/m³]			Orientation	Size
	Open	TCM (global)	Sealed	Sealed	Sealed
NE	0.163	3.299	3.136	All(global)	All(global)
NS	0.094	2.150	2.056	All(global)	All(global)
NW	0.098	1.608	1.51	All(global)	All(global)
EW	0.039	n/a	n/a	All(global)	All(global)
HZ	0.141	0.640	0.499	All(global)	All(global)

2.4 Natural Fracture Shape for FFM01 and FFM06

Fractures can be approximated as planar, circular discs with thickness described as a parameter (aperture), and having radii independent of position. While the fractures in the rock are probably neither circular nor planar, there appears to be insufficient data to mathematically characterize deviations from these two idealizations. It is noted by Fox et al. (2007) that in outcrop the deviations from planarity do not appear to be large, and it is highlighted that there are also mechanical reasons to suppose that the actual fracture shapes may tend towards being equant. This is since the mechanical layering present in sedimentary rocks, which generally promotes non-equant fracture shape, is potentially less well-developed in the crystalline rocks at Forsmark.

On this basis the DFN fracture shapes adopted in the current investigations are chosen as equant six sided hexagonal fractures. It is recognised however that locations at Forsmark which may have undergone significant deformation (e.g. deformation zones) fractures may be more prone to exhibiting significant aspect ratios in terms of elongation and height.

2.5 Rock Mechanical Properties

The rock mechanical properties are important for assessing the stability of any fractured rock mass since the properties directly influence the deformation and failure of the rock mass. The primary rock mass properties can effectively be classified into three different types of properties, these are:

- Intact rock properties.
- Fracture strength properties; and
- Fracture compliance.

2.5.1 Intact Rock Properties

Table 2-8 summarises the basic intact rock properties extracted from Glamheden et al. (2007). These data are considered approximate averages for the various tables originally reported, and provides averaged elastic properties, of Young's Modulus, Poissons ratio, and the Bulk Density, as well as estimate values of the intact material Mohr coulomb failure envelope. Intact elastic properties refers to the solid un-fractured rock existing in-between the nature fractures.

Table 2-8. Basic Intact Rock Properties from Glamheden et al. (2007).

Material Property	Average Property Value
E, Young's Modulus [MPa]	76 000(**)
v, Poisson Ratio [–]	0.23(**)
RhoB, Bulk Density [g/cc]	2.70
Intact Mohr Coulomb Phi [deg]	59.00(**)
Intact Mohr Coulomb Cohesion [MPa]	28.50(**)

Note: (**) – averaged reported values by Glamheden et al. (2007).

Of the properties provided in Table 2-8 only the bulk density property is required for the current implementation of the rock wedge analysis, since this value is used to derive the self-weight for each of the individual rocks blocks identified through the analysis process. Future analyses integrating the full in situ stress description with kinematic stability will require full use of all properties listed in Table 2-8.

2.5.2 Fracture Strength Properties

Results of the direct shear tests originally undertaken are summarised in detail by Glamheden et al. (2007) with support from other SKB reports (see also Chryssanthakis 2003, 2004 a, b, c, d, Jacobsson 2005, Jacobsson and Flansbjer 2005). It is noted, that in the original reporting, frictional response of the natural fractures are not distinguished between domains FFM01 and FFM06, this is since no samples were taken for testing for domain FFM06. It is noted however by Glamheden et al. (2007), that the frictional properties of the natural fractures in domain FFM06 are likely to be similar to those for domain FFM01. In the following subsections, the fracture surface strength properties are detailed for the Open Fractures, and Sealed Fractures types.

Open Fractures

The surface friction properties of the open natural fractures were originally evaluated from 57 direct shear test investigations (see Glamheden et al. 2007, Tables 4-7 and 4-8). A summary of the derived Coulomb strength properties are provided in Table 2-9 and Figure 2-3.

Table 2-9. Coulomb Strength Surface Properties for Open Fractures from Glamheden et al. (2007).

Strength Property	Average	St Dev	Minimum	Maximum
Coulomb Friction, Phi [degrees]	36.60	2.90	29.30	42.00
Coulomb Cohesion [MPa]	0.80	0.30	0.20	1.30

Figure 2-3 shows the relative relationship of the average, minimum and maximum shear (frictional) strength envelopes of the available data in terms of fracture normal stress. It is seen that the properties are similar to those noted by Hoek (2006), with the exception that the cohesion value is noticeably higher.

Sealed Fractures

In addition to the open fracture types, strength properties are also provided for the more spatially dominant sealed fracture types, these are shown in Table 2-10 and Figure 2-4. These data are detailed in the original report by Glamheden et al. (2007).

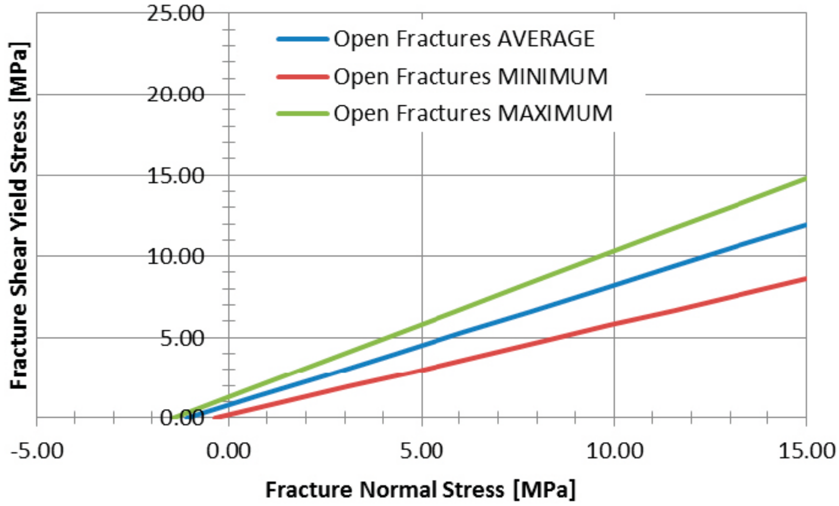

Figure 2-3. *Coulomb Strength Envelopes for Open Fractures from Glamheden et al. (2007).*

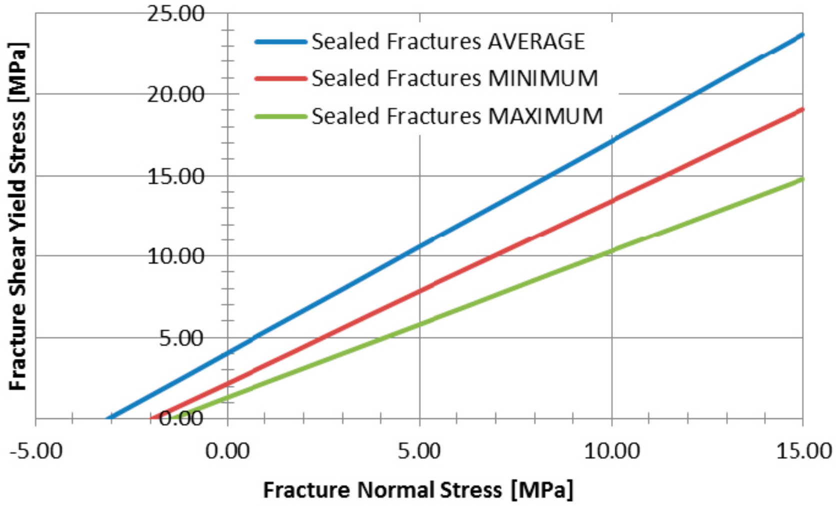

Figure 2-4. *Coulomb Strength Envelopes for Sealed Fractures from Glamheden et al. (2007).*

Table 2-10. Averaged Coulomb Strength Surface Properties for Sealed Fractures from Glamheden et al. (2007).

Strength Property	Average	St Dev	Minimum	Maximum
Coulomb Friction, Phi [deg]	52.60	4.90	48.30	57.90
Coulomb Cohesion [MPa]	4.06	2.99	2.21	7.50

It is evident that the sealed natural fractures have significant increased shear resistance compared to the open natural fractures. This increase is due to the significant increase in the (normal stress independent) cohesion parameter of the shear strength model used.

It is reported that most natural fractures in the Forsmark repository area are considered as sealed; indicating that the shear (slip) strength or resistance of the natural fracture sets is significant.

Fracture Stiffness Properties

In addition to the frictional response of the natural fractures at the Forsmark location, specification of the fracture normal (Kn) and tangential (Kt) stiffness (compliance) properties are also essential material properties. Compliance data is essential for understanding how the fractures respond under normal compressive loading. Table 2-11 specifies the normal and tangential fracture stiffness values.

Table 2-11. Normal and Shear Stiffness Values (from Glamheden et al. 2007, Table 4-17).

Forsmark 2.2 Properties	Mean [GPa/m]	St Dev [GPa/m]	Min [GPa/m]	Max [GPa/m]
Kn, Secant Normal Stiffness (0.50–10 MPa confinement)	607	483	115	2445
Kt, Tangential Stiffness (10 MPa confinement)	33	10	18	62

2.6 Appropriate Model Configurations

In the previous report sections, details of the main properties of the natural fractures are identified. These relate to both the fracture geometry as well as the mechanical properties. These are provided for all, open and sealed fracture types for each of the two fracture domains FFM01 and FFM06 being investigated. In the following subsections the available model configurations and the selected model case are considered.

2.6.1 Available Model Configurations

In Table 2-12 all possible model configurations put forward for the kinematic stability assessment of Task 1.2 of Phase I are identified. From the identified model configuration a smaller selection of configurations are selected for analysis.

Table 2-12. Summary of Possible Model Configurations for Analysis.

Cases for Each Domain		Reference Data	Arguments For?	Arguments Against?
A	FFM0x (All).	Geo DFN TCM, Fox et al. (2007, Tables 6-34 and 6-37).	Straight use of Geo DFN, TCM model. Reflects complete fracture statistics in Forsmark.	GeoDFN not necessarily developed for this usage. No distinction of sealed/open.
	TCM with all fractures using mechanical properties from ”open” fractures on all global sets.	Mechanical properties in Glamheden et al. (2007, Table 4-7).	Conservative by using open fracture mech properties on all fractures. Both domains treated identical. ”Worst case scenario”.	Overestimating probability of blockfalls. Large models – complex analysis.
B	FFM0x (Open)	Hydro DFN, SKB (2010, Table 6-75) mixed with size from GeoDFN TCM, Fox et al. (2007, Table 6-34).	Focus on open fractures only – quick analysis. Including depth dependence.	No influence of complete fracture network may underestimate blocks.
	Hydro DFN derived model using only open fractures with open fracture mechanical properties.	Mechanical properties in Glamheden et al. (2007, Table 4-7).	Appropriate properties from open fractures only.	A mix of DFN properties from Hydro and Geo which are somewhat unclear.
C	FFM0x (Open/Sealed).	Mix between GeoDFN TCM, Fox et al. (2007, Tables 6-34, 6-37) and Hydro DFN, SKB (2010, Table 6-75).	Treating both sealed and open. Includes depth dependency of open.	A mix of DFN properties from Hydro and Geo which are somewhat unclear.
	TCM/Hydro DFN derived model separating open and sealed fractures. Using Open and sealed mechanical fracture properties.	Mechanical properties, Glamheden et al. (2007, Tables 4-7 and 4-9).	Using mechanical properties of both sealed and open.	Large models – complex analysis.

Table 2-12 identifies there are three cases available for each rock domain for investigation. Each of which corresponds to the cases of A) all, B) open, and C) open/sealed fracture types respectively. For each of the cases identified Table 2-12 also provides summary arguments for and against evaluation of each.

2.6.2 Selected Model Configurations

Based on the possible cases in Table 2-12, it is proposed the Case A configuration is pursued for analysis of both domains FFM01 and FFM06. Details on the analyses carried forward are provided in Table 2-13.

Table 2-13. Model Cases Selected for Analysis.

Fracture Set Id	Type	Orientation	Intensity	Size
FFM01 (All, global sets)	All fractures	TCM	TCM	Power law, r_0 TCM
FFM06 (All, global sets)	All fractures	TCM	TCM	Power law, r_0 TCM

The adopted configuration of Table 2-13 provides a conservative approach in which all fractures are treated as potentially block forming rather than just analysing the effect of unstable blocks on a particular sub-set of the whole population. In addition, the cases also directly provide compliance to the complete set of fracture statistics observed at Forsmark location.

2.7 Deposition Tunnel Geometry

The anticipated geometry of the repository at the Forsmark Site is shown in Figure 2-5. From this figure, two tunnel orientations are identified, these correspond to a primary tunnel direction N233 (i.e. 233 degrees from North), and a secondary tunnel orientation of N143. In addition the figure also highlights some of the tunnel geometries and locations which are not considered in the current investigations.

In addition to Figure 2-5, the geometry of the deposition tunnel is shown in Figure 2-6, additionally a representation of the FracMan tunnel geometry model is provided for comparison. It is evident in Figure 2-6 that the tunnel geometry provided by SKB is fairly regular, but does include some smaller scale detail which may be important. The smaller scale details are located where the sidewall transition to the tunnel crown (roof), and there the tunnel invert (floor) transitions to the sidewall locations, see Figure 2-7.

The following section reports on the development and analysis of the kinematic block stability model (i.e. Phase I Task 1.2) based on the fracture domain configurations and tunnel geometries identified. The fracture properties employed in the configurations are those identified previously in Section 2.

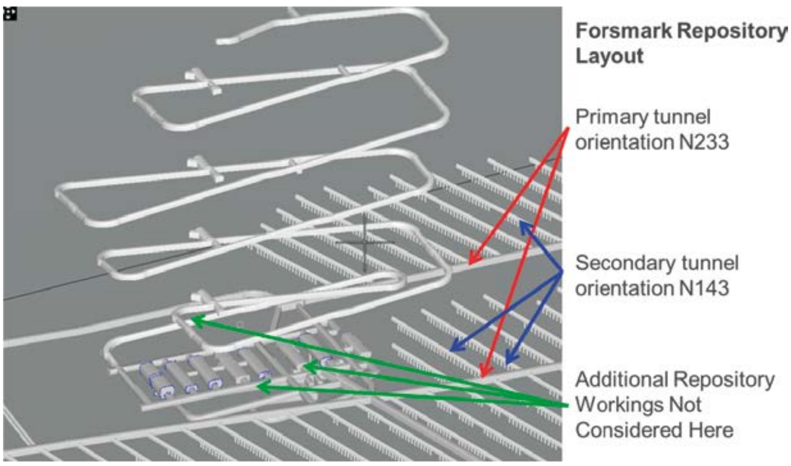

***Figure 2-5.** Representation of Anticipated Forsmark Repository D2 Layout (Vidstrand P 2015, personal communication).*

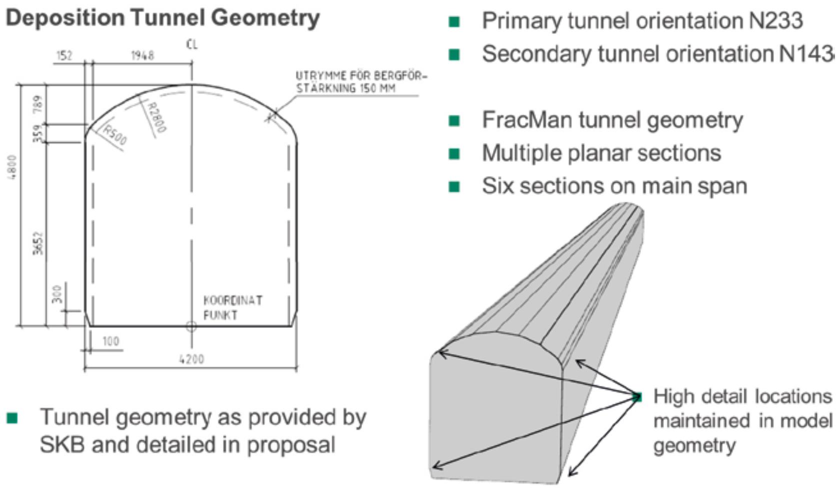

Figure 2-6. *Schematic of Tunnel Geometry (Vidstrand P 2015, personal communication).*

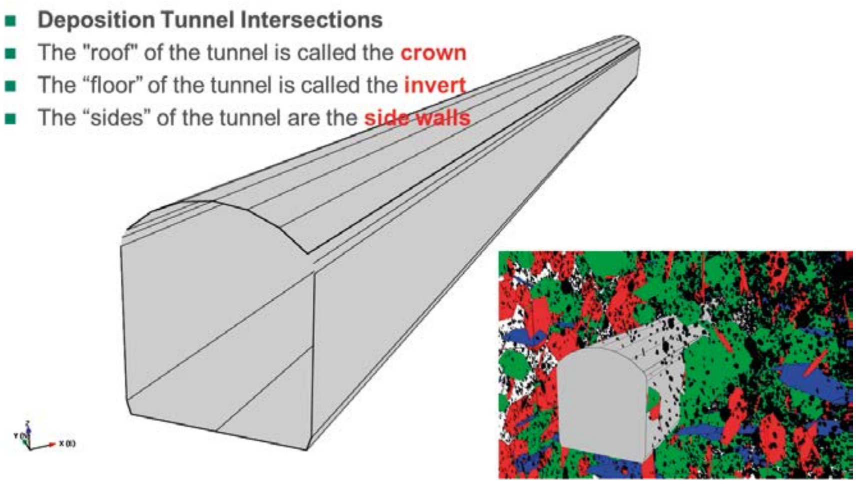

Figure 2-7. *Tunnel Intersections in FracMan Model and the Surrounding Fracture Network Model. DFN Configuration Shown if FFM01 Fracture Model.*

3 Task 2: Probabilistic Assessment of Rock Block Kinematic Stability

This section presents the development and assessment of the rock block kinematic stability assessment of the deposition tunnel geometries embedded in the discrete fracture models of the Forsmark rock domains FFM01 and FFM06. In the following sections, the process of the workflow definition, model construction, and kinematic stability assessment are provided.

3.1 DFN Generation Workflow

Summarized in Figure 3-1 is the typical workflow used for parameterising, constructing and applying a DFN model, and includes the typical data types and sources used for model construction. The workflow begins on the left with data sources, which are then integrated to form a calibrated hydrostructural model, and are then carried into geomechanics and engineering analyses.

Whilst the Figure 3-1 presents a typical DFN model workflow, the specific workflow used in this work is provided below in Figure 3-2.

3.1.1 DFN Model Creation

Using the DFN workflow, the simplified construction of the required tunnel scale DFN model is divided into three key stages, these are:

- **Stage 1:** Generation of a DFN to 100 × 100 × 100 metre sized box full of the global fracture sets.
- **Stage 2:** Clipping the DFN down to 25 × 100 × 25 metre sized box; and
- **Stage 3:** Clipping the fractures out within the tunnel from DFN 25 × 100 × 25 box. At the end of the Stage 3, we have a local (25 × 100 × 25 metre) model full of four fracture sets intersected by the planned tunnel.

The fracture sets in the DFN model are generated based on the orientation, intensity, and size data presented for the TCM fracture sets in the previous sections.

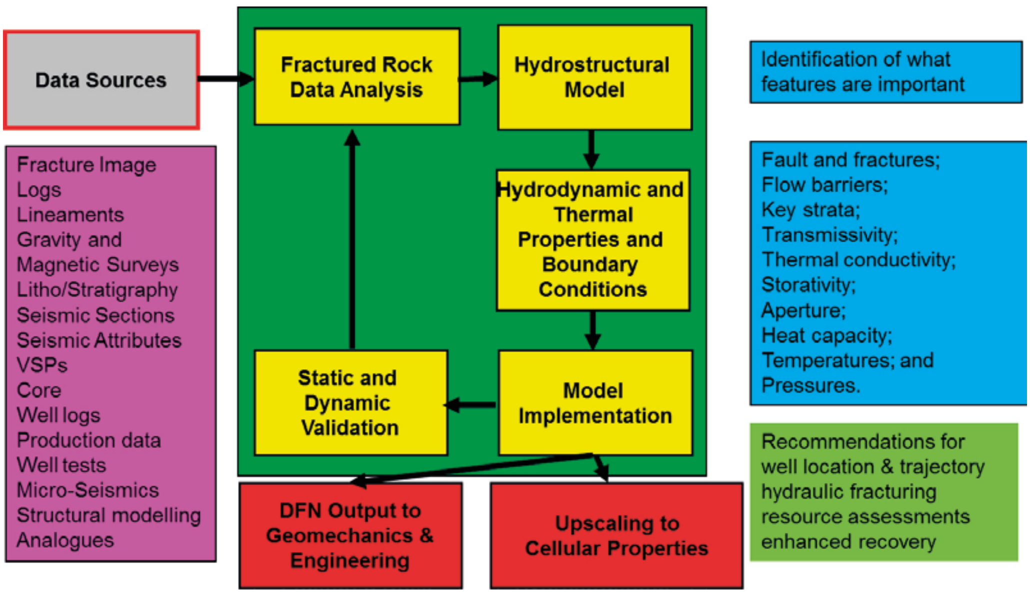

Figure 3-1. *DFN Workflow Defining Data Types, Model Construction and Analysis.*

As illustrated below in Figure 3-3, Stage 1 consists of filling a large 100 × 100 × 100 metre box with the global fracture sets for each of the respective fracture domains FFM01 and FFM06 respectively. Beginning with the larger 100 metre wide box domain initially is to allow for the inclusion of the larger sized natural fractures which are relatively few in number but are still important to the overall model.

Stage 2 provides for the reduction in overall model size down to a size appropriate for the kinematic rock wedge analysis that is ultimately being considered.

The final Stage 3 is the final step of the model conditioning, in this step the tunnel geometry is clipped away from the inside of the fracture network block.

3.1.2 Validating Optimised DFN Model Creation

Whilst the model workflow detailed provides creation of the DFN model and tunnel for use in the kinematic stability assessment, the initial creation of the large 100 × 100 × 100 metre sized domain with all natural fractures makes the DFN model initially computationally inefficient. In improving the efficiency of the DFN model created, the model is reduced down to a 25 × 100 × 25 metre sized region.

The acceptability of the smaller model is assessed by generating the fractures at both box scales and then by direct comparison of tracemap statistics sampled from the local and large scale fracture network models. Comparison of traceplane statistics from the two models are shown in Figure 3-4.

Comparison of the traceplane statistics obtained from the large and local scale DFN box are detailed in Table 3-1 below. To ensure proper representation these statistics have been obtained from an average of three individual realisations of each DFN model for each generation region and averaged.

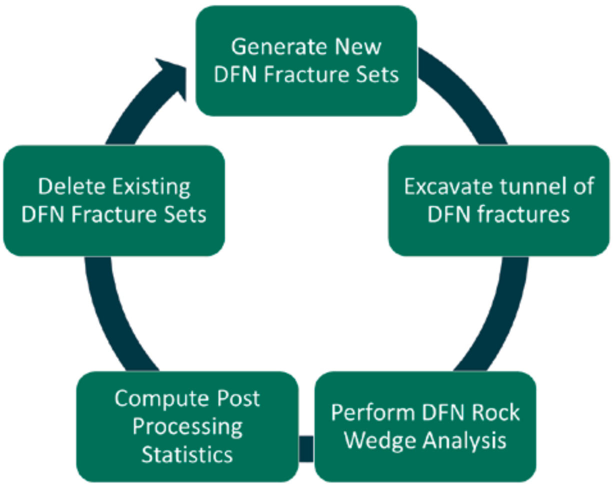

Figure 3-2. *Specific DFN Kinematic Stability Analysis Workflow.*

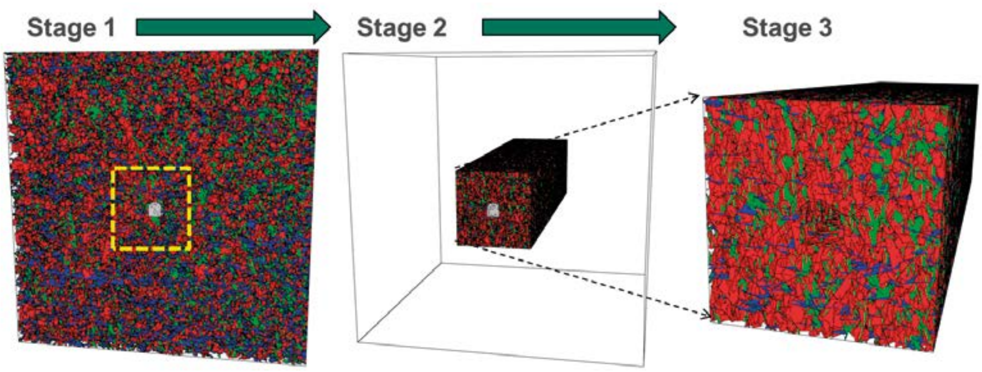

Figure 3-3. *The Stages of the DFN generation, Note Grey Tunnel Region in Centre of Model.*

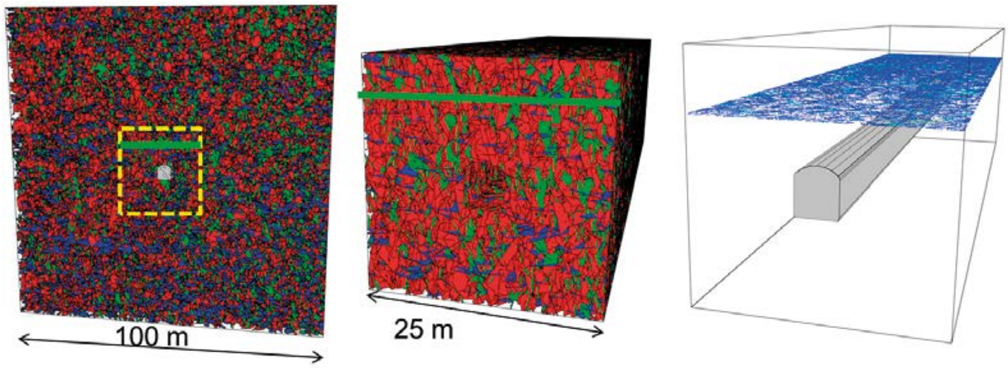

Figure 3-4. *Traceplane Comparison Model for Large (100 × 100 × 100) and Small (25 × 100 × 25) Region Around the Model Deposition Tunnel Geometry. Traceplane is Green Surface Located 8 Metres Above Tunnel Centre.*

Table 3-1. Comparison of Traceplane Statistics for Large and Small Generation Regions.

Traceplane Property	100 × 100 × 100 Generation Region	25 × 100 × 25 Generation Region
# of Segments [–]	77 324	77 463
# of Intersections [–]	27 710	27 690
Total trace length [m]	10 103.04	10 248.84
Intensity P_{21} [m/m^2]	4.04	4.09
Trace length mean [m]	0.364	0.370
# of fractures per area	11.08	11.07

It is evident in Table 3-1 that the creation of the DFN fracture at both the large and small sized generation regions provides traceplane statistics that are suitably comparable to each other. On this basis, an optimisation to the workflow is that the DFN model generation is not sensitive to model size within the tested limits such that it can be reduced down to the more efficient 25 × 100 × 25 metre domain.

3.1.3 Final DFN Model

The adopted local scale model includes additional sampling points to allow simple assessment of how the generated DFN model statistically interacts with the inserted model geometry. Three sampling locations are included in the model, there is the traceplane positioned above the tunnel, there is an offset vertical borehole positioned adjacent to the tunnel, and there is the tunnel itself which is also sampled for intersecting natural fractures. The sampling locations are shown in Figure 3-5.

In terms of the sampling locations identified in Figure 3-5, the model includes a horizontally orientated tracemap positioned midway between the top of the tunnel crown and the upper edge of the model.

In addition, a vertical verification borehole offset to one side of the tunnel at the mid position along the tunnel is also included. A third verification sampling location is the tunnel geometry itself, the tunnel geometry provides opportunity to sample for fracture intersections.

3.2 FracMan Kinematic Stability Analysis

Using the FracMan kinematic stability approach, models for rock domains FFM01 and FFM06 is tested for fracture intersections and connection maps, and specifically assesses the stability condition of the rock block geometry at the exposed faces of the tunnel.

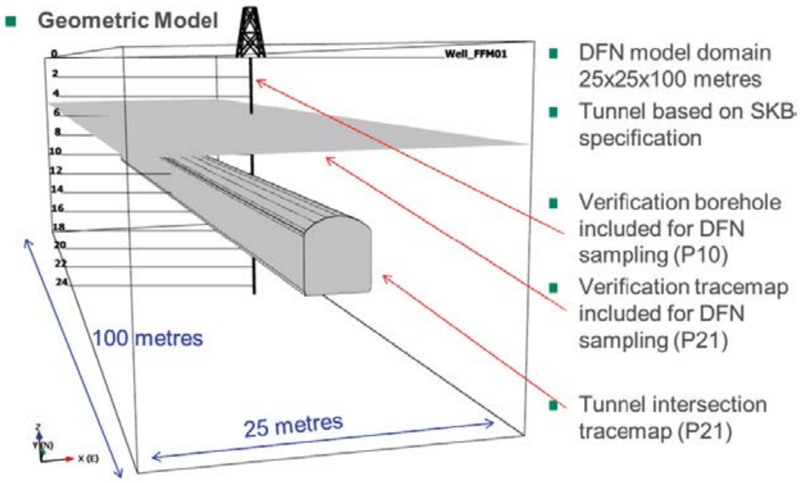

***Figure 3-5.** Model Sampling Locations of the DFN Fracture Model.*

3.2.1 Rock Wedge Kinematic Stability Theory

The analysis approach in FracMan is able to simulate rock block stability on tunnels, slopes or mine voids, allowing a truly probabilistic assessment of the kinematic stability in surface and underground rock excavations. This analysis is carried out upon realistic multifaceted rock blocks defined by the users DFN model and therefore not subjected to any of the conventional limitations of block stability being defined by a prescribed number of fracture sets. This approach therefore considers the probability of adverse wedge formation rather than just the possibility of them.

Modelling the Rock Mass Fracture has a Number of Advantages

Modelling the rock mass fracture system using FracMan DFN has a number of advantages, including:

- The flexibility to realistically model a wide range of fracture scenarios.
- The ability to constrain and condition the model to a range of data sources including 1D, 2D and 3D data sources.
- To be able to produce models that realistically reproduce observed fracture properties without excessive simplification.
- Monte Carlo support for running and analysing multiple realizations for constraining the likelihood of outcomes; and
- Integration with other numerical codes for realistic simulation.

Kinematic Stability Analysis Workflow

The workflow employed in the analysis is detailed in the following itemised points.

1) Determine the wedge geometry using classical block theory (Goodman and Shi 1985).
2) Determine all of the individual forces acting on a wedge, and then calculate the resultant active and passive force vectors for the wedge.
3) Determine the sliding direction of the wedge.
4) Determine the normal forces on each wedge plane.
5) Compute the resisting forces due to joint shear strength, and tensile strength (if applicable); and
6) Calculate the Factor of Safety.

Wedge Forces

All forces on the wedge can be classified as either Active or Passive. In general, the Active Forces represent driving forces in the safety factor calculation, whereas the Passive Force terms represent the resisting terms.

Active Forces

The Active Forces (A) is defined by the following items:

- A = W + C + X + U + E
  - A = Resultant active force vector.
  - W = Wedge weight vector (= volume x density x gravity).
  - C = Shotcrete weight vector (= density x area x thickness x gravity).
  - X = Pressure force (external) (=stress x area x unit normal).
  - U = Water Pressure (=water pressure x unit normal); and
  - E = Seismic force vector (= seismic coefficient x density x volume).

Passive Forces

Similarly to the Active Forces, the resisting Passive Forces (P) are defined by the following items:

- P = H + Y + B
  - P = Resultant passive force vector.
  - H = Shotcrete shear resistance force vector.
  - Y = Passive pressure force vector; and
  - B = Resultant bolt force vector.

Sliding Direction

One of the principal calculations performed in the kinematic stability assessments, is in the calculation of the resultant sliding direction of each rock wedge identified. The sliding direction calculation is based only on the Active Force components only – the Passive force terms are not considered influential on the sliding direction. The implemented algorithm for calculation of the sliding direction is similar to that presented in the classical rock block text presented by Goodman and Shi (1985).

It should be noted, that the calculation of the sliding direction is considered a two-step process. Firstly all possible sliding directions are identified, and secondly each of the sliding directions is appraised and those that are considered invalid are eliminated from further calculation. Invalid sliding directions are those directions which are considered geometrically inadmissible.

Forces, Failure Models and Factor of Safety

The following subsections provide explanation on the approaches used for calculation of the normal and shear force components on each block face, the shear and tensile strength limits, and the failure mode classification and Factor of Safety calculation for each block identified.

Normal and Shear Force

- The calculation of the normal forces on each of the joint planes first requires the calculation of the sliding direction.
- Using the sliding direction, the normal forces are then used to calculate a resultant force vector, F; which in turn provides the shear force component; and
- The resultant vector, F, is generally either the active or the passive resultant force vector.

Shear and Tensile Strength

- There are two joint strength models available in FracMan's kinematic stability approach: 1) Mohr-Coulomb (Coulomb 1776), and 2) Barton-Bandis (Barton and Choubey 1977, Barton and Stephansson 1990). These shear failure models are easily calibrated using simple rock mechanical approaches.
- The surface shear (yield) strength is computed based on the magnitude of the normal stress projected onto each joint plane for each block identified; and
- The normal stress is computed based on the active and passive normal forces computed on the joint planes using the equations in the previous section.

Failure Model and Factor of Safety Calculation

- For each wedge identified FracMan computes a specific failure mode indicator, the failure indicator differentiates between those blocks that are a) freefall blocks, b) blocks that are kinematically stable (shear and tensile strength, if applicable, keeps them stable), and c) blocks that are geometrically stable (shaped such that they cannot fall out); and
- The limit equilibrium safety factor calculations only consider force equilibrium in the resultant direction of sliding. Moment equilibrium (rotation) is not considered as part of the solution process.

Factor of Safety Calculation

The Factor of Safety (FOS) assessment for each rock block identified on the sampling structure (the tunnel or slope) is a primary output of the analysis. The Factor of Safety is simply calculated based on the following equation:

- Factor of Safety = (Resisting Forces) / (Driving Forces).

Failure Mode Calculation

In parallel to the Factor of Safety (FOS) calculation, the employed approach also computes a respective failure mode for each block identified. The calculation of the block failure mode, and their relation to FOS, is detailed in the following points:

- Kinematically Inadmissible Blocks (FOS = 100).
- Stable Blocks (FOS $\geq$ 1.00).
- Unstable Sliding Blocks (FOS $<$ 1); and
- Free Falling Gravity Blocks (FOS = 0).

Limitation of Approach

It is recognised however, that in all of the analyses undertaken the proper post-excavation in situ stress field has not be considered. Therefore, the fracture normal stress responsible for the fracture frictional strength is only induced by each block self-weight. This is expected to affect the results considerably, and should be more fully addressed in future investigations.

Composite Blocks

FracMan is able to provide a post processing option in which it will report on blocks that are contiguous as a single block volume which are formed from multiple individual connected blocks. This form of output is called Composite Block output, an example is provided in Figure 3-6. Here it is shown how two blocks (one red and one green) may exist aligned and adjacent, therefore contiguous to each other. When FracMan computes the required block statistics (block geometry, failure mode, and factor of safety) these are based on the combined block geometry – the composite geometry.

For all model analyses presented in this report, the FracMan analyses only consider the use of composite block output. No results output is provided considering the smaller sub block geometry and attributes. It may be of interest in future investigations related to the repository construction phase to consider the smaller sub blocks also.

Required Input Data

The required input elements for execution of the rock wedge analysis are defined in the following points:

- The local DFN model, of which the workflow is detailed in Section 3.1, and the parameters from Sections 2.1 to 2.5 including fracture definitions for orientation, intensity, size and rock mechanical properties including fracture shear strength and pore pressure state; and
- Inclusion of the sampling structure (tunnel), defined in Figure 2-7 from Section 2.7.

Analysis Output Data

Implementation of the kinematic stability analyses provides the following information at the completion of each of the analysis runs:

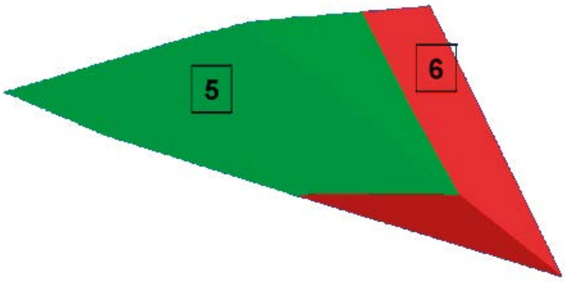

Figure 3-6. *FracMan Rock Wedge Analysis Results Composite Block Example.*

(a)

- Identification of unstable blocks surrounding the tunnel (see Figure 3.7(b), red blocks).
- Identification of stable and unstable blocks (see Figure 3.7(b), green and red blocks).
- Calculation of the block failure mode for each block formed,
- Calculation of the block Factor of Safety for each block formed,
- Calculation of the block dimensions for each block formed; and
- Calculation of a tunnel tracemap for all fractures intersecting the sampling structure.

(b)

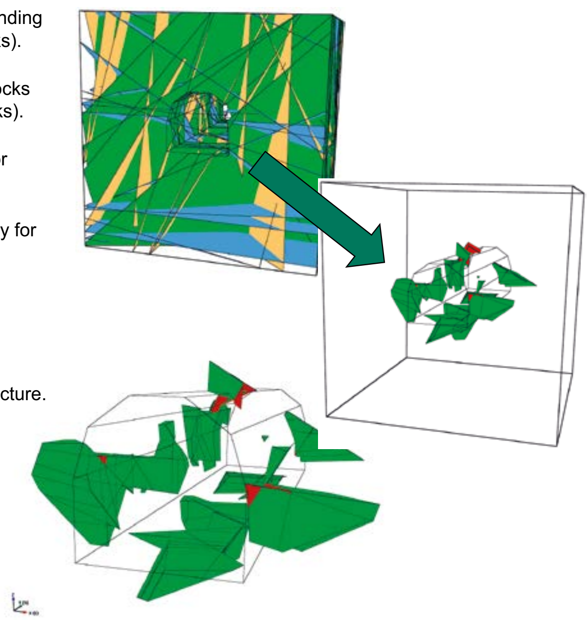

Figure 3-7. *FracMan Rock Wedge Analysis Results, Showing Red Blocks are Kinematically Unstable Blocks, and Green Blocks are Kinematically Stable Blocks.*

3.2.2 Baseline Configurations Initially Investigated

The following Sections 3.3 to 3.5 presents the baseline model analyses undertaken for rock domains FFM01 and FFM06 respectively. Table 3-2 specifies both the fracture geometrical descriptions and the fracture frictional properties and fracture fluid (pore) pressure loading.

Table 3-2. Baseline Model Cases Selected for Rock Wedge Analysis.

Domain	Fractures	Orientation	Intensity	Size	Friction	Pore Load
FFM01 (All)	All fractures	TCM*	TCM*	TCM*	Open Fractures	Zero
FFM06 (All)	All fractures	TCM*	TCM*	TCM*	Open Fractures	Zero

* From Fox et al. (2007).

It should be noted that in the presented models no fracture truncation has been included. The created DFN models honour the full unmodified fracture intensity values derived from previous SKB reporting. Fracture truncation is typically omitting fractures that are either particularly small or large in size, and serves to reduce the fracture numbers and therefore complexity of the analysed fracture model.

3.3 FFM01 – Baseline Kinematic Stability Analysis

The results of the baseline stability analysis for the domain FFM01 are presented in the following sections. The sections presented consider the following items:

- Model Configuration.
- Tunnel Fracture Intersection Analysis; and
- Tunnel Kinematic Stability Analysis.

3.3.1 Model Configuration

The global fracture sets included in the developed model are detailed below. The tunnel orientation considered in this baseline analysis is N233 only – no alternative tunnel orientations have been considered at this stage.

In Figure 3-8 the orientations of the four fracture sets have been evaluated identifying the natural fractures that intersect the vertically deviated borehole included in the model. A contoured stereoplot describing the intersecting fracture orientation is shown in Figure 3-9. It is seen that the fracture orientations of the intersecting fractures relate appropriately to the orientation parameters specified. Further plots of the individual fracture set orientations are detailed in the included Appendices.

In addition to the fracture geometrical data, the following Table 3-3 provides the frictional properties assigned to the created fractures. No differentiation has been applied between the fractures sets, all sets have identical strength property distributions assigned.

Table 3-3. Coulomb Strength Properties Assigned to the Fracture Sets in Rock Domain FFM01.

Surface Strength Property	Average	St Dev	Minimum	Maximum
Coulomb Friction, Phi [degrees]	36.60	2.90	29.30	42.00
Coulomb Cohesion [MPa]	0.80	0.30	0.20	1.30

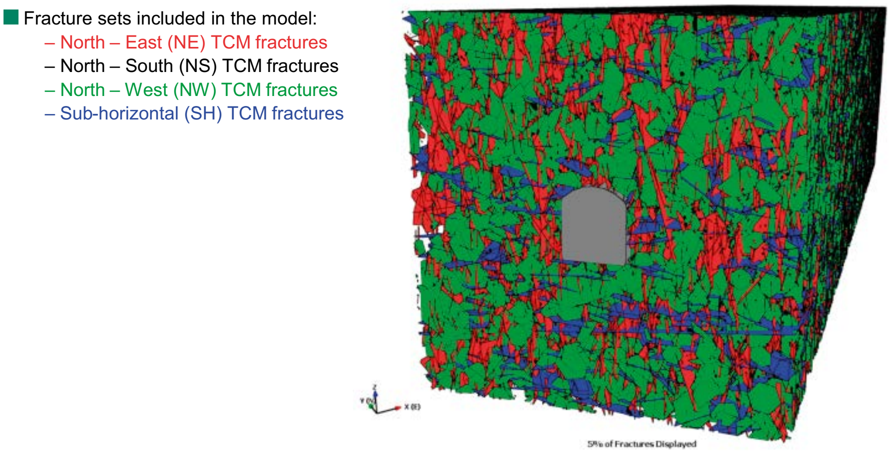

Figure 3-8. Local DFN Model of Domain FFM01.

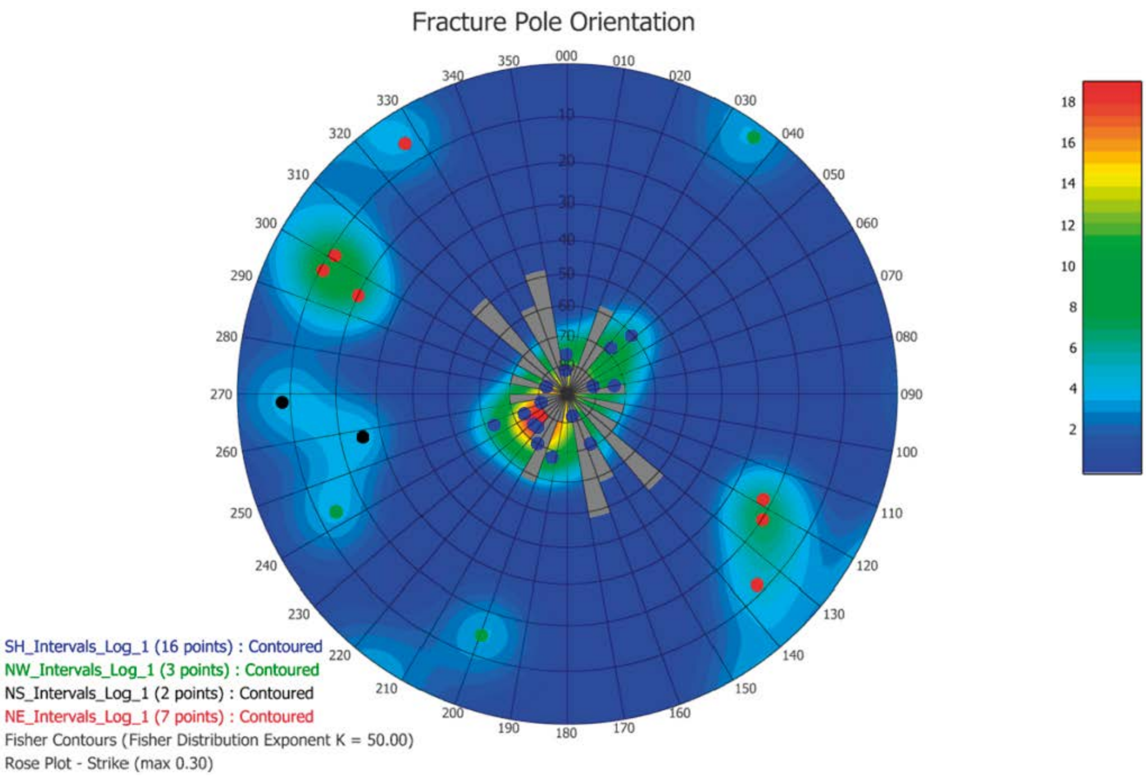

Figure 3-9. Contoured Stereoplot of the Fracture Set Intersections for the Domain FFM01 Model Borehole.

3.3.2 Tunnel Kinematic Stability Analysis

The primary analysis undertaken considers the kinematic stability of the rock blocks identified around the tunnel geometry. The below Figure 3-10 provides the typical rock wedge kinematic stability statistics obtained from a single realisation of the DFN for the Forsmark FFM01 domain.

It is evident in Figure 3-10 that most of the rock blocks identified are kinematically stable. Over the interval assessed a total of 207 blocks are identified. Of these, 194 blocks are kinematically stable, no blocks are kinematically unstable, and a relatively small number (13 blocks) are considered as being freefall.

Name	WedgeAnalysis_1:Composite_1
Total Blocks	207
Stable Blocks	194
Unstable Blocks	0
Free Fall Blocks	13
Maximum block weight [tonne]	0.45713175
Average block weight [tonne]	0.01691218
Maximum block volume [m³]	0.16930806
Average block volume [m³]	0.0062637704
Maximum block height [m]	1.1499506
Average block height [m]	0.16655193
Maximum block width [m]	2.3506571
Average block width [m]	0.45804374
Maximum block surface area [m²]	2.6150814
Average block surface area [m²]	0.19214331
Maximum unstable block weight [tonne]	0
Average unstable block weight [tonne]	0
Maximum freefall block weight [tonne]	0.21148027
Average freefall block weight [tonne]	0.01665191
FracMan 7.50.1	
Version 750.1 (Build 2015.06.30)	
Wednesday, July 08, 2015	

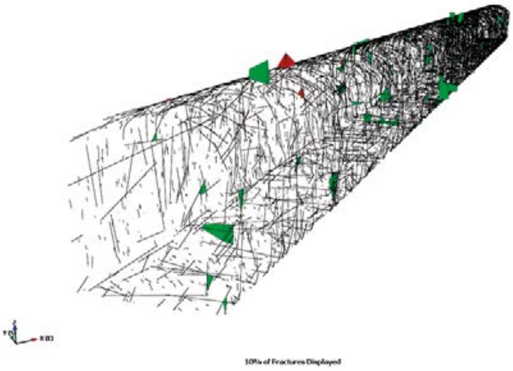

Tunnel Orientation: N233
Fracture Domain: FFM01
Fracture Sets Model: TCM
Fracture Sets: NW, NS, NW, and SH

Figure 3-10. *Kinematic stability statistics obtained from single realisation of TCM DFN for Domain FFM01.*

It is evident in Figure 3-10 that for the analysis of a 100 metre length of N233 aligned deposition tunnel located in the FFM01 domain, that most of the rock blocks identified are relatively small. Over the 100 metre interval assessed, a total of 207 blocks are identified, and these blocks have an average block weight of approximately 17 kg (or an average volume of 0.006 m^3).

The levels of block stability and block geometries are considered in more detail in the following sections.

Block Failure Indicator

In addition to the summary statistics provided in Figure 3-10, the following Figure 3-11 provides where the rock blocks identified are located on the tunnel geometry. It is evident that the (green coloured) kinematically stable blocks are founded in both the crown and sidewalls of the tunnel, whereas it is seen that the fewer unstable (freefall) blocks are solely confined to the crown roof location.

Block Factor of Safety

In addition to the block failure indicators shown in Figure 3-11, the following Figure 3-12 provides a schematic of the block factor of safety values and locations for the baseline analysis case for FFM01.

It is seen in Figure 3-12 that the factor of safety values reflect the failure mode indicators seen previously. The blocks that are considered freefall have a factor of safety equal to zero. In addition, it is also evident that most of the other blocks (coloured white) exhibit factors of safety that are greater than 5.0 – so are therefore considered stable.

There are a very small number of blocks identified that exhibit a factor of safety in the crucial 1.0 to 2.0 range. These few blocks are seen to be located in the crown of the tunnel.

Block Volumes

In addition to assessing block stability by way of the calculated factor of safety, an additional results obtained from the analyses are the evaluation of the geometry of the blocks intersecting with the tunnel. The volumes of the intersecting block and the associated distribution of the block volumes is provided in Figure 3-13.

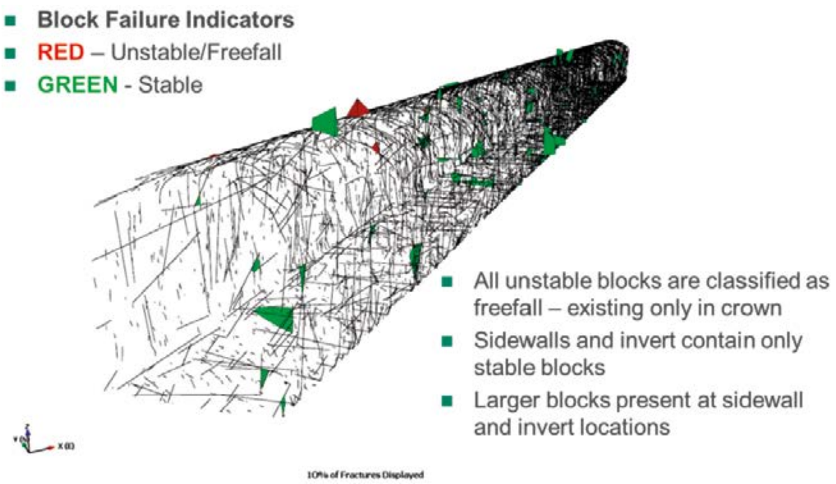

Figure 3-11. *Kinematic Stability Failure Indicator obtained from single realisation of TCM DFN for Domain FFM01.*

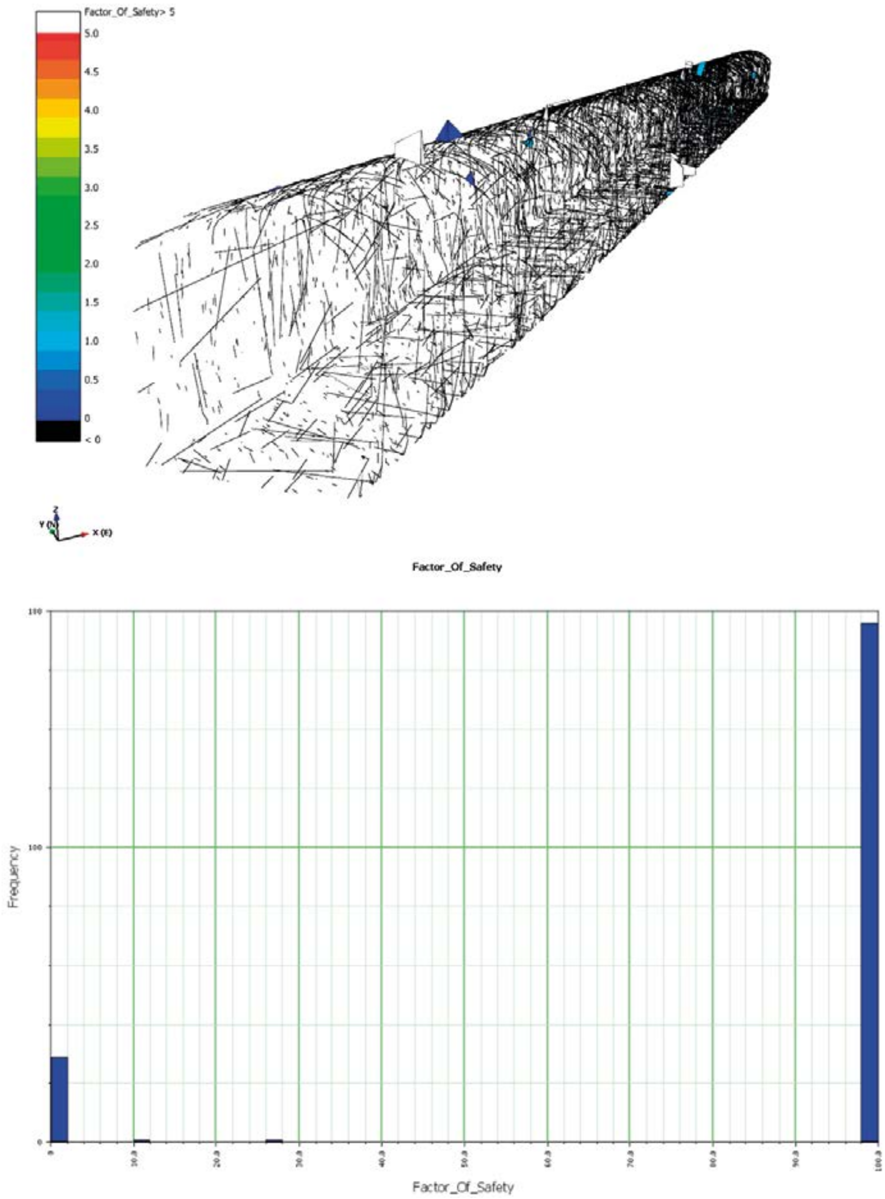

Figure 3-12. *Kinematic Stability Factor of Safety obtained from single realisation of TCM DFN for Domain FFM01.*

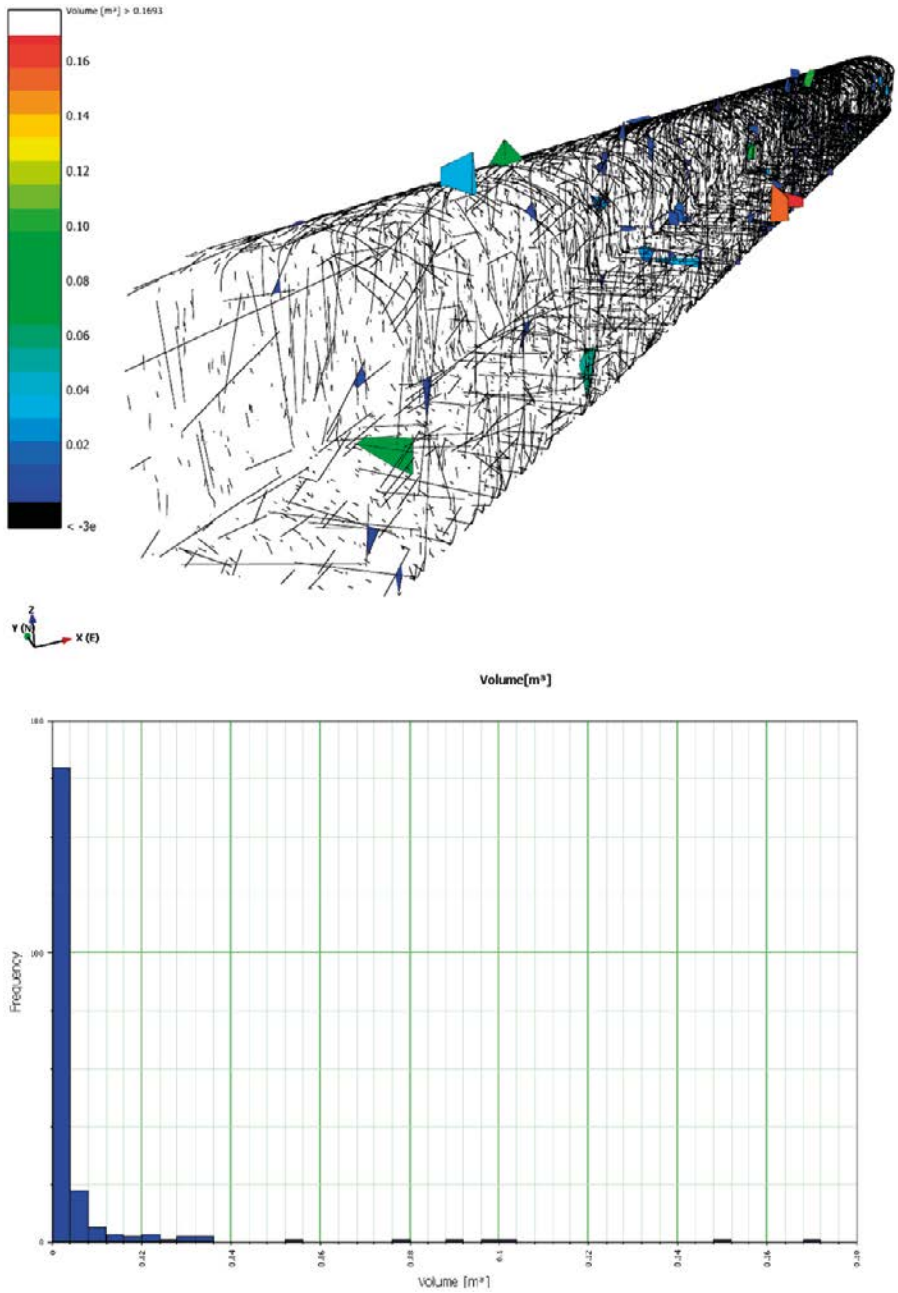

Figure 3-13. *Block volumes obtained from single realisation of TCM DFN for Domain FFM01.*

It is evident from Figure 3-13 that most of the block volumes identified at the tunnel faces are relatively small in size, with typical volume of < 0.020 m^3 (soccer football size). In addition, it is identified that the largest block size present is 0.17 m^3 and the block is located in the tunnel sidewall.

Block Weights

Providing similar understanding to the block volume results provided in Figure 3-13, the following Figure 3-14 provides the block weight predictions.

Following the volume results seen previously, it is evident that the largest block is approximately 460 kg in weight, and is positioned in the sidewall location. It is seen that the very largest blocks identified all exist in the sidewalls, there are however a number of blocks weighing 100 to 300 kg existing in the tunnel crown and invert locations. Most blocks identified though are small in volume and weight and typically less than 20 kg.

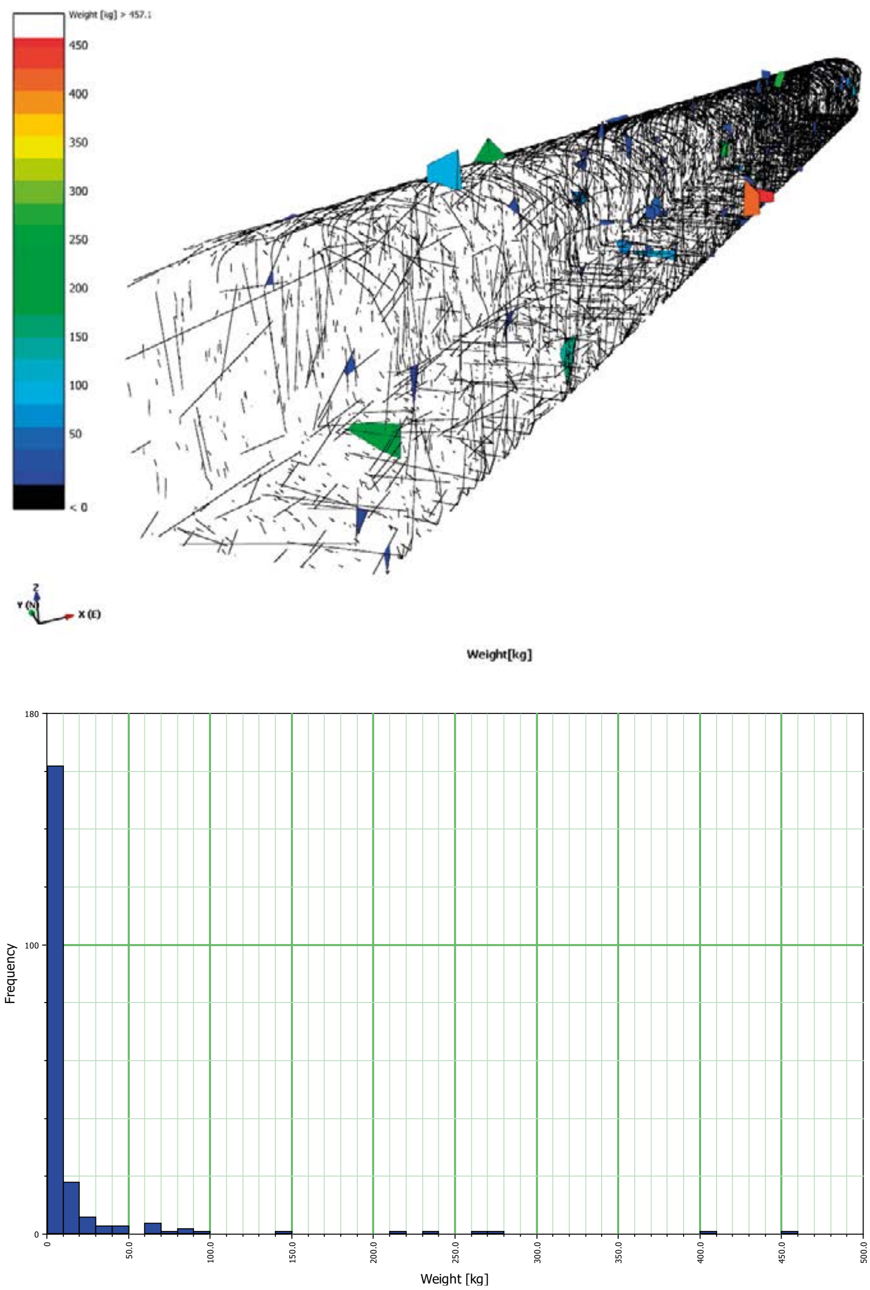

Figure 3-14. *Block Weights obtained from single realisation of TCM DFN for Domain FFM01.*

3.4 FFM06 – Baseline Kinematic Stability Analysis

The results of the baseline rock wedge analysis for the domain FFM06 are presented in the following sections. The sections presented consider the following items:

- Model Configuration.
- Tunnel Fracture Intersection Analysis; and
- Tunnel Kinematic Stability Analysis.

3.4.1 Model Configuration

The global fracture sets included in the developed model are detailed below. The tunnel orientation considered in this baseline analysis is N233 only – no alternative tunnel orientations have been considered.

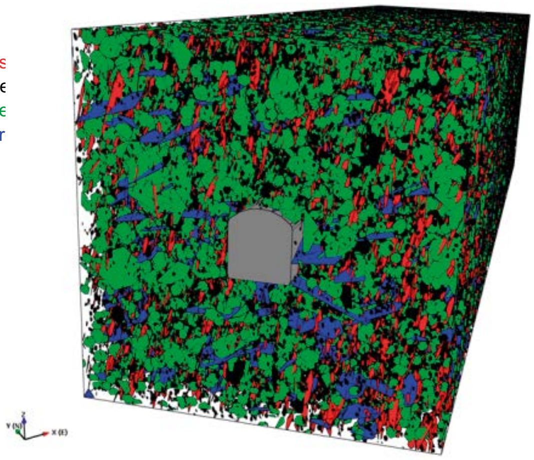

Figure 3-15. Local DFN Model of Domain FFM06.

Using Figure 3-16 the orientations of the four fracture sets have been evaluated identifying the natural fractures that intersect the vertically deviated borehole included in the model. A contoured stereoplot describing the intersecting fracture orientation is shown. It is seen that the fracture orientations of the intersecting fractures relate appropriately to the orientation parameters specified.

It is seen in Figure 3-16 that there exists a dominant fracture set intersected by the borehole, this relates to the NE orientated set.

In addition to the fracture geometrical data, the following Table 3-4 provides the strength properties assigned to the created fractures. Analyses for domain FFM01 and FFM06 have utilised the same fracture frictional strength properties.

Table 3-4. Coulomb Strength Properties Assigned to the Fracture Sets in Rock Domain FFM06.

Surface Strength Property	Average	St Dev	Minimum	Maximum
Coulomb Friction, Phi [degrees]	36.60	2.90	29.30	42.00
Coulomb Cohesion [MPa]	0.80	0.30	0.20	1.30

3.4.2 Tunnel Kinematic Stability Analysis

The primary analysis undertaken considers the kinematic stability of the rock blocks identified around the tunnel geometry. Figure 3-17 provides the rock wedge kinematic stability statistics obtained from the single realisation of the FM006 DFN for Forsmark. It is evident in Figure 3-17 that the basic number of rock blocks formed for domain FFM06 is effectively double that seen previously for domain FFM01. Despite the large increase in the block count, the vast majority of blocks formed remain kinematically stable. There still exists a relatively small number (= 16) of blocks that are classified as being freefall. Similarly to the FFM01 results seen previously, there are no other kinematically unstable blocks detected.

In terms of block sizing and dimension, it is seen that the blocks formed for domain FFM06 are smaller than those encountered for domain FFM01. For domain FFM06 the average block weight is approximately 4.3 kg, this in turn, corresponds to an average block volume of 0.001 m^3. The maximum block weight and volume encountered in this realisation are 412 kg and 0.15 m^3 respectively.

Block Failure Indicator

In addition to the basic statistical results provided in Figure 3-17, the following Figure 3-18 considers where the rock blocks identified are located on the tunnel geometry and their associated failure mode. It is again evident that the (green coloured) kinematically stable blocks are found on both the crown and sidewalls of the tunnel, whereas it is seen that the fewer unstable (freefall) blocks are largely confined to the crown or tunnel roof location.

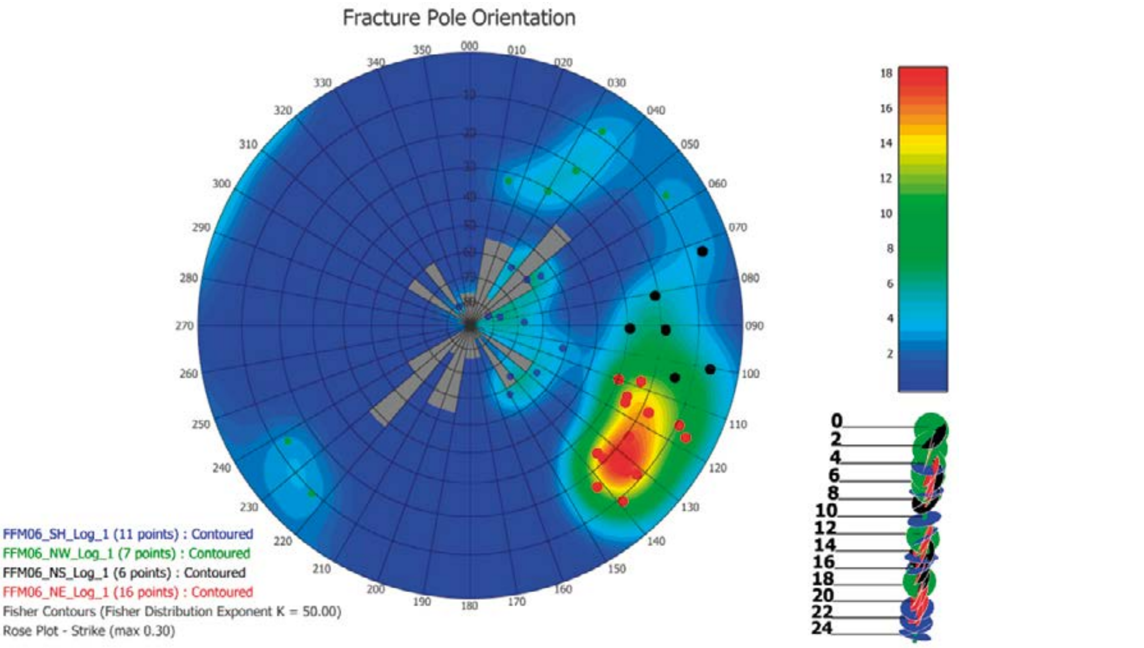

***Figure 3-16.** Contoured Stereoplot of the Fracture Set Intersections for the Domain FFM06 Model Borehole.*

Name	WedgeAnalysis_1:Composite_1
Total Blocks	438
Stable Blocks	422
Unstable Blocks	0
Free Fall Blocks	16
Maximum block weight [tonne]	0.41240787
Average block weight [tonne]	0.0043563445
Maximum block volume [m^3]	0.15274366
Average block volume [m^3]	0.0016134609
Maximum block height [m]	0.8423596
Average block height [m]	0.11853924
Maximum block width [m]	6.0967351
Average block width [m]	0.3246387
Maximum block surface area [m^2]	3.3213454
Average block surface area [m^2]	0.078028017
Maximum unstable block weight [tonne]	0
Average unstable block weight [tonne]	0
Maximum freefall block weight [tonne]	0.0037203008
Average freefall block weight [tonne]	0.00041032776
FracMan 7.50.1	
Version 750.1 (Build 2015.06.30)	
Wednesday, July 08, 2015	

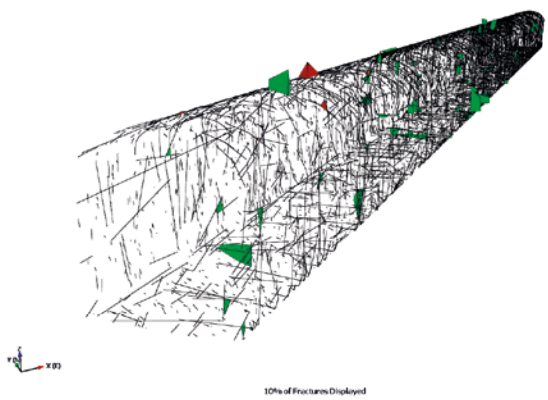

Tunnel Orientation: N233
Fracture Domain: FFM06
Fracture Sets Model: TCM
Fracture Sets: NW, NS, NW, and SH

***Figure 3-17.** Kinematic Stability Statistics Obtained From Single Realisation Of TCM DFN For Domain FFM06.*

Factor of Safety

In addition to the block failure indicators shown in Figure 3-18, the following Figure 3-19 provides a schematic of the block factor of safety values and locations for the baseline case for FFM06.

It is evident from Figure 3-19 that similarly to the results from domain FFM01, the factors of safety calculated for the FFM06 domain indicate that besides a small number of freefall blocks, most of the identified blocks are kinematically stable. It is evident that the freefall blocks are confined to the tunnel crown location.

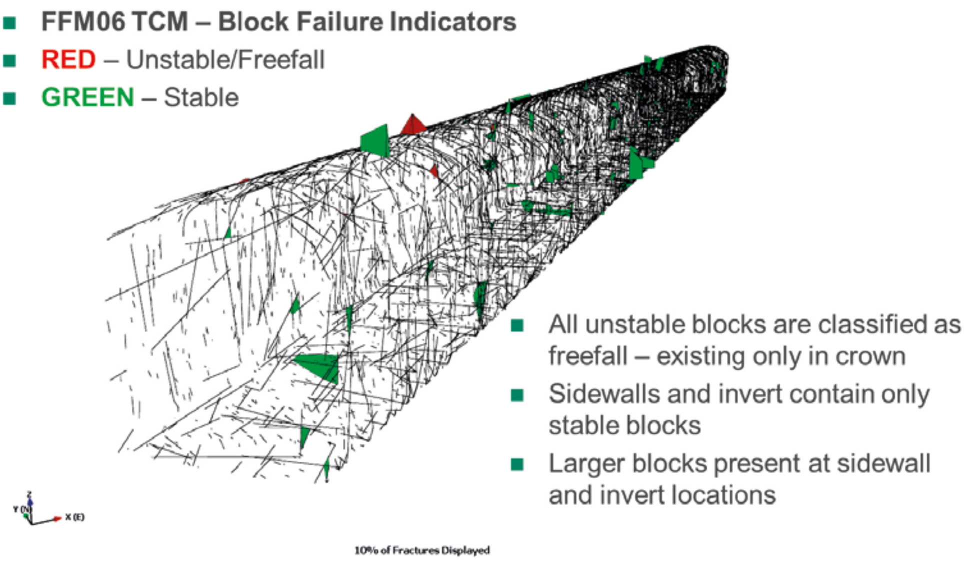

Figure 3-18. Kinematic stability failure indicator obtained from single realisation of TCM DFN for Domain FFM06.

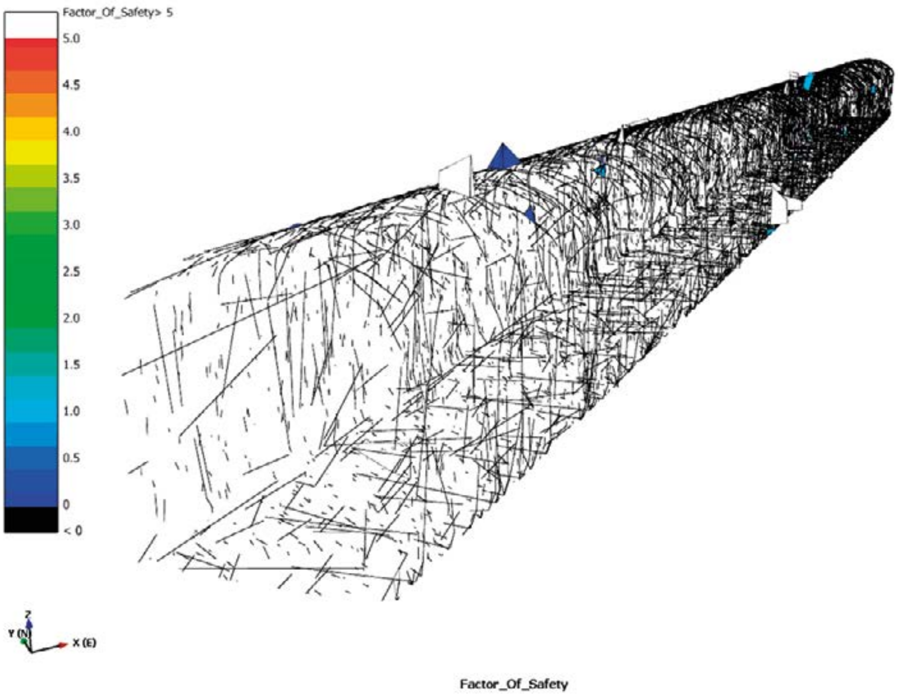

Figure 3-19. Kinematic stability factor of safety obtained from single realisation of TCM DFN For Domain FFM06.

Block Volumes

In addition to the calculated factor of safety, the following Figure 3-20 details the block volumes realised from the single realisation of the FM006 fracture model. Similarly to that observed for FFM01, it is seen that most of the rock blocks at the tunnel face are small, with volumes typically less than 0.02 m^3. In addition, the largest block seen is located in the tunnel sidewall with a volume of 0.17 m^3.

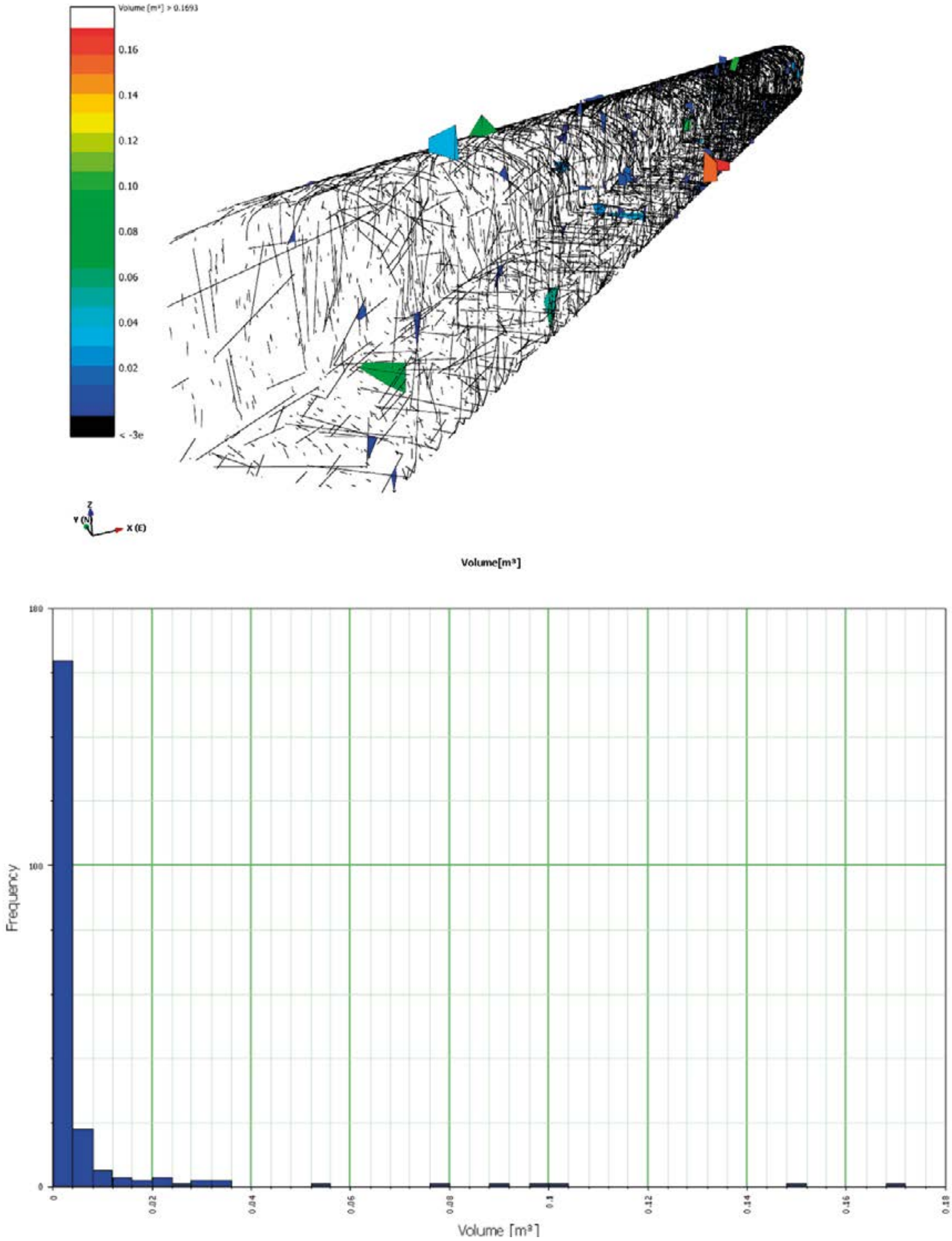

***Figure 3-20.** Block volumes obtained from single realisation of TCM DFN for Domain FFM06.*

Block Weights

Providing similar understanding to the block volume results provided in Figure 3-20, the following Figure 3-21 provides the block weight predictions for FFM06. Similarly to block volumes it is seen the largest block size in in the sidewall.

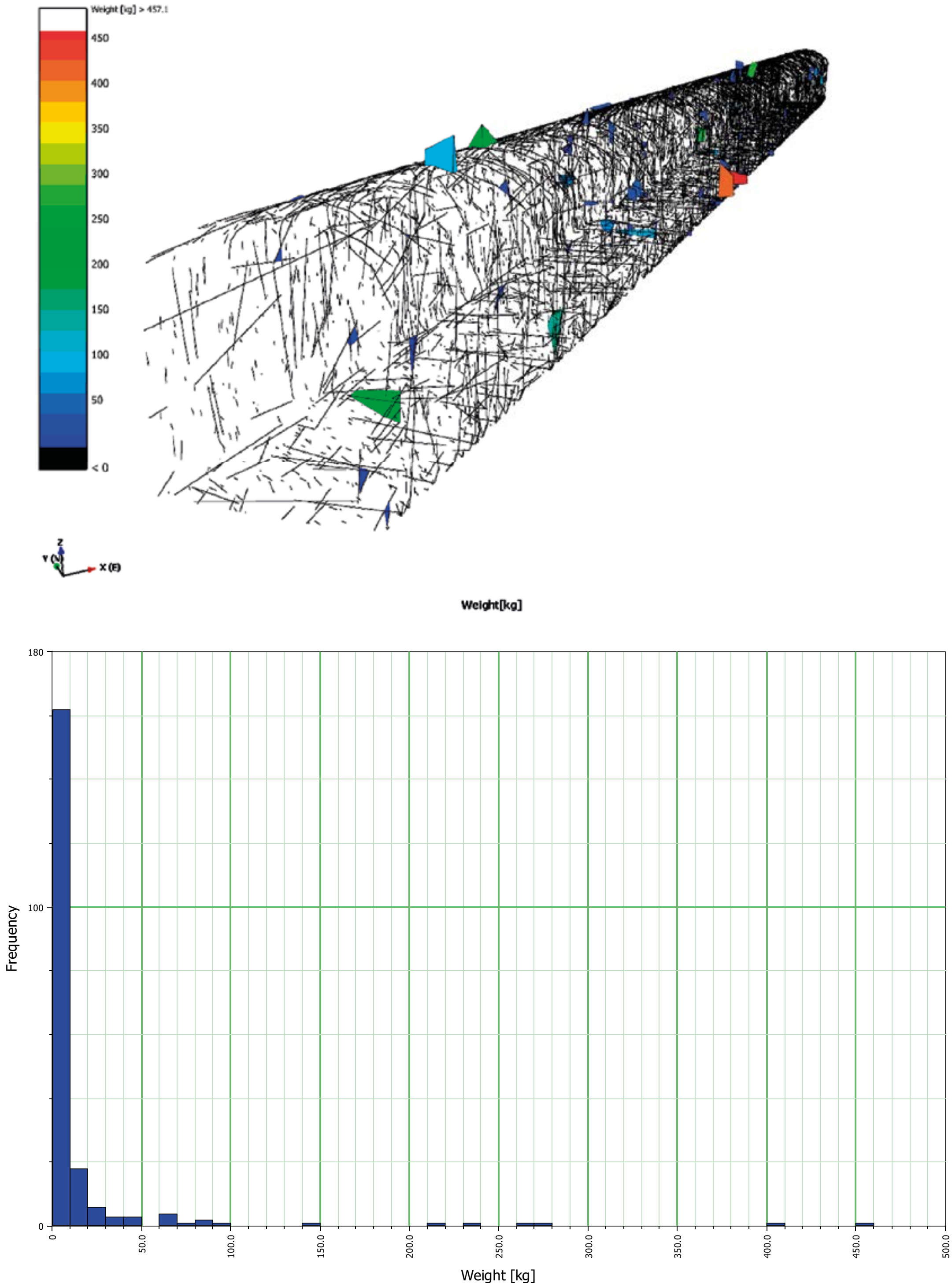

***Figure 3-21.** Block weights obtained from single realisation of TCM DFN for Domain FFM06.*

3.5 Summary Comparison Block Stability for FFM01 and FFM06

The following Table 3-5 provides a general comparison of the rock block attributes predicted for the 100 metre tunnel profile when positioned in domains FFM01 and FFM06 respectively. It is seen that the number of rock blocks formed for domain FFM06 is effectively double those formed for domain FFM01. From this, comparison of the block volume shows that in domain FFM06 the average block volumes are approximately three times smaller than those seen in domain FFM01. In terms of maximum block size, it is seen that the two domains have similar values at approximately 0.169 m^3.

Table 3-5. Comparison of N233 Tunnel Rock Block Attributes for Domain FFM01 and FFM06.

Rock Block Property	Domain FFM01	Domain FFM06
Number(#) of Blocks / 100 metre	207	438
# of Unstable Blocks / 100 metre	0	0
# of Freefall Blocks / 100 metre	13	16
# of Stable Blocks / 100 metre	197	422
Block Weight (min, max, ave)	n/a, 457 kg, 16.90 kg	n/a, 412 kg, 4.35 kg
Block Volume (min, max, ave)	n/a, 0.169 m^3, 0.006 m^3	n/a, 0.153 m^3, 0.002 m^3

3.6 Probabilistic Assessment Approach

The previous Sections 3.3 to 3.5 considered the basic results obtained from single realisations of the TCM based fracture models for domains FFM01 and FFM06. Section 3.6 details an approach which has been used to provide automated import and analysis of multiple kinematic stability analysis results to allow presentation of probabilistic based distributions collated from multiple realisations.

3.6.1 Monte Carlo Realisation Analysis

The use of the Monte Carlo approach allows the generation and analysis of multiple versions of stochastic fracture sets in order to create a large sample size. This in turn permits the assessment of a likelihood of a range of outcomes when the realisation results are considered. A simplified workflow of the Monte Carlo analysis process is provided in Figure 3-22.

It is seen in Figure 3-22 that the Monte Carlo process for the current project involves generations of the required fracture sets followed by undertaking of the kinematic stability analysis. This is then followed by accrual of the necessary analysis statistics and the deletion of the fracture sets. The loop then repeats to provide the required number of user specified realisations.

Implementation of the outline workflow detailed in Figure 3-22 has been implemented in FracMan using currently available macro language functionality. The use of the macro language approach is primarily to allow inclusion of the tunnel formation (clipping) operation from inside the DFN fracture network block. The macro language employed in the executed macro files is detailed in Figure 3-23. It is seen that the main steps detailed in Figure 3-23 reflect those shown in the outline workflow of Figure 3-22.

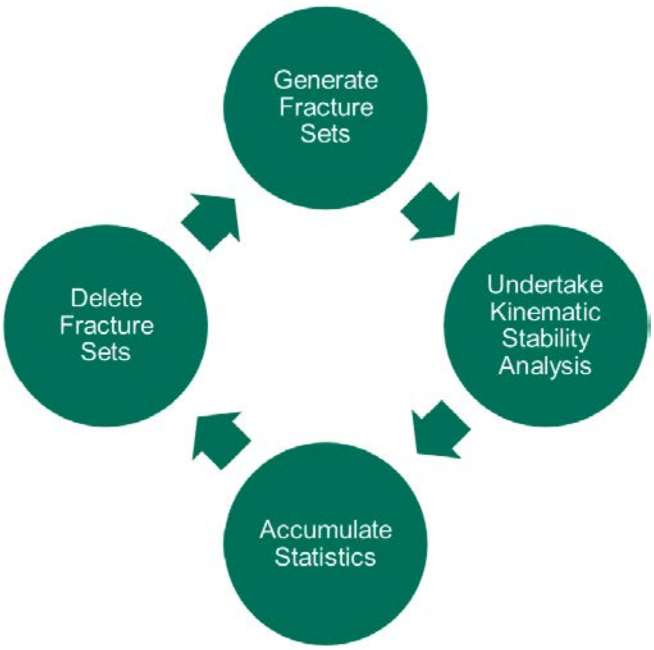

Figure 3-22. *Workflow of the Monte Carlo Analysis.*

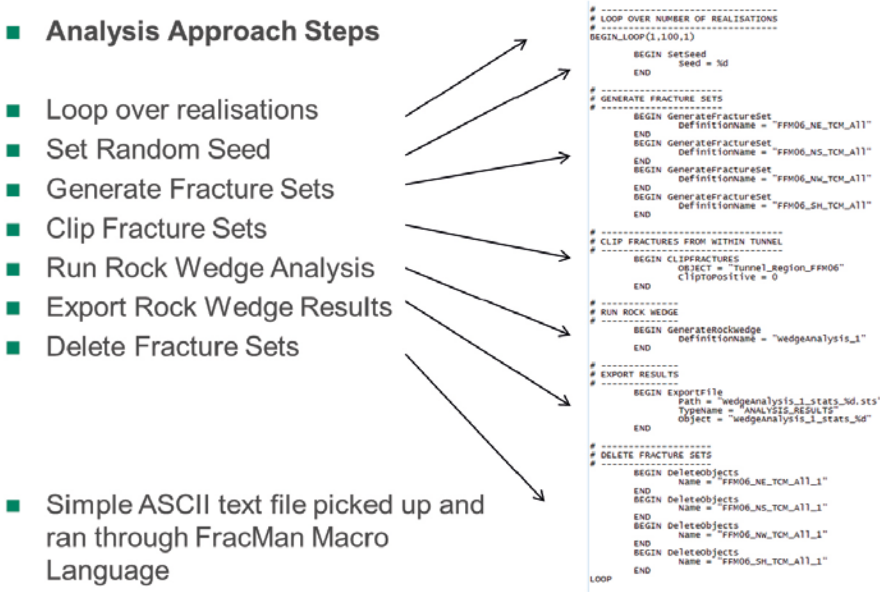

Figure 3-23. *Macro language implementation of the Monte Carlo based analysis.*

3.6.2 Automated Rock Wedge Statistical Analysis

To provide support to the Monte Carlo results produced by each of the realisations executed by FracMan, an external Excel based tool has been tailored to provide automatic collation and analysis of the combined set of realisation results from each configuration run. Based upon the collated results the tool calculates a results summary of the main geometrical variables and also provides histograms and cumulative based curves of the primary measures. The primary measures include:

The described tool is based on Microsoft Excel 2010 and makes use of the embedded VBA programming language. The tool includes a front page which presents the main results graphs, as well as a number of secondary analysis sheets in which the required calculations are processed. The main components of the interface and analysis tool are:

- **“Front Page”** – is the analysis sheet that controls the basic user functions, and provides linkages to the main analysis pages and factor of safety.
- **“Results Data”** – is the analysis sheet that controls the import process and collation of the statistical kinematic results from each of the FracMan realisations.
- **“Results Summary”** – is the analysis sheet that controls the creation of all of the available histograms and charts available from the imported data; and
- **“Results Factor of Safety”** – is the analysis sheet where the important Factor of Safety data is reported.

Further details on each of the listed components are provided in in the following identified subsections.

“Front Page” Analysis Sheet

It is seen in Figure 3-24 that the main results display is centrally positioned on the front page, and consists of nine histogram and cumulative based charts. These charts report the breakdown between state, unstable, and freefall blocks, block geometry (volume, surface area, height and width), block weight (freefall, stable and unstable), and block Factor of Safety.

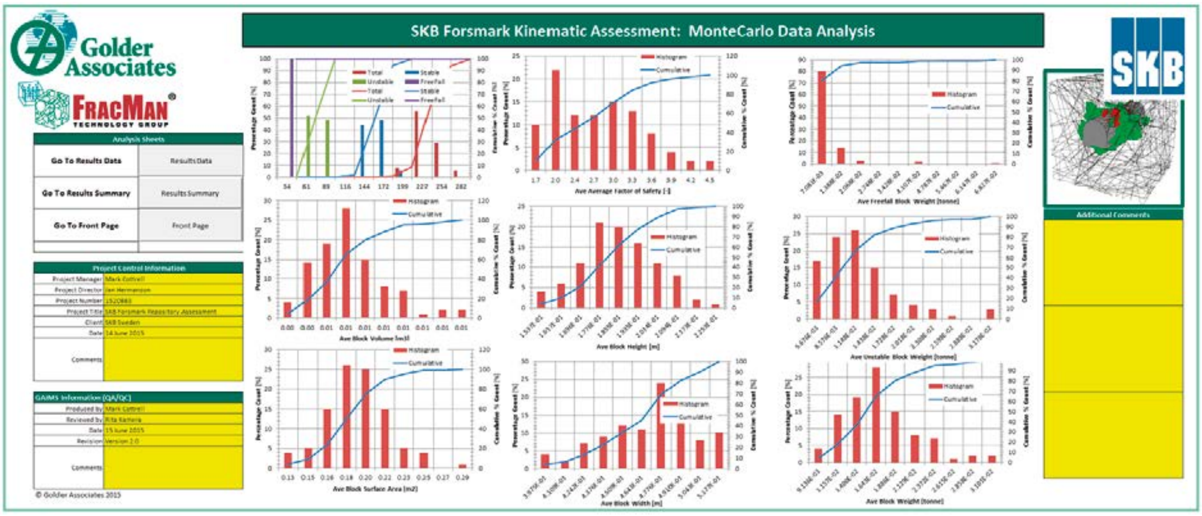

***Figure 3-24.** Front Page of Monte Carlo Results Collation and Post Processing User Interface.*

On the left hand side of the interface, in Figure 3-24, the user has the option of going to the Results Data and Results Summary calculation pages. To the lower left and right hand side of the Front Page there are several boxes filled yellow which provide opportunity for the user to provide notes style documentation.

"Results Data" Analysis Sheet

The Results Data sheet allows the specification and import of the main statistical data that is reported from each of the FracMan kinematic stability analyses. The sheet provides collation of all data imported and collation of baseline statistics (e.g. minimum, maximum, average, and deviation) for each of the analysis variables brought in from FracMan. It is on this sheet that the user is able to specify the path and basic analysis name of the result files that are then automatically imported. See Figure 3-25.

"Results Summary" Analysis Sheet

The Results Summary page, shown in Figure 3-26, provides reporting of histogram and cumulative based charts for the rock block measures that are calculated during the import and processing of the FracMan output.

"Results Factor of Safety" Analysis Sheet

The Results Factor of Safety page, shown in Figure 3-27, provides reporting of histogram and cumulative factor of safety data. For this result variable, the user is able to manually specify the interval bin sizes used by the histogram reporting.

3.7 Probabilistic Analyses and Results

A total of seven analyses have been undertaken making use of the Monte Carlo based approach available from FracMan. A total of 50 new realisations are performed for each of the 100 metre long tunnel configurations detailed in Table 3-6. A large number of realisations is required to allow creation of relatively smooth probabilistic type curves using the automated results processing facility detailed in Section 3.6.2.

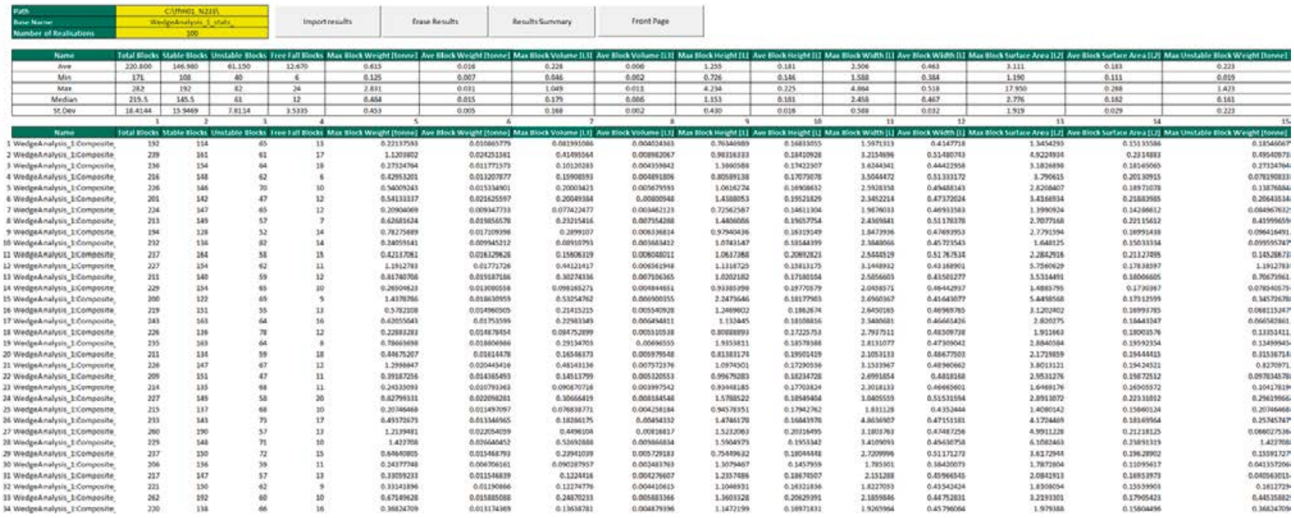

Figure 3-25. Monte Carlo realisation results data read and stored from each output results file.

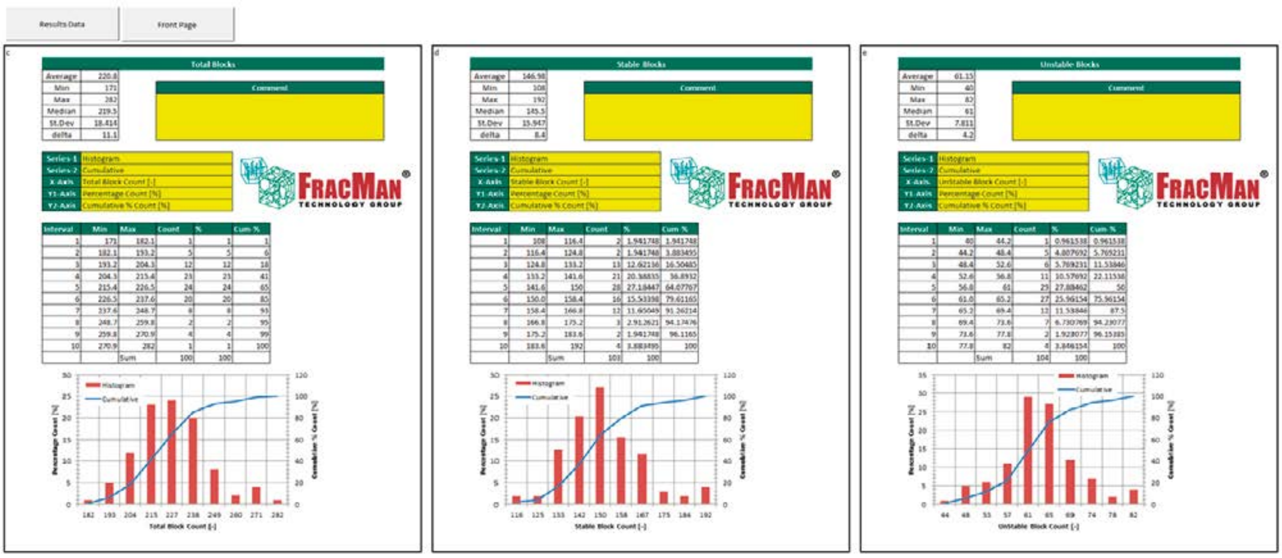

Figure 3-26. Monte Carlo realisation results charts created from statistics of combined output results files.

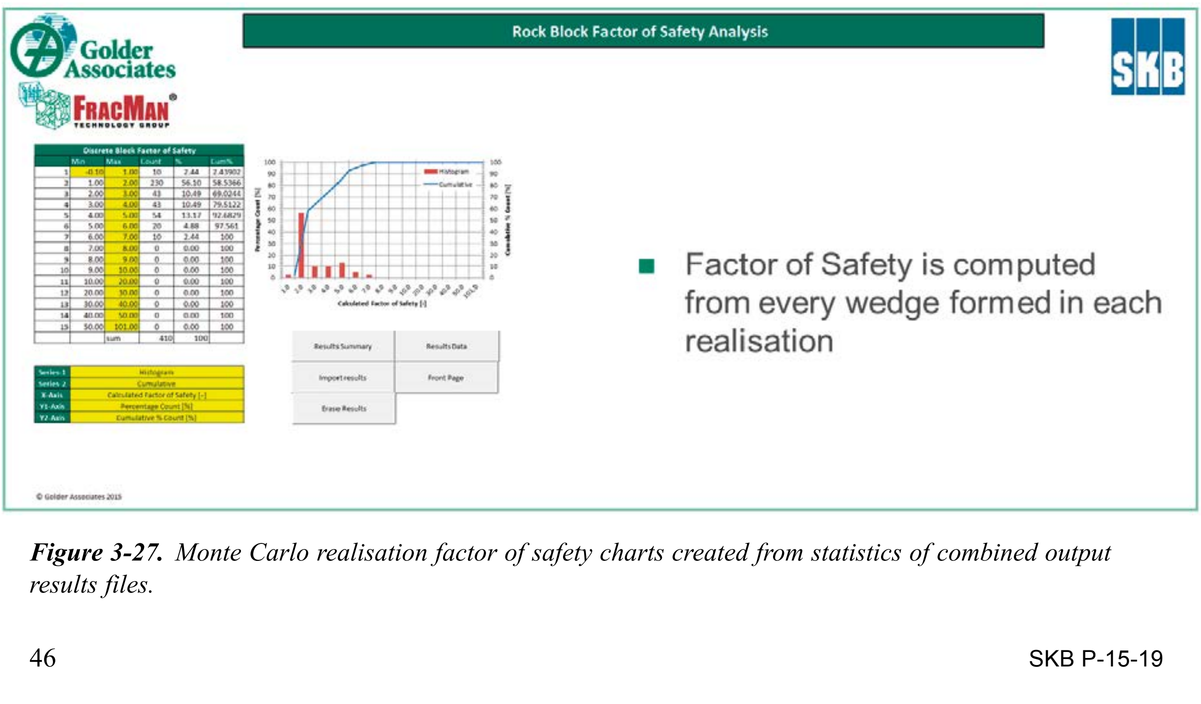

Figure 3-27. Monte Carlo realisation factor of safety charts created from statistics of combined output results files.

Table 3-6. Probabilistic Analysis Configurations Investigated.

Case	Domain	Fracture Data				Tunnel Direction	Fracture Strength	Pore Level
		Type	Orientation	Intensity	Size			
I	FFM01	TCM	TCM	TCM	TCM	N233	Open	0 MPa
II	FFM01	TCM	TCM	TCM	TCM	N143	Open	0 MPa
III	FFM06	TCM	TCM	TCM	TCM	N233	Open	0 MPa
IV	FFM06	TCM	TCM	TCM	TCM	N143	Open	0 MPa
V	FFM01	TCM	TCM	TCM	TCM	N233	Open	Hydro
VI	FFM06	TCM	TCM	TCM	TCM	N233	Open	Hydro
VII	FFM01	TCM	TCM	TCM	TCM	N233	Reduced	0 MPa

The configurations detailed in Table 3-6 have been undertaken since they consider identified models drivers including fracture domains and fracture strength properties, as well as important tunnel orientation and pore water loading conditions. The following sections present summaries of the results obtained from the specified realisations of each configuration, and consider block counts, block volumes and dimensions, block weights, and factor of safety histograms.

3.7.1 Results: Configuration-I

The initial configuration analysed, using the 50 realisation Monte Carlo analysis approach, considers the properties detailed in Table 3-7.

Table 3-7. Analysis Details – Configuration-I.

Configuration Component	Configuration Description
Rock Domain	FFM01
Fracture Model Description	TCM global fracture sets, TCM properties for orientation, size and intensity
Tunnel Orientation	N233
Friction Properties	Properties for Open fractures uniformly assigned
Pore Pressure Conditions	No fluid pressure included. 0 MPa

Block Count and Factor of Safety

The block count and factor of safety result charts from the implemented realisations are shown in Figure 3-28. The resulting Block Count results are provided in Figure 3-28 a, here it is seen that the 50 realisations of the 100 metre long tunnel typically yields approximately 250 rock blocks on the tunnel perimeter (i.e. crown, invert and sidewalls). Of these, it is seen that the number of freefall rock blocks is relatively low and accounts for about 8 % of the total blocks formed. Inspection of the data shows that an average of 16 freefall blocks are formed, with a total range of 8 to 29 blocks typical from the realisation set. Of the 250 blocks typically formed, it is seen that only a very small number of blocks are considered unstable. The number of unstable blocks formed typically ranges 0 to 2, equating to an average of 0.03 unstable blocks per realisation. Based on the very small numbers of freefall and unstable blocks formed during the realisations, it is evident that a large percentage (92 %) of the blocks formed are considered kinematically stable. An average of 225 stable blocks are identified as forming over the 100 metre tunnel length, with a range of 130 to 320 stable blocks per realisation.

The Factor of Safety results are provided in Figure 3-28 b, it is seen that approximately 6–7 % of blocks are marked as being freefall or unstable. Approximately 4 % of stable block exist but with a very moderate (< 1.50) factor of safety. Reflecting this, it is evident over 90 % of the blocks formed have very large factors of safety (FOS > 100), indicating they are both geometrically and kinematically stable.

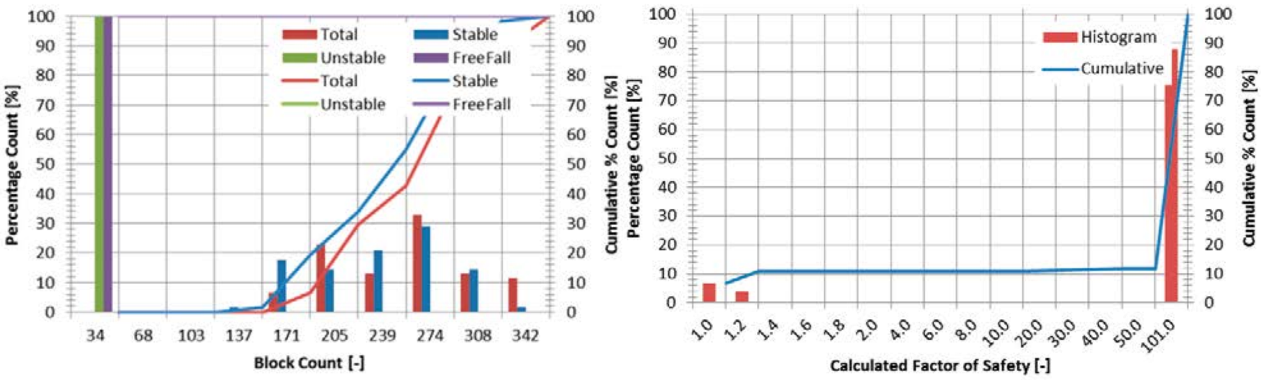

***Figure 3-28.** Monte Carlo Results for Configuration-I, Showing a) Block Count Data, and b) Factor of Safety.*

Block Volumes & Dimensions

In addition to the factor of safety data, the set of (50) realisations also provides detailed information concerning the block geometry of the rock blocks formed, see Figure 3-29. The results provide indication of the levels of variability in terms of block sizing seen from the multiple realisations performed.

From the realisations performed, it is seen that for this configuration approximately 90 % of the rock blocks formed have a volume of 0.01 m^3 or less. In addition, it is seen that the individual block dimensions tend to vary between 0.15 to 0.20 metres for height, and vary between 0.40 to 0.60 metres for width.

Block Weights

In addition to the block volumes and dimensions detailed in the previous section and Figure 3-29, the following Figure 3-30 provides details concerning the distribution of blocks weights predicted from the fifty realisations.

It is evident in Figure 3-30 a the histogram of the average block weight suggests most of the blocks identified are relatively small, in the 10 to 40 kg range. It is seen that approximately 60 % of the rock blocks identified reside in the 18 to 23 kg weight range. In terms of unstable block weight, Figure 3-30 b provides the distribution of unstable block weights, here it is seen that almost 100 % of the blocks exist in the <20 kg category, there a very small number of unstable blocks >150 kg in weight that exist. There appear to be no unstable blocks existing in the in-between 20 to 150 kg weight interval. Of the freefall blocks, it is evident in Figure 3-30 c that these blocks are small in weight compared to the overall block weight distribution, it is seen that nearly 90 % of the freefall blocks weigh typically less than 10 kg. In terms of most frequent, it is shown that over 50 % of the freefall blocks formed weigh less than 7 kg.

Summary and Conclusions

In terms of the salient features identified through this group of analyses, the following are seen:

- Approximately 6 % of blocks are considered freefall.
- Approximately 4 % of blocks are stable but with a low >1 FOS.
- Approximately 90 % of blocks exhibit high level of kinematic stability, FOS > 100; and
- Typical block weights are in the region of 20 kg.

3.7.2 Results: Configuration-II

The second configuration analysed considers the model properties detailed in Table 3-8, this configuration has the tunnel orientation changed to align to N143 compared to N233 for Configuration-I. All other properties remain as previously used.

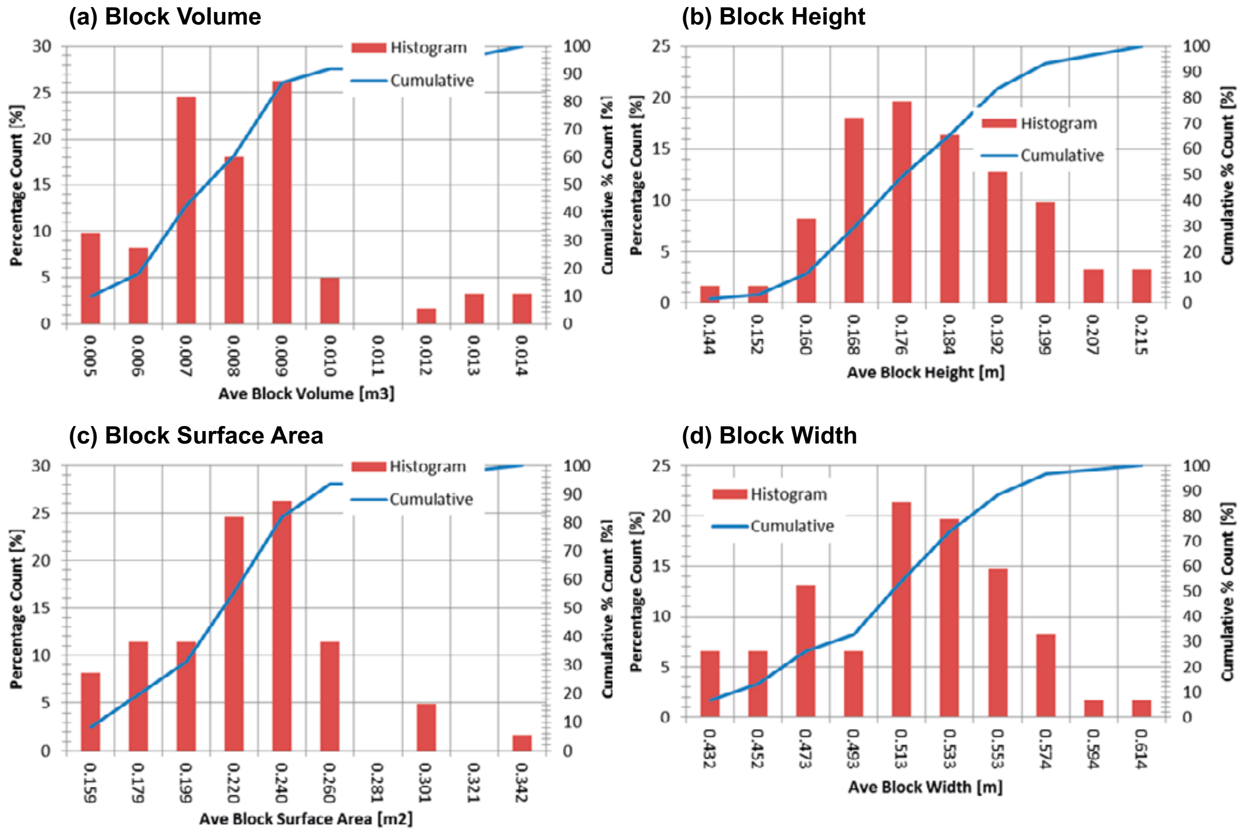

__Figure 3-29.__ Monte Carlo Results for Configuration-I, Showing a) Block Volume, b) Block Height, c) Block Area, and d) Block Width.

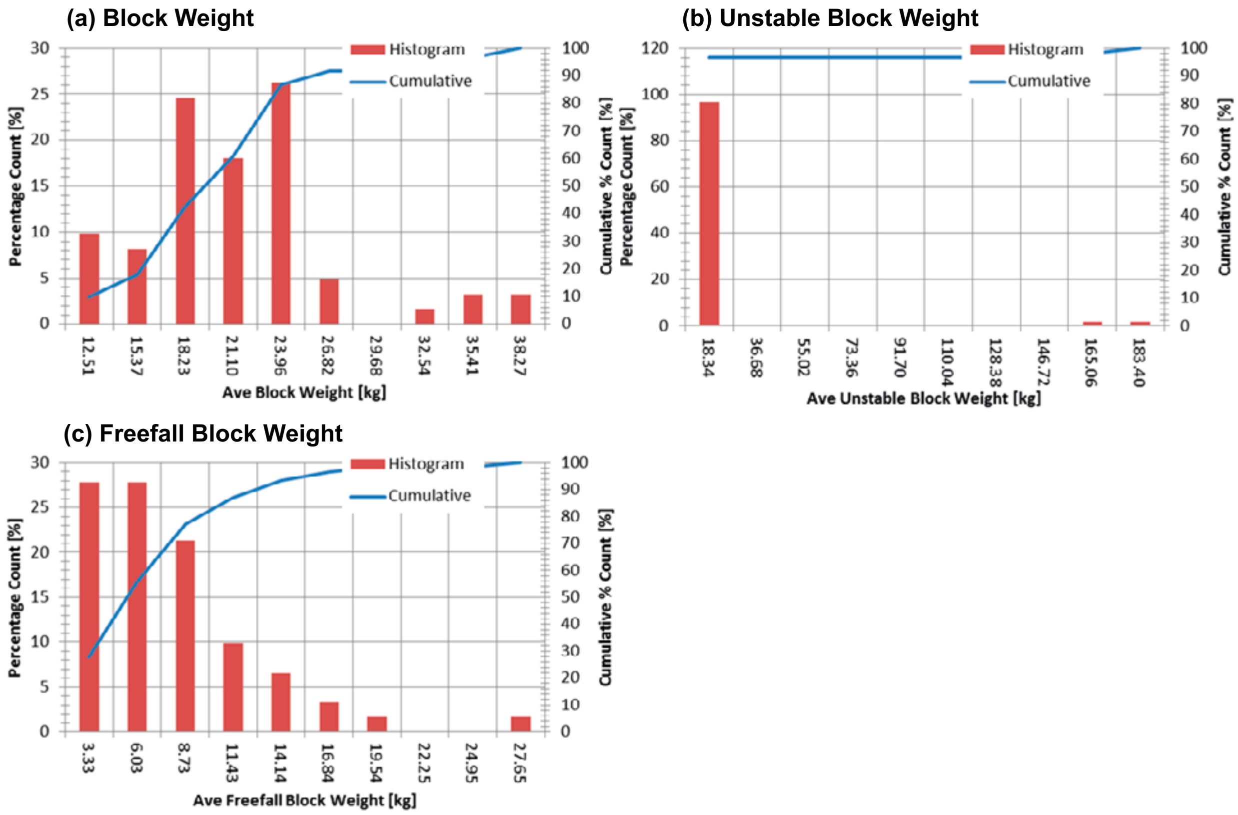

__Figure 3-30.__ Monte Carlo Results for Configuration-I, Showing a) Block Weight, b) Unstable Block Weight, and c) Freefall Block Weight.

Table 3-8. Analysis Details – Configuration II.

Configuration Component	Configuration Description
Rock Domain	FFM01
Fracture Model Description	TCM global fracture sets, TCM properties for orientation, size and intensity
Tunnel Orientation	N143
Friction Properties	Properties for Open fractures uniformly assigned
Pore Pressure Conditions	No fluid pressure included. 0 MPa

Block Count and Factor of Safety

The block count and factor of safety result charts from the implemented realisations are shown in Figure 3-31. It is seen in Figure 3-31 a that the block count distributions are very similar to those realised in Configuration-I, confirming that tunnel orientation has little influence on the block count data. It is again seen that the number of freefall blocks are low, typically < 15 blocks per 100 metre tunnel length. Similarly, the number of unstable blocks is very small, typically varying 0 to 1 per realisation (average 0.05), and the number of stables blocks is seen to be comparable to Configuration-I with approximately 250 blocks identified per realisation.

In terms of Factor of Safety, Figure 3-31 b provides a distribution that is very similar to that obtained previously. It is seen that nearly 90 % of the blocks formed are considered very stable, with approximately 12 % of the total blocks formed being either freefall/unstable and those with a relatively small factor of safety (i.e. FOS < 1.20).

Block Volumes and Dimensions

In addition to the block count and factor of safety distributions, the following Figure 3-32 (a–d) provides description of the distributions generated from the Monte Carlo probabilistic analysis of Configuration-II. Similarly to that derived for Configuration-I, the results for the second configuration exhibit similar attributes in terms of block size distribution. It is seen that nearly 90 % of formed rock blocks are 0.010 m^3 volume or less, the block height is seen to typically vary 0.17 to 0.22 metres, and the larger block width variable varies approximately 0.40 to 0.60 metres. All of these dimensions concur with those identified previously for Configuration-I.

Block Weights

In terms of block weights, the results obtained for Configuration-II indicate relatively small (<20 kg) sized blocks being most common for both the stable and unstable blocks. See Figure 3-33.

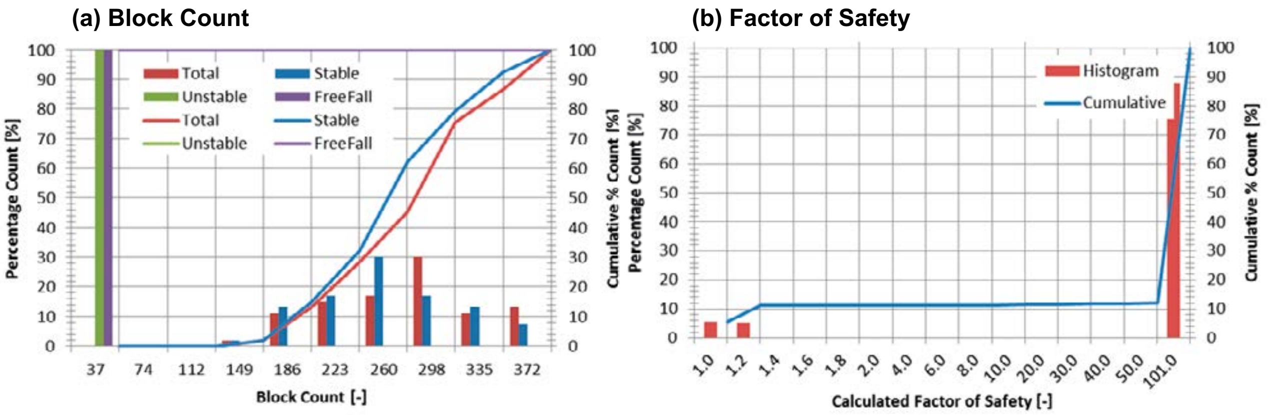

Figure 3-31. Monte Carlo Results for Configuration-II, Showing a) Block Count Data, and b) Factor of Safety.

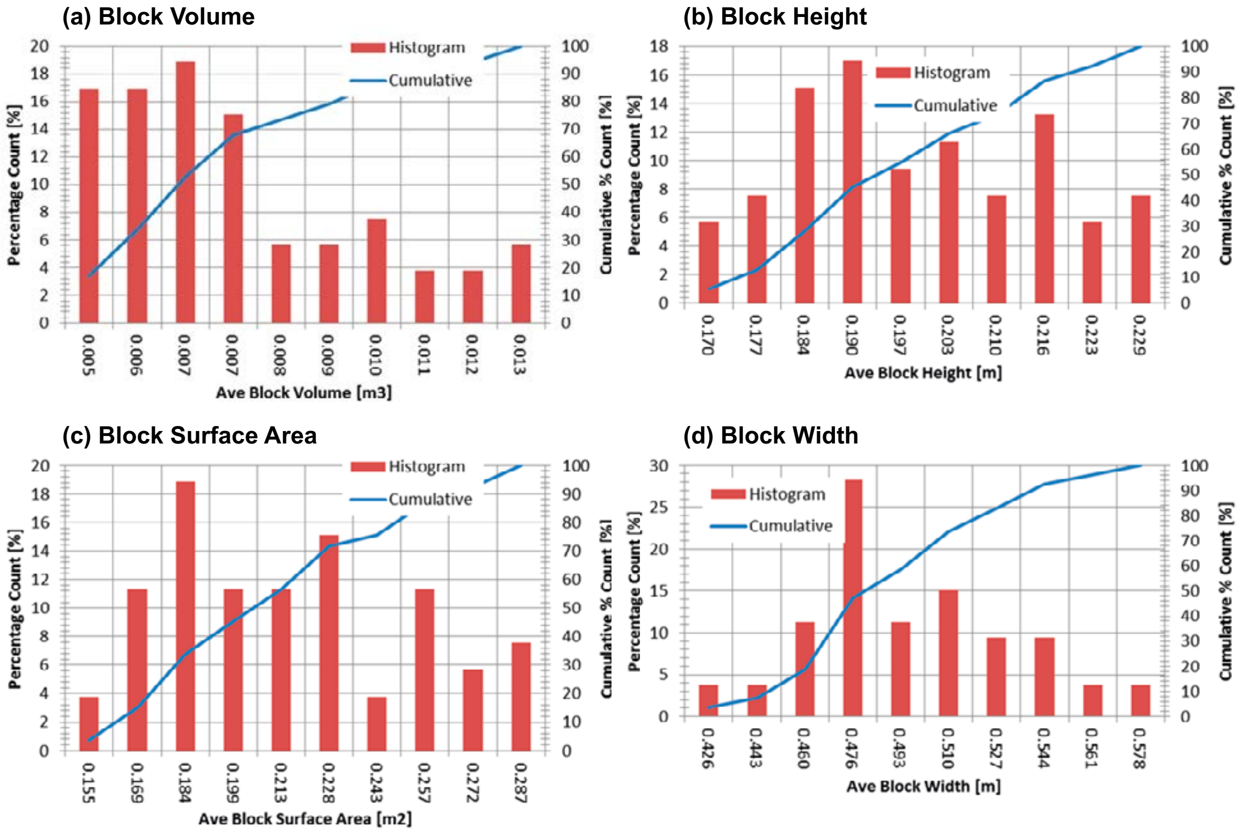

Figure 3-32. *Monte Carlo Results for Configuration-II, Showing a) Block Volume, b) Block Height, c) Block Surface Area, and d) Block Width.*

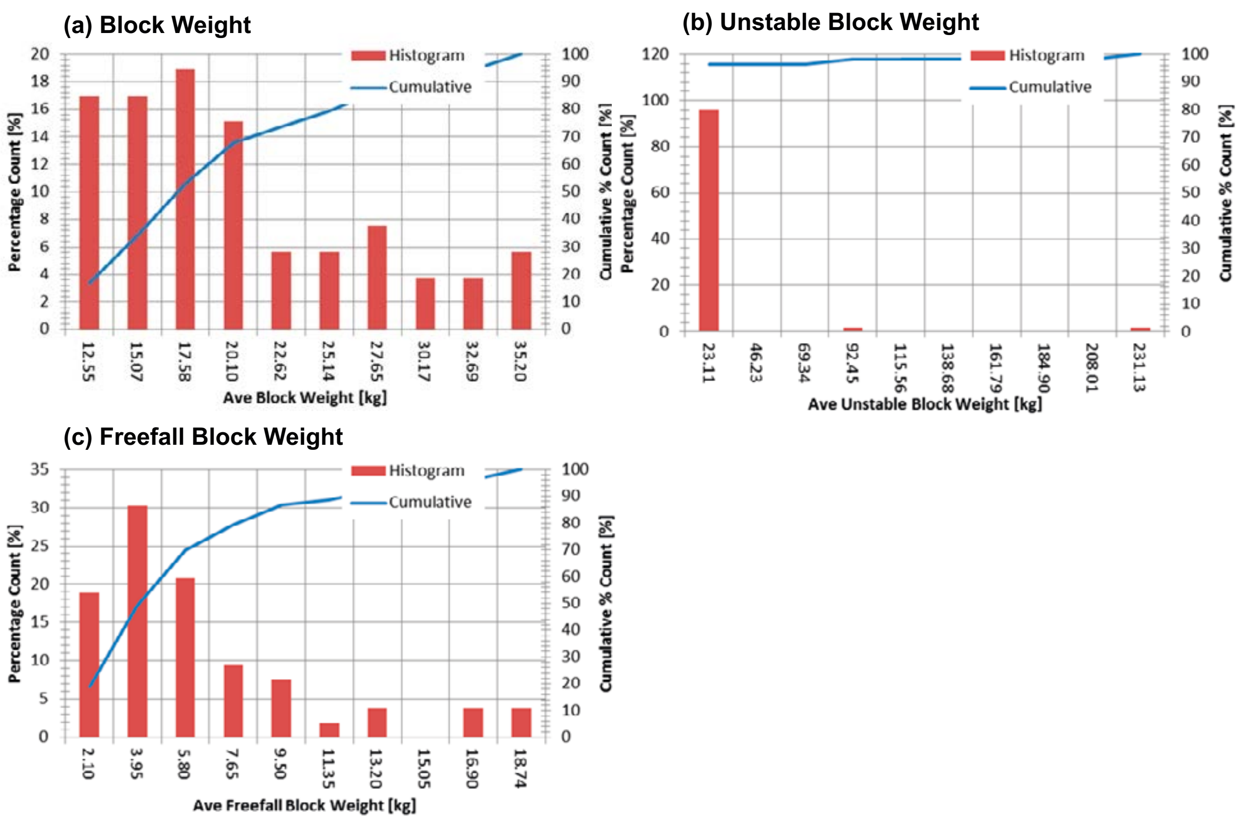

Figure 3-33. *Monte Carlo Results for Configuration-II, Showing a) Block Weight, b) Unstable Block Weight, and c) Freefall Block Weight.*

In it evident in Figure 3-33 a that most of the stable block weights vary between 12 and 35 kg, with the blocks weighing 20 kg or less accounting for approximately 60 %. In addition, it is seen in Figure 3-33 b that of the unstable blocks identified over 90 % of these blocks weigh approximately 23 kg or less. It is seen however two significantly larger block sizes are realised, one at around 90 kg and a second at 230 kg respectively. The occurrence of these two larger blocks is relatively small in terms of percentage from the completed realisations.

In Figure 3-33 c, the distribution of block weights derived from the realisation process is provided. It is seen once more that the freefall blocks are dominated by very small sized blocks, with 90 % of these blocks having a typical weight of 10 kg or less. It is seen that nearly 50 % of the freefall blocks identified weigh 4 kg or less. The largest size freefall block weight derived is approximately 20 kg.

Summary and Conclusions

In terms of the salient features identified through this group of analyses, the following are seen:

- The distribution of block is comparable in number and dimension compared to that seen for domain FFM01 with tunnel orientation N233 (Configuration-I).
- Approximately 6 % of blocks are classified as freefall.
- Approximately 6 % of blocks are classified as stable with low >1 FOS; and
- Approximately 88 % of blocks are classified as extremely stable FOS > 100.

3.7.3 Results: Configuration-III

The third configuration analysed, using the Monte Carlo analysis approach, considers the properties detailed in Table 3-9. The primary difference of Configuration-III compared to the previous Configure-I and -II is this results sets is based on the fractures identified for rock domain FFM06.

Table 3-9. Analysis Details – Configuration-III.

Configuration Component	Configuration Description
Rock Domain	FFM06
Fracture Model Description	TCM global fracture sets, TCM properties for orientation, size and intensity
Tunnel Orientation	N233
Friction Properties	Properties for Open fractures uniformly assigned
Pore Pressure Conditions	No fluid pressure included. 0 MPa

Block Count and Factor of Safety

The block count and factor of safety distributions obtained from the multiple realisations of the configuration defined in Table 3-9 are detailed in Figure 3-34.

Based on the charts in Figure 3-34 a, it is evident that the number of rock blocks forming around the tunnel is significantly more when compared to those seen previously for domain FFM01. For FFM06 the total number of blocks formed around the 100 metre intervals is typically around 425 in number. This is nearly double the total number of blocks usually identified for the same tunnel located in domain FFM01.

Of the total number of blocks identified, approximately 5 % (23) of the blocks are identified as being freefall; this typically varies between 10 and 32 blocks per realisation. In addition, it is seen that the number of unstable blocks again is very low in number, with 0 to 2 blocks being identified for each realisation (average 0.05/realisation). In terms of stable blocks, an average of 400 (94 %) of the total number of blocks are identified, covering a range of 350 to 450 stable blocks per realisation.

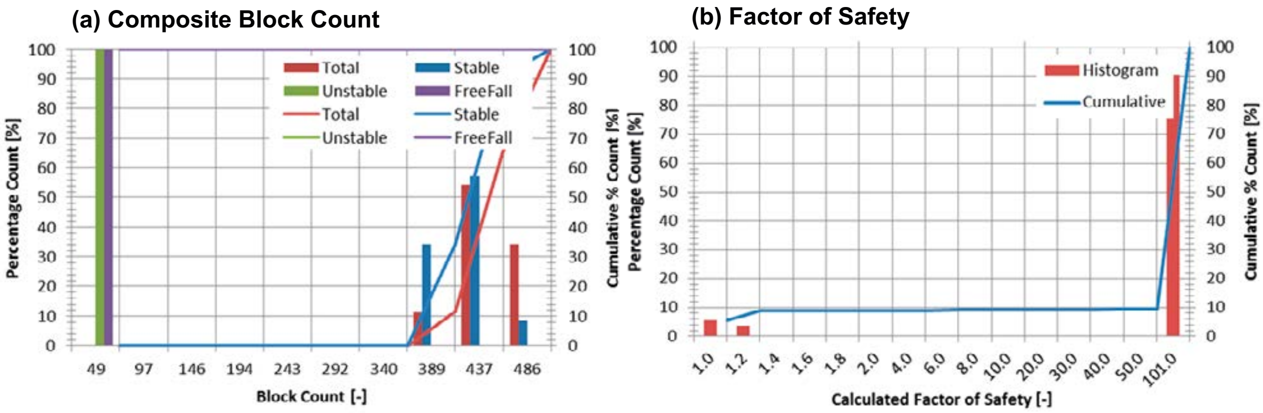

Figure 3-34. *Monte Carlo Results for Configuration-III, Showing a) Block Count Data, and b) Factor of Safety.*

Figure 3-34 b provides the factor of safety information obtained from the realisations, here it is seen that as seen previously the large majority of rock blocks formed during the analysis are considered to have high kinematic stability. It is seen that over 91 % of the rock blocks identified around a 100 metre long tunnel have a high factor of safety FOS of >100. Similarly, it is seen that just over 5 % of blocks formed are freefall/unstable, and just under 4 % of blocks are stable but with a low factor of safety, varying 1.0–1.2.

Block Volumes

The following Figure 3-35 provides the results of the block volume and size distributions realised for Configuration-III.

Block Weights

In addition to the block volume distributions presented in the previous section, the following Figure 3-36 considers the distribution of block weights realised. It is evident in Figure 3-36 a that on average the rock blocks tend to be smaller in size than those identified for rock domain FFM01. For domain FFM06 approximately 80 % of the blocks are seen to weight 4 kg or less. In addition, it is seen that both the freefall and unstable block weight are also suitable small – with blocks being typically 5 kg or less.

Summary and Conclusions

In terms of the salient features identified through this group of analyse, the following are seen:

- Higher number of blocks formed (~425 per 100 metre run) compared to equivalent configuration for domain FFM01;
- Blocks are generally smaller in volume and weight (4 kg) compared to that seen for domain FFM01; and
- Over 90 % of blocks formed have sufficiently high Factor of Safety predicted (FOS > 100).

3.7.4 Results: Configuration-IV

The fourth configuration analysed, using the Monte Carlo analysis approach, considers the properties detailed in Table 3-10. The primary difference of Configuration-IV compared to the previous Configuration-III is solely the tunnel orientation.

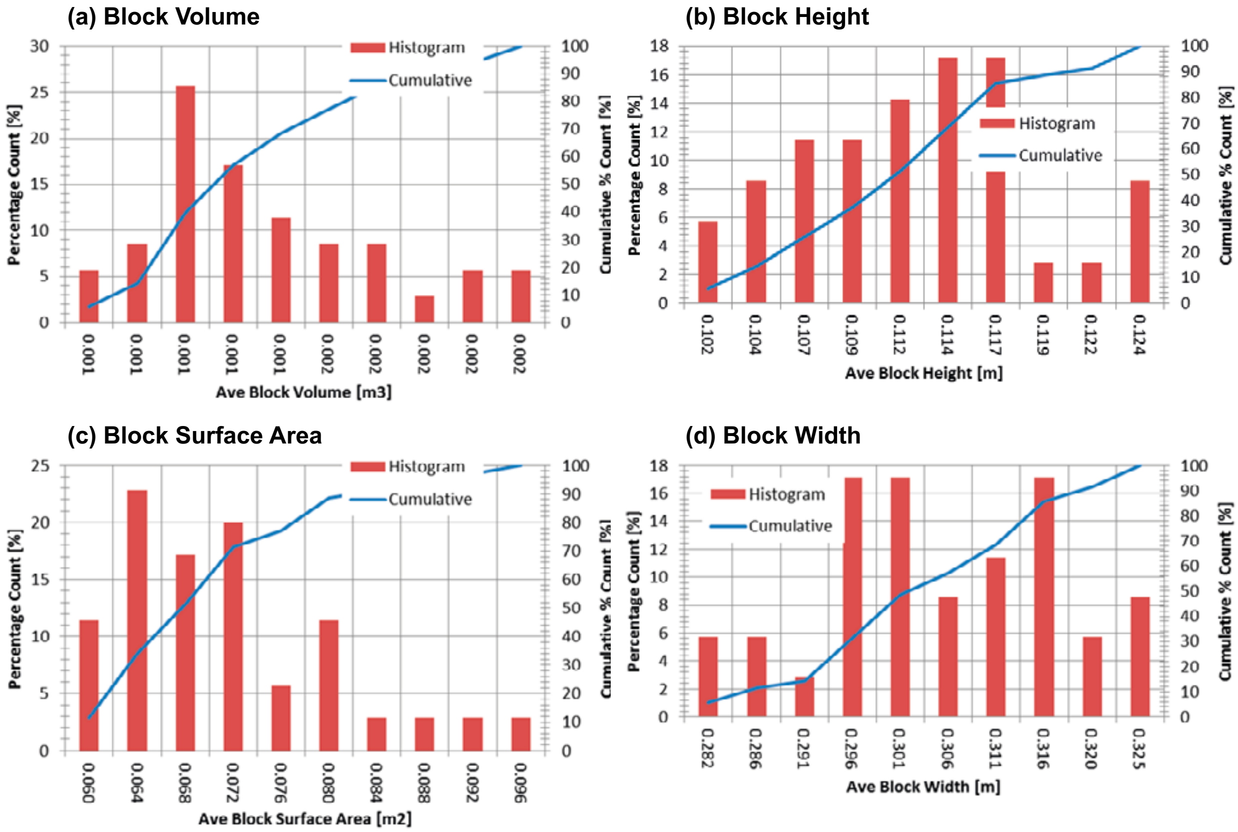

Figure 3-35. Monte Carlo Results for Configuration-III, Showing a) Block Count Data, and b) Factor of Safety.

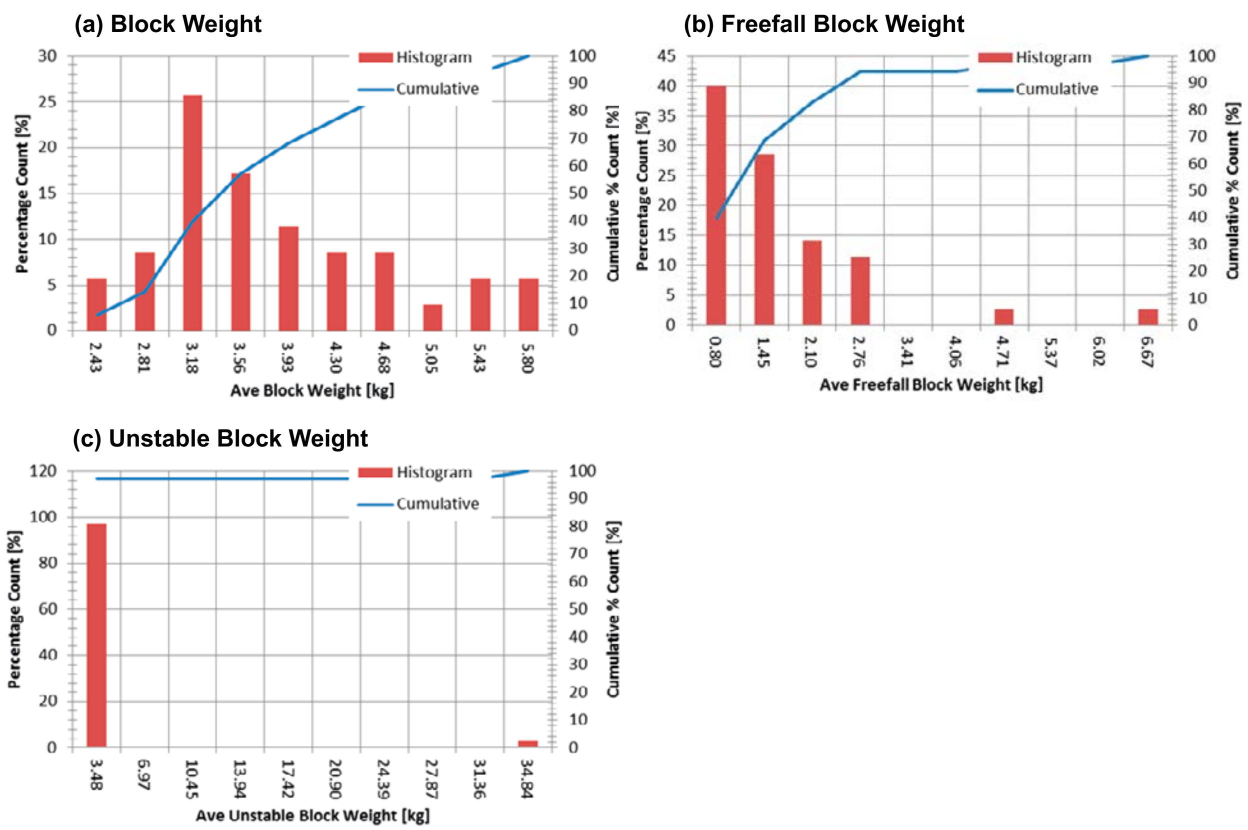

Figure 3-36. Monte Carlo Results for Configuration-III, Showing a) Block Weight, b) Freefall Block Weight, and c) Unstable Block Weight.

Table 3-10. Analysis Details – Configuration-IV.

Configuration Component	Configuration Description
Rock Domain	FFM06
Fracture Model Description	TCM global fracture sets, TCM properties for orientation, size and intensity
Tunnel Orientation	N143
Friction Properties	Properties for Open fractures uniformly assigned
Pore Pressure Conditions	No fluid pressure included. 0 MPa

Block Count and Factor of Safety

The block count and factor of safety distributions obtained from the multiple realisations of the configuration defined in Table 3-10 are detailed in Figure 3-37.

The distributions provided in Figure 3-37 relate to the block count and factor of safety data obtained from the fifty realisations of Configuration-IV. It is again seen, similarly to Configuration-III, that the pattern of natural fracturing in domain FFM06 realises a significant increase in the total number of blocks being formed. As seen previously, in excess of 400 blocks are realised for domain FFM06. In addition, the number of freefall blocks remains relatively low with an average of 22 blocks (ranging 8–39) being predicted for this configuration. In terms of factors of safety, it is again seen that approximately 90–91 % of blocks are extremely stable, and the remaining 9–10 % of blocks are either freefall/unstable (5.5 %) or are stable but with a very low safety margin accounting for approximately 3.5 %.

Block Volumes

In addition to the block count and factor of safety of data, the following Figure 3-38 provides details of the distributions obtained from the collation of the realisation data in terms of block sizing and geometry. It is seen in Figure 3-38 again that the most frequent block volumes are in the region of 0.001 m^3, with the block height seen to generally vary between 0.11 to 0.14 metres, and the block width varying slightly more between 0.28 to 0.33 metres.

Block Weights

In terms of block weights, the following Figure 3-39 presents a summary of the Monte Carlo results obtained from Configuration-IV realisations. It is again seen that the block weights are typically smaller than those calculation previously for rock domain FFM01.

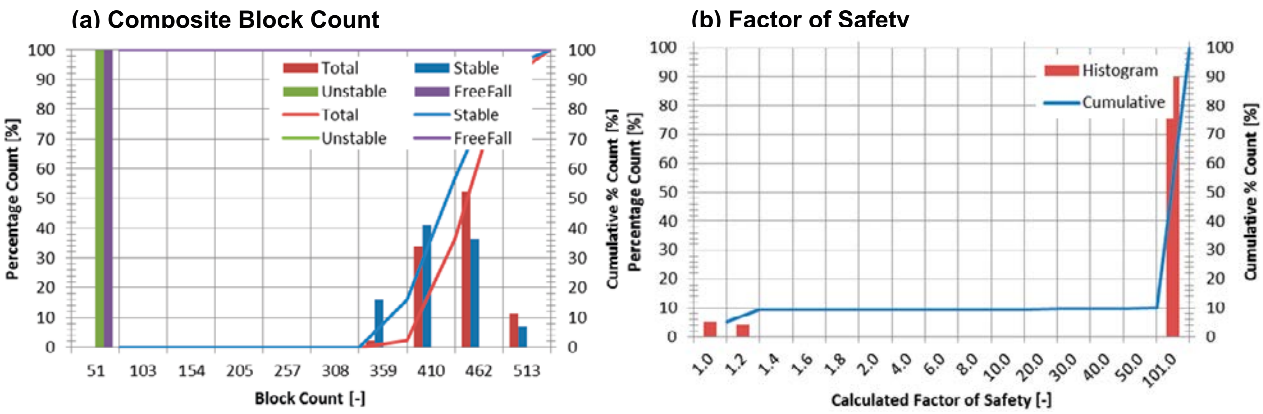

Figure 3-37. Monte Carlo Results For Configuration-IV, Showing a) Block Count, and b) Factor of Safety.

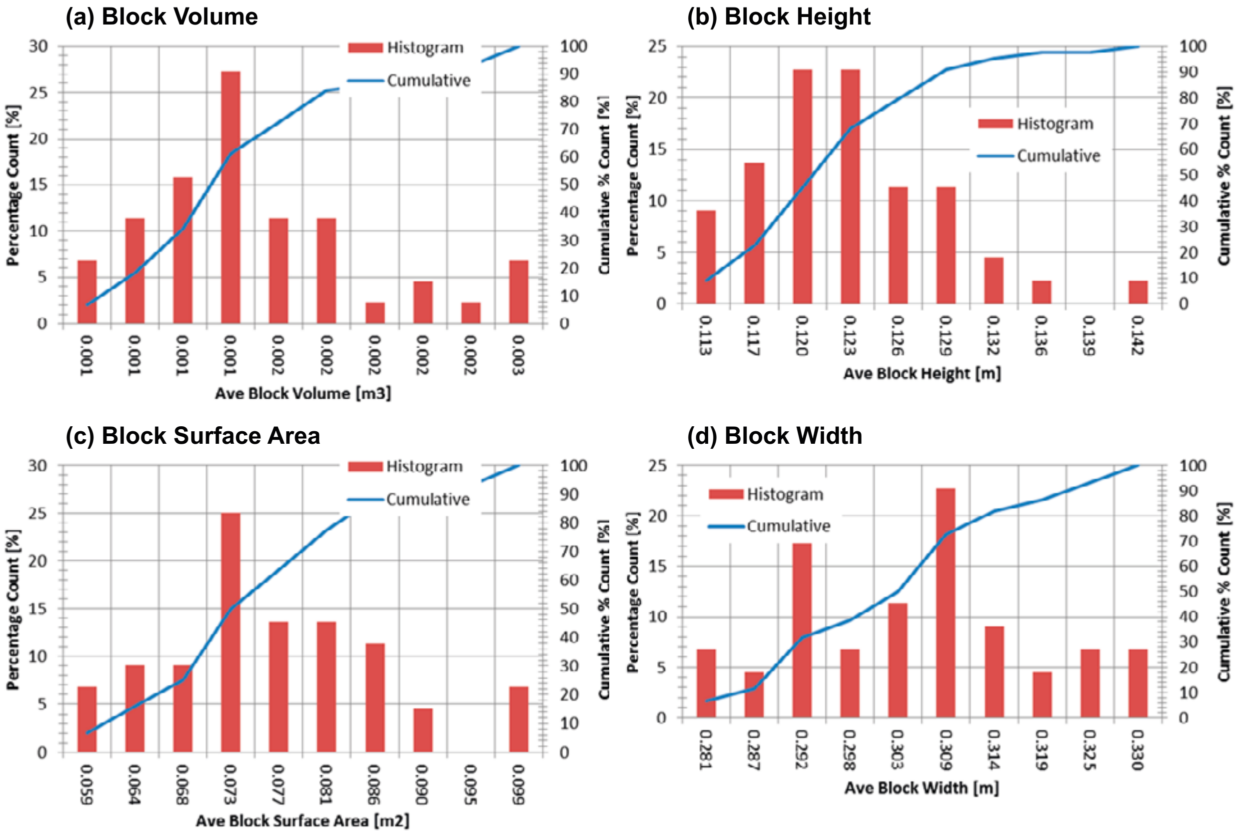

Figure 3-38. *Monte Carlo Results for Configuration-IV, Showing a) Block Volume, b) Block Height, c) Block Surface Area, and d) Block Width.*

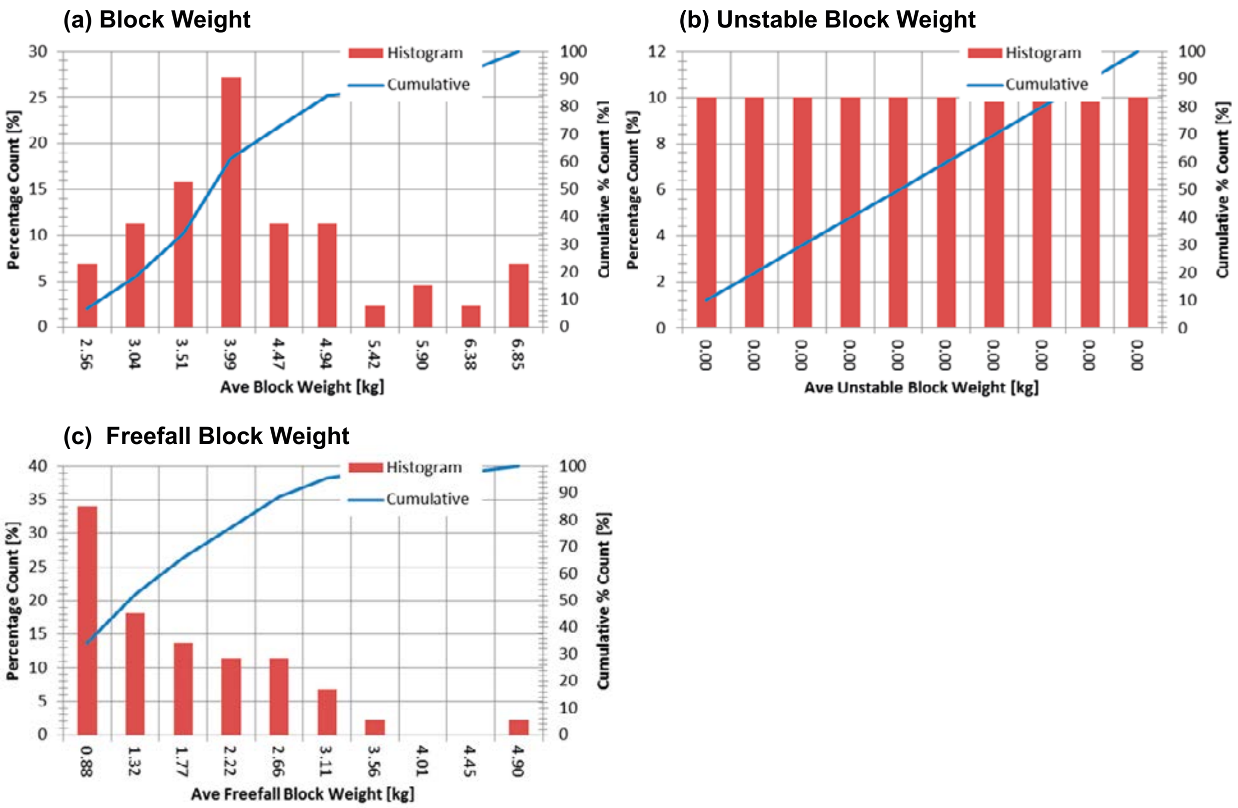

Figure 3-39. *Monte Carlo Results for Configuration-IV, Showing a) Block Weight, b) Unstable Block Weight, and c) Freefall Block Weight.*

Summary and Conclusions

In terms of the salient features identified through this group of analyses, the following are seen.

- High number of smaller blocks formed compared to FFM01; and
- Number of freefall blocks remains low at approximately 5–6 %.

3.7.5 Results: Configuration-V

The fifth configuration analysed considers the model properties detailed in Table 3-11. This configuration has the tunnel orientation as the original N233 direction in the FFM01 domain, with the main difference being a nonzero pore fluid pressure condition included. All other properties remain as previously used.

Table 3-11. Analysis Details – Configuration-V.

Configuration Component	Configuration Description
Rock Domain	FFM01
Fracture Model Description	TCM global fracture sets, TCM properties for orientation, size and intensity
Tunnel Orientation	N233
Friction Properties	Properties for Open fractures uniformly assigned
Pore Pressure Conditions	Hydrostatic fluid pressure included. 5 MPa

Block Count and Factor of Safety

Summary charts of the results obtained for the FFM01 rock domain results for the case where a hydrostatic pore fluid loading is included in the analysis approach are shown in Figure 3-40. Figure 3-40 a provides the average block counts of each type formed per realisation around the 100 metre tunnel model. Based on the 50 realisation approach, it is evident that approximately 250 discrete blocks are formed. This approximates the same number seen previously for Configurations-I and –II. Of these blocks it is again seen that a low percentage of these blocks are considered freefall, typically 14 by number (6 %) on average, with a general range of between 8–23 blocks per realisation.

Of the average 250 blocks per realisation, it is seen that on average approximately 43 % (~ 110 per realisation) are considered kinematically stable, this represents a significant reduction in stable blocks compared to that realised when the pore pressure field is zero (see Configuration-I). Accompanying the reduction in stable block numbers, there is a corresponding increase in the number of unstable blocks, accounting for approximately 47 % of the total block count. The combined freefall and unstable blocks account for approximately 53 % in Figure 3-40 b.

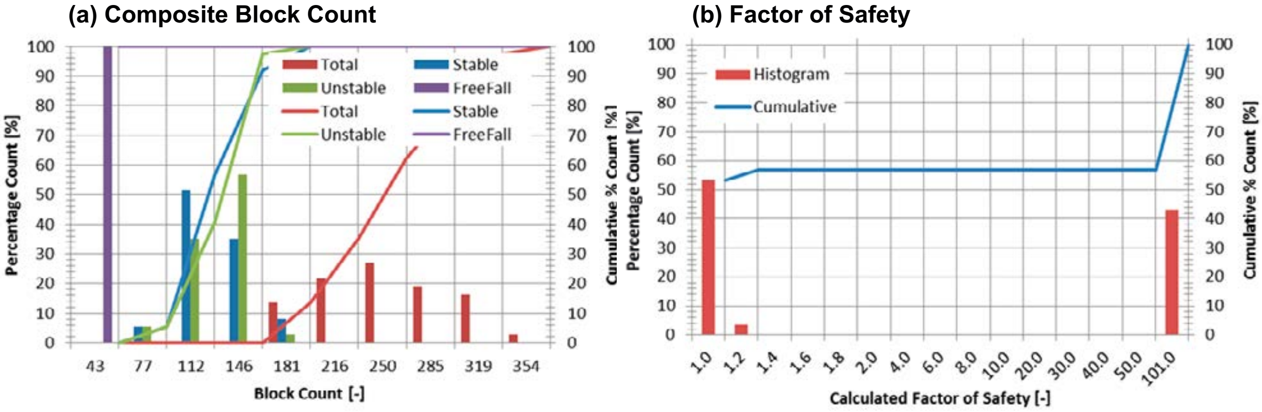

Figure 3-40. Monte Carlo Results for Configuration-V, Showing a) Block count, and b) Factor of Safety.

Block Volumes

The block volume data for the set of realisations is presented in Figure 3-41, it is evident that this data reflects the levels seen in the previous configurations for domain FFM01.

Block Weights

The corresponding block weight data for the set of realisations assessed is provided in Figure 3-42. It is again seen, like the volume data, that this data reflects the levels seen in the previous configurations for domain FFM01. The overall range of block weights varies between approximately 10 to 25 kg in weight, with the greatest number of blocks being approximately 20 kg. It is also seen that over 40 % of the freefall blocks that are identified are particularly small, at 4 kg in weight.

Summary and Conclusions

In terms of the salient features identified through this group of analyse, the following are seen:

- Increases to the pore pressure to 5 MPa level are seen to noticeably increase the number of unstable blocks formed; and
- Approximately 47 % of blocks formed are unstable, similarly to previously just 6 % of blocks are considered freefall, and the remaining 47 % of blocks formed remain stable.

3.7.6 Results: Configuration-VI

The sixth configuration analysed considers the model properties detailed in Table 3-12. This configuration has the tunnel orientation as the original N233 direction, but the main difference is a nonzero pore fluid pressure condition is included where in the preceding analyses it remained at zero. All other properties remain as previously used.

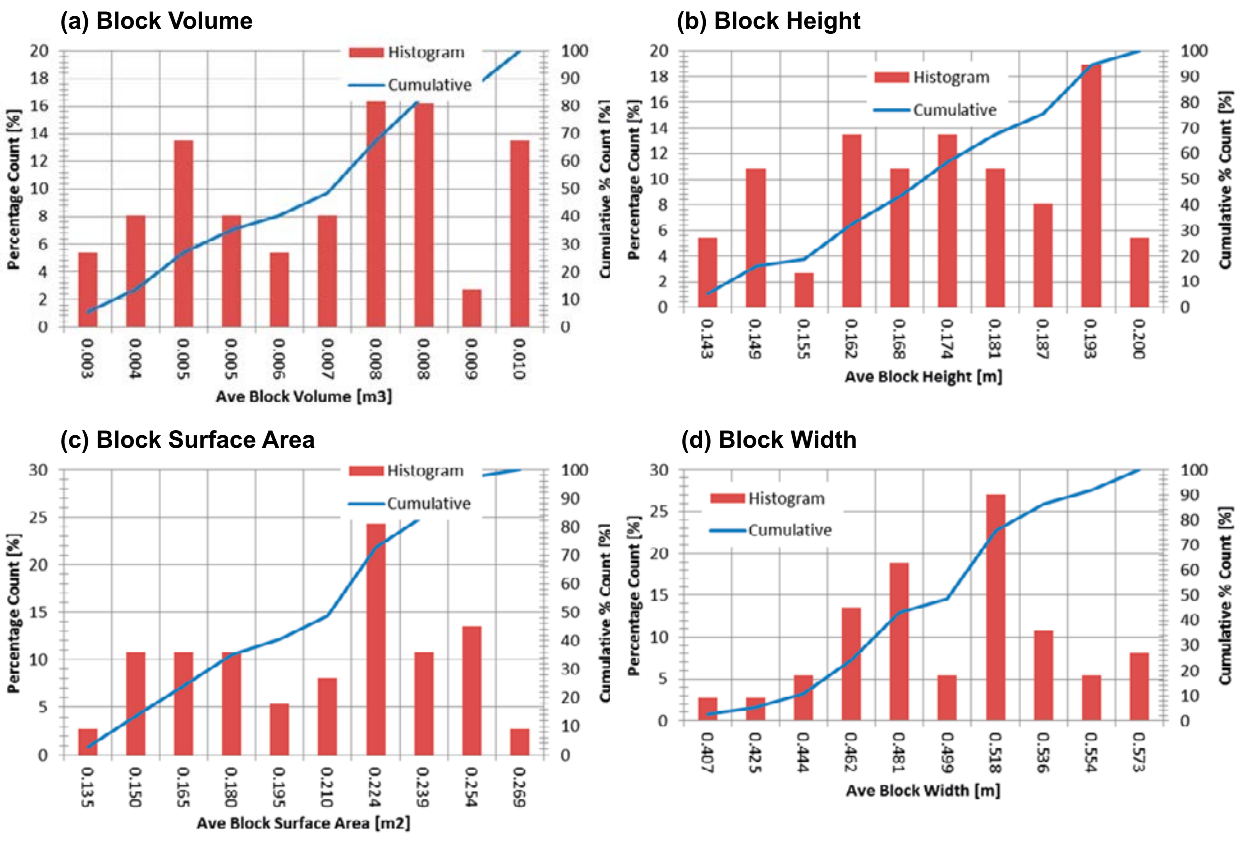

Figure 3-41. Monte Carlo Results for Configuration-V, Showing a) Block Volume, b) Block Height, c) Block Surface Area, and d) Block Width.

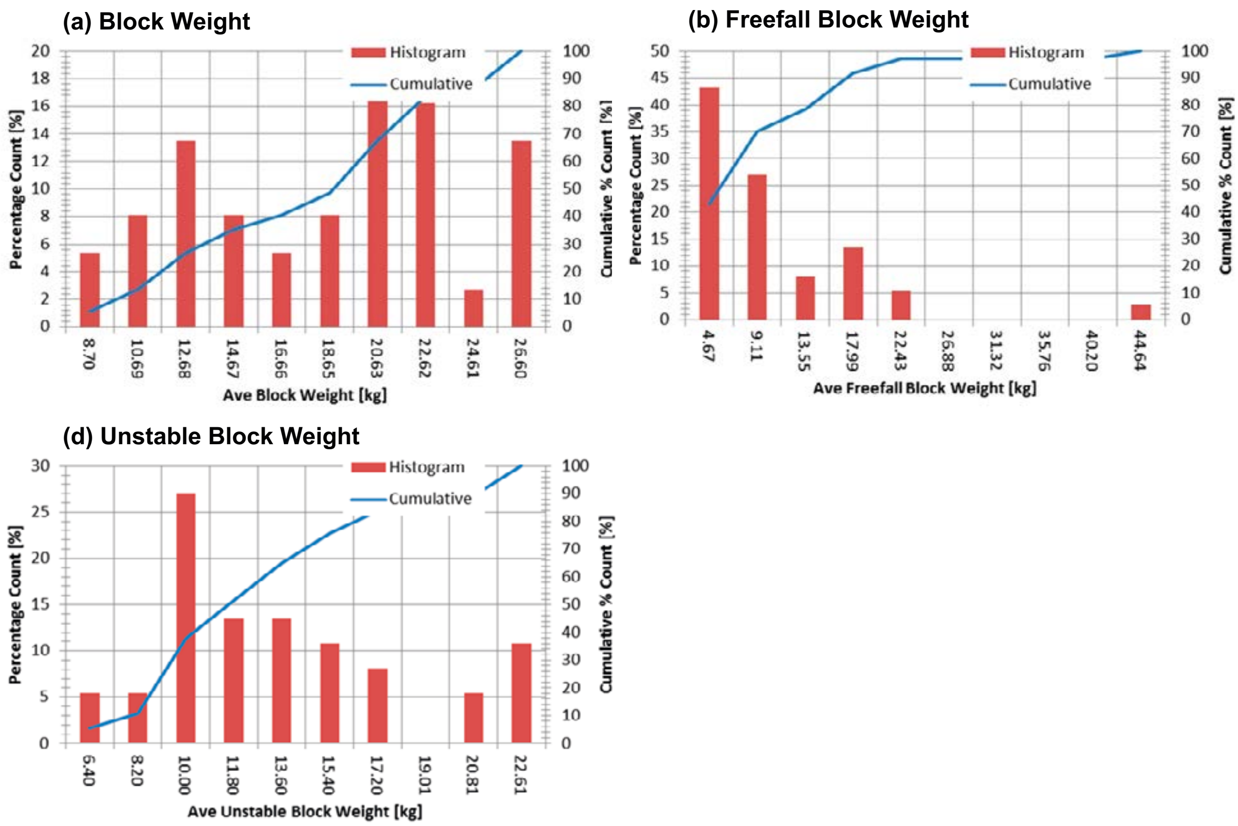

***Figure 3-42.** Monte Carlo Results for Configuration-V, Showing a) Block Weight, b) Freefall Block Weight, and c) Unstable Block Weight.*

Table 3-12. Analysis Details – Configuration-VI.

Configuration Component	Configuration Description
Rock Domain	FFM06
Fracture Model Description	TCM global fracture sets, TCM properties for orientation, size and intensity
Tunnel Orientation	N233
Friction Properties	Properties for Open fractures uniformly assigned
Pore Pressure Conditions	Hydrostatic fluid pressure included. 5 MPa

Block Count and Factor of Safety

The realised block count and factor of safety distributions obtained for the Monte Carlo analyses are provided in Figure 3-43. Similarly to the original case where there was no pore pressure the number of rock blocks identified as existing around the N233 aligned tunnel remains high compared to that seen for domain FFM01 with a typical total number of 400 blocks being realised. Of these, the number of freefall blocks remains low, with approximately 22 (6 %) being realised, typically varying 8–23 blocks.

It is seen however, that through introduction of a 5 MPa pore fluid pressure, the number of unstable blocks increases significantly. When there is no pore pressure component the number of unstable blocks is very close to zero, however it is evident that increasing the fluid pressure to hydrostatic levels (5 MPa) increases the number of unstable blocks significantly, realising approximately 185 (46 %) unstable blocks per realisation. The number of stable blocks varies 147–250 per realisation, averaging 192 (48 %) of the total number of blocks formed.

Block Volumes

The block volumes realised are comparable to those seen previously in the other FFM06 domain based analyses. These FFM06 blocks are once more noticeably smaller than those observed for domain FFM01. See Figure 3-44.

Block Weights

In terms of block weights, the results for this configuration are seen to be similar to those observed previously for rock domain FFM06. Again, the block sizes are smaller compared to those predicted for domain FFM01. For the FFM06 configuration the blocks are typically 4 kg in weight, see Figure 3-43.

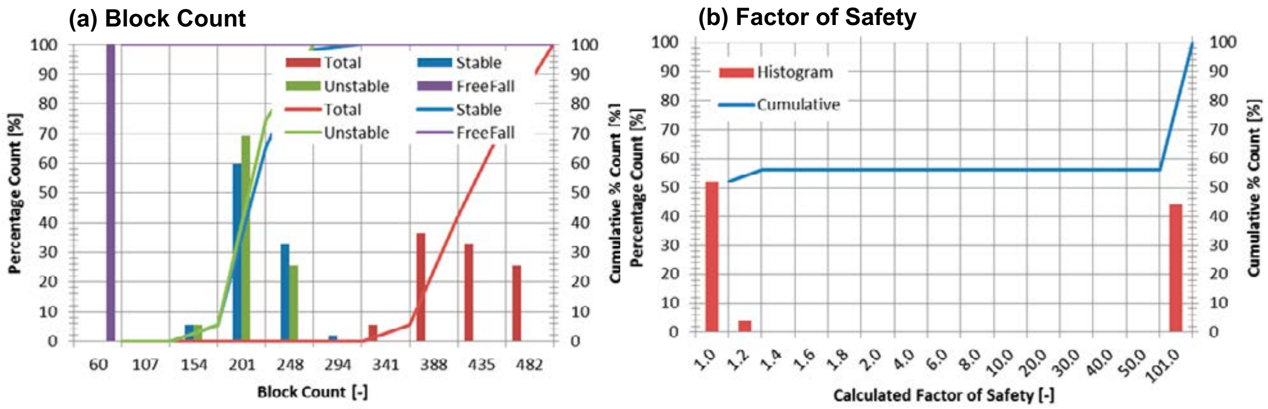

***Figure 3-43.** Monte Carlo Results for Configuration-VI, Showing a) Block Count, b) Factor of Safety.*

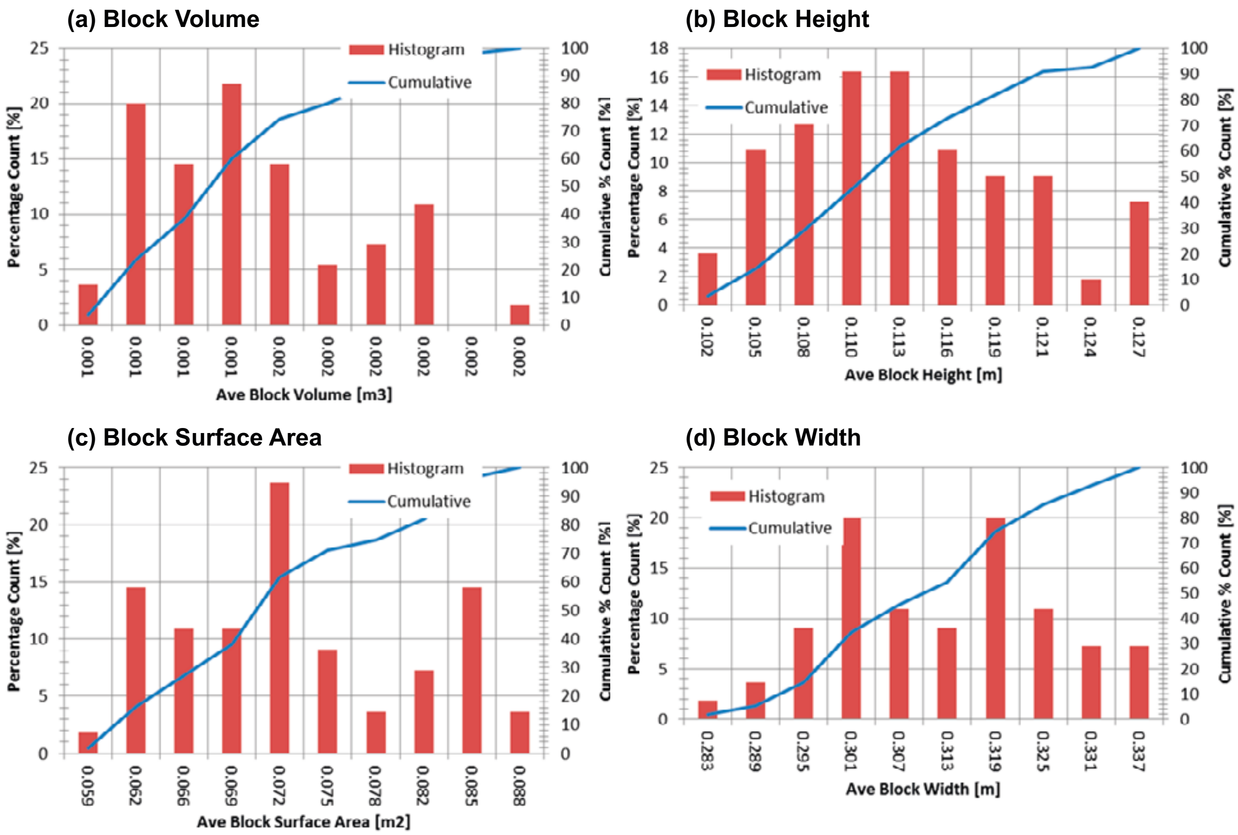

***Figure 3-44.** Monte Carlo Results for Configuration-VI, Showing a) Block Volume, b) Block Height, c) Block Surface Area, and d) Block Width.*

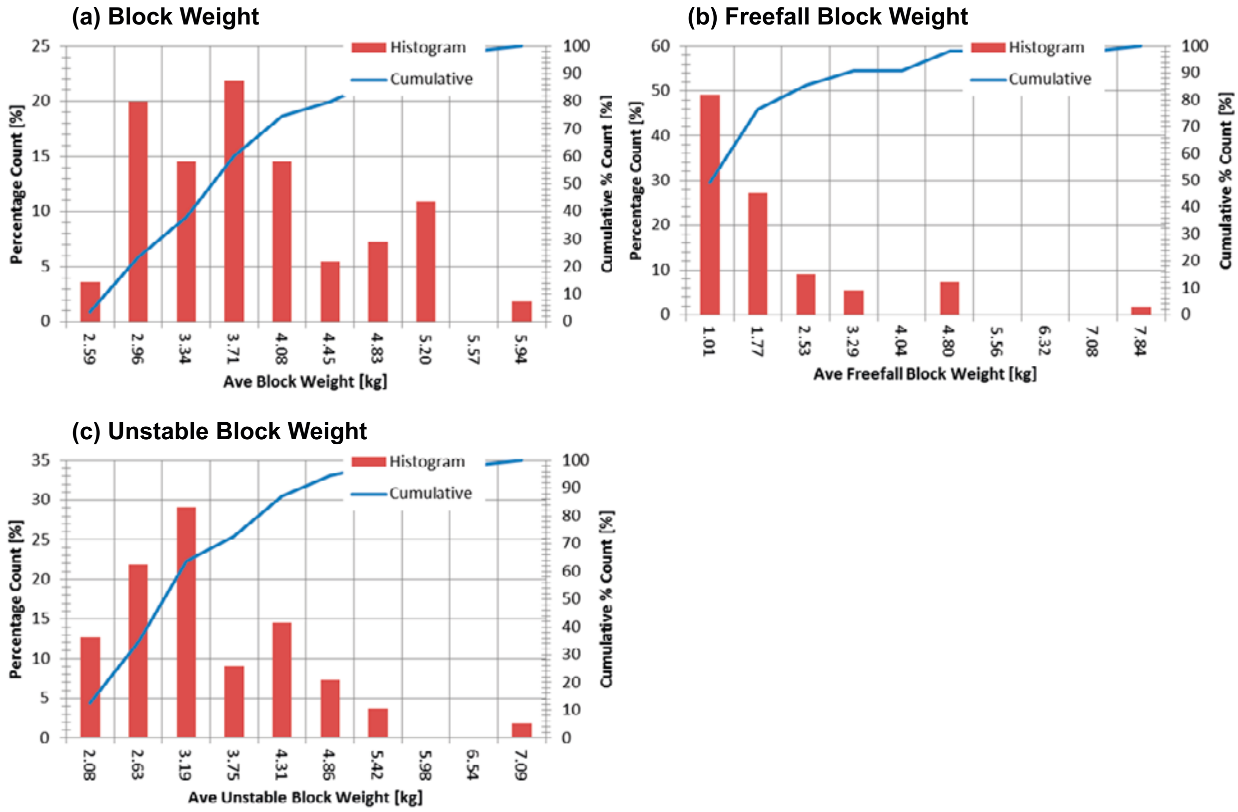

Figure 3-45. *Monte Carlo Results for Configuration-VI, Showing a) Block Weight, b) Freefall Block Weight, and c) Unstable Block Weight.*

Summary and Conclusions

In terms of the salient features identified through this group of analyses, the following are seen:

- Increased pore pressure levels are, similarly to domain FFM01, seen to noticeably increase the number of unstable blocks formed; and
- Approximately 46 % of blocks formed are unstable, just 6 % of blocks are considered freefall, 48 % of blocks formed are stable.

3.7.7 Results: Configuration-VII

The seventh configuration analysed considers the model properties detailed in Table 3-13. This configuration has the tunnel orientation as the original N233 direction, but the main difference is the open fracture frictional properties have been significantly reduced to test the sensitivity of the fracture mechanical properties. All other properties remain as previously used.

Table 3-13. Analysis Details – Configuration-VII.

Configuration Component	Configuration Description
Rock Domain	FFM01
Fracture Model Description	TCM global fracture sets, TCM properties for orientation, size and intensity
Tunnel Orientation	N233
Friction Properties	Reduced friction properties, friction angle 26 degrees
Pore Pressure Conditions	No fluid pressure included. 0 MPa

Block Count and Factor of Safety

The data shown in Figure 3-46 shows the block count and factor of safety distributions, it is seen that based on the 50 realisations the number of unstable blocks expectedly increases with the reduction in frictional strength. It is seen that of the typical 200 blocks identified per realisation approximately 38 % are unstable, 5 % are stable with particularly low factors of safety, and the remaining 57 % of blocks are those with factors of safety greater than 1.4. It is seen that over 40 % of blocks are calculated with higher factors of safety >50.

Block Volumes

The calculated block volume distributions are provided in Figure 3-47, it is seen that these results are consistent with what has been seen previously for the rock domain FFM01.

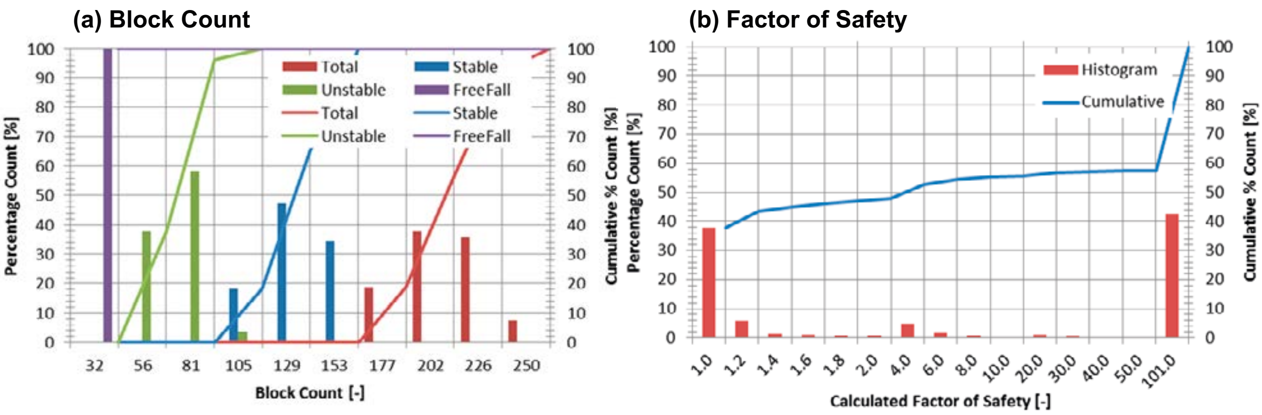

Figure 3-46. *Monte Carlo Results for Configuration-VII, Showing a) Block Count, and b) Factor of Safety.*

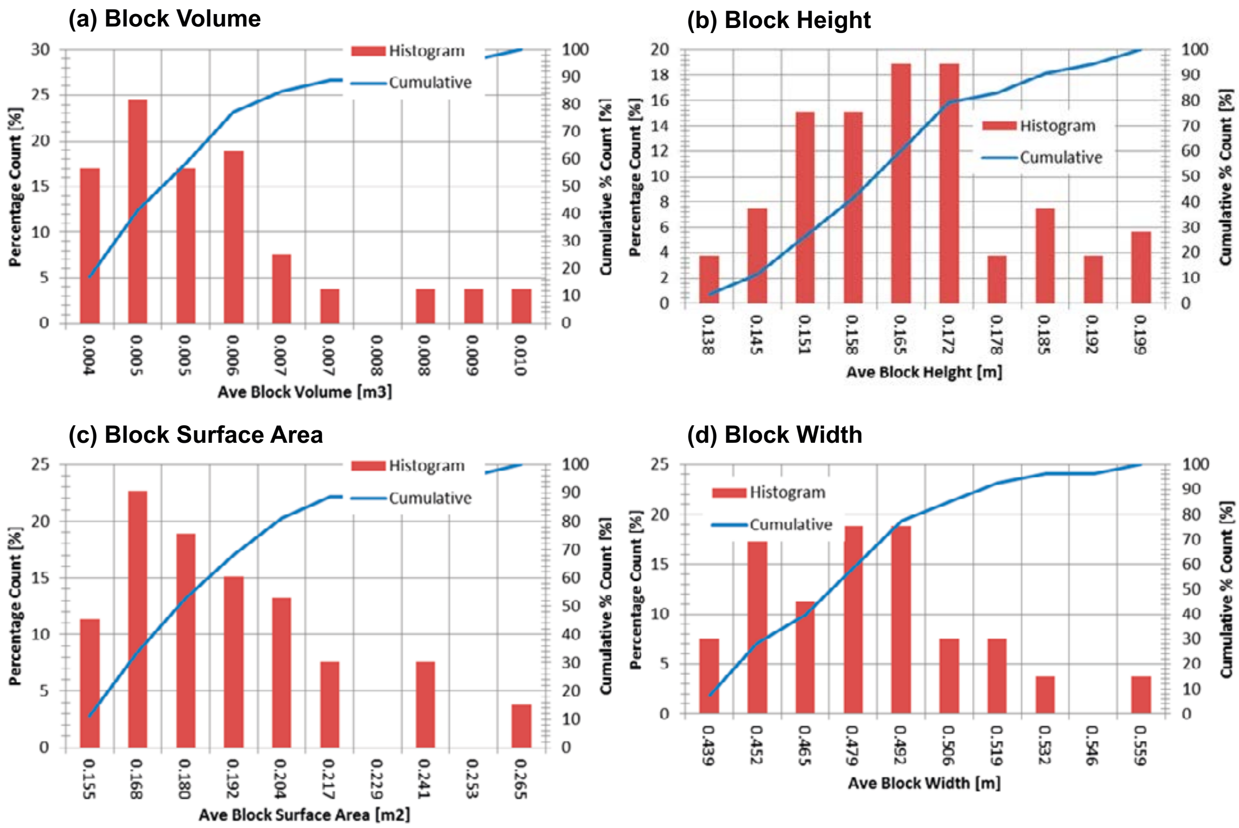

Figure 3-47. *Monte Carlo Results for Configuration-VII, Showing a) Block Volume, b) Block Height, c) Block Surface Area, and d) Block Width.*

Block Weights

The calculated block weight distributions are provided in Figure 3-48 it is seen that these results are consistent with what has been seen previously for the rock domain FFM01.

Summary and Conclusions

In terms of the salient features identified through this group of analyse, the following are seen:

- Using common distribution of strength parameters for all global fracture sets included in assessment – impact of this is currently uncertain
- Reduction in fracture surface friction gives significant increase in number of unstable blocks; and
- Combined free fall and unstable blocks accounts for nearly 40 % of blocks formed.

3.7.8 Results Summary

The following Table 3-14 provides succinct summary of the key variables obtained from the performed realisations of each of the configurations identified.

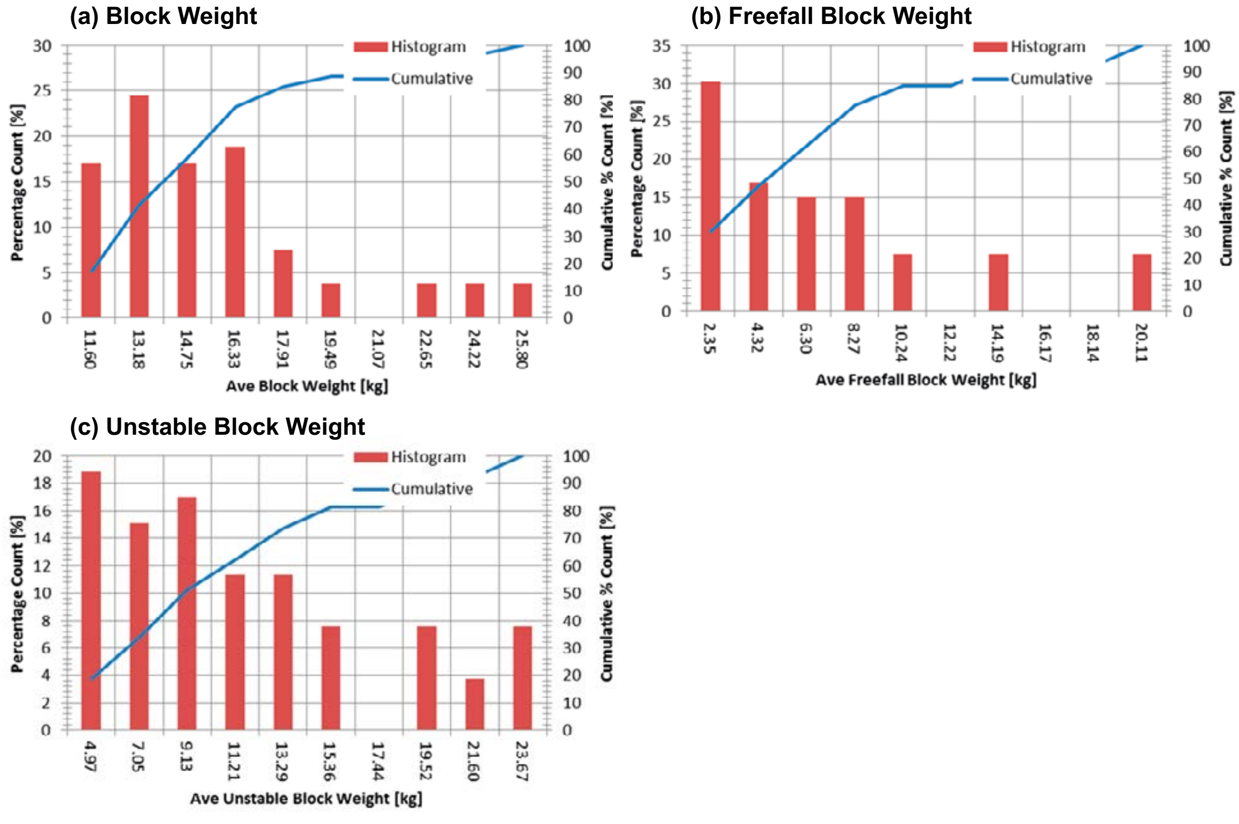

Figure 3-48. Monte Carlo Results for Configuration-VII, Showing a) Block Weight, b) Freefall Block Weight, c) Unstable Block Weights.

Table 3-14. Summarised Realisation Results.

Cases	Block Counts [–] / 100 metre tunnel				Block Weights [kg]			Factor of Safety [%]		
	Total	Stable	Unstable	Freefall	Min	Max	Ave	0–1	1–5	5+
FFM01 (N233) (I)	242.71	225.97	0.03	16.71	9.65	38.27	20.01	6.90	4.09	89.02
FFM06 (N233) (II)	425.00	401.50	0.06	23.43	2.06	5.80	3.62	5.53	3.50	90.97
FFM01 (N143) (III)	262.91	247.74	0.05	15.11	10.03	35.20	19.08	5.77	5.55	88.68
FFM06 (N143) (IV)	425.21	402.89	0.00	22.32	2.08	6.85	3.97	5.25	4.29	90.46
FFM01 (N233) Pore 5 MPa (V)	231.92	108.80	107.45	15.04	6.72	26.60	17.80	53.14	3.60	43.26
FFM06 (N233) Pore 5 MPa (VI)	400.87	192.31	186.08	22.49	2.22	5.94	3.66	52.03	3.96	44.01
FFM01 (N233) Friction 26 deg (VII)	215.25	141.55	60.02	13.68	10.02	25.80	14.86	37.75	16.60	45.65

Of the data presented in Table 3-14, it is evident that:

- Models for domain FFM01 averages 250 blocks/100 metre run, average block weights are 20 kg, approximately 6 % of the formed blocks being freefall.
- Models for domain FFM06 averages 425 blocks/100 metre run, average block weights are 4 kg, approximately 5 % of the blocks freefall.
- In both FFM01 and FFM06 rock domains the percentage of unstable blocks is very low < 1 %, typically only 1–2 blocks per 100 metre tunnel run seen.
- Tunnel orientation is seen to have little sensitivity in terms of unstable block formation. It is seen tunnel orientation accounts for a 10 % increase in total block count for FFM01, but for FFM06 block count is unaffected by orientation.
- Block kinematic stability shows significant sensitivity to pore pressure. Increasing the pore pressure levels from zero to a uniform 5 MPa results in the number of unstable blocks increasing. Increasing the pore pressure indicates between 20–30 % of the blocks are unstable compared to dry case where <10 % are either unstable/freefall; and
- The simulations indicate that if the fracture strength properties are lower than currently has been estimated, then there is significant sensitivity and risk to increased levels of block instability.

4 Summary and Conclusions

The current piece of work has assembled existing data and reporting to provide an assessment of the kinematic stability of the rock wedges surrounding proposed tunnel geometries inserted into the Forsmark repository location.

The investigations have considered identification of the main fracture attributes for the version 2.2 of the Forsmark GeoDFN fracture sets, these attributes include the natural fracture sets orientation, intensity, size, as well as the fracture mechanical properties including friction, cohesion and compliance (compressibility). Different types of fractures have been included in the initial assembly of data, including GeoDFN derived fractures following the TCM model (Fox et al. 2007), open fractures and sealed fractures from SKB (2010).

The TCM description, in which fractures at the outcrop and borehole scale are considered as the main fracture description is utilised in the current investigations. For each of the two rock domains investigated, FFM01 and FFM06, the principal fracture properties have been assembled for the global North-East (NE), North-South (NS), North-West (NW) and Sub Horizontal (SH) fracture sets. Each of the four fracture sets exists in each of the two rock domains but with different describing parameters sets respectively. For the case of fracture intensity, the sealed fracture parameters have been indirectly calculated from the difference between the volumetric intensity of all (TCM) and open (hydrogeological) fracture descriptions.

In terms of rock mechanical properties assigned to each of the individual fracture sets, the analyses require principally shear strength based descriptions. Examination of the available literature provides coulomb strength envelopes, however it is noted that the provided strength envelopes appear both fracture set and fracture domain independent. In addition, examination of the fracture shear strength envelopes indicate that there is significant shear resistance present for open, healed and broken fracture types. Although it is recognised from existing reporting that most of the natural fracture are in fact healed, in the implemented analysis the weaker open fracture strength properties have been used. Use of the open fracture strength properties represents a conservative position in terms of block interface strength.

Section 2.6 identifies the possible model configurations put forward for kinematic stability assessment of Task 1.2 of Phase I. For each of the cases identified a summary of the arguments for and against evaluation is also provided. The end of this section provides the selection of the model configurations that are then investigated further in terms of block kinematic stability assessment. The two model cases that are then followed through with assessment are FFM01 and FFM06 with the main fracture models following the TCM descriptions.

The design of the tunnel used for analysis is based on that put forward by SKB, and in the current investigation two different tunnel orientations are assessed, the first orientation at N143 and at N233.

The development of the DFN model is described in terms of the model geometry in which the fracture set definitions are applied. Detailed checks were undertaken to ensure that the necessary pattern of natural fracturing was not influenced by the size of the model. The model size used is numerically efficient but has shown to provide similar fracture trace statistics to a significantly larger fracture model.

Carrying forward the development of the tunnel scale DFN fracture model, the report goes on to provide a detailed description of the kinematic stability analysis approach employed. Description of the underlying theory of block stability and how it translates into the calculation of the varying active and passive (resistive) force terms is also provided. Details concerning the available output options from the kinematic stability are provided, further the results produced from the analyses are presented in terms of composite block descriptions. The composite block approach means that contiguous block fragments are considered and presented as a single block entity.

Single realisations have been presented initially for baseline cases of rock domain FFM01 and FFM06, see Sections 3.3 and 3.4, and the summary provided in Section 3.5. For each of the two baseline analyses, both tunnel-fracture intersection and kinematic block stability is assessed. The tunnel fracture intersection is considered in terms of the areal fracture intensity realised on the tunnel crown, sidewall and invert positions. It is evident from these baseline analyses that for tunnel in rock domain FFM01 the P_{21} fracture intensity expected on the crown, sidewall and invert positions is largely uniform at approximately 3.30 m/m^2 average. However, for domain FFM06 it is seen that the level of areal fracture intensity is significantly higher on the sidewalls ($P_{21} = 7.2$ m/m^2) than the crown and invert positions ($P_{21} = 5.25$ m/m^2) on average.

The impact of the increases in areal fracture intensity is further realised when the distribution of rock blocks is assessed from the kinematic stability analysis results. It is seen for the 100 metre length tunnel model, that domain FFM01 realises approximately 200 rock blocks, whereas domain FFM06 on average realises nearly 450 rock blocks per 100 metre tunnel length. In terms of block geometry, it is also seen in Table 3-5, that the average block weight encountered for domain FFM06 (4.35 kg) is approximately 25 % of that predicted for domain FFM01 (16.90 kg). The perceived reduction in block size tying to the increased areal fracture intesity for domain FFM06.

Extension of the baseline analyses through use of a Monte Carlo based approach has been implemented to allow a more appropriate probabilistic assessment of the likely block geometry and kinematic stability. In facilitating the probabilistic assessment, an Excel macro based approach for seamless integration and analysis of results from multiple stochastic realisations is detailed. The developed tool provides histogram and cumulative based graphs of each of the main result variables produced by each kinematic analysis. The composite results include block count, block geometries (size, volume, and weights), as well as block factor of safety.

Implementation of the probabilistic assessment has taken on the form of assessing seven different configurations; these are detailed in Table 3-6 of Section 3.7. For each of the configurations identified systematic variation to the tunnel orientation, frictional properties and pore water level has been investigated for each of the two rock domains FFM01 and FFM06 respectively. It is seen generally small numbers of freefall blocks are formed for either of the two domains. Confirming with previous observations it is seen that the formed blocks for domain FFM06 are on average much greater in number (factor × 2) but also significantly smaller in weight (factor × 5) than those typically seen for domain FFM01. Typically, for the baseline configurations of: all TCM fractures, default frictional properties, and no pore water pressure, on average 6 % of blocks are freefall, 4 % of block are stable but with low factor of safety, and an overwhelming 90 % of blocks are extremely stable (FOS > 5.00). It is seen, that the variation of tunnel orientation between N143 and N233 have overall little impact in terms of the block stability behaviour.

Greater system sensitivity is seen however when pore fluid pressures become non zero or fracture frictional strength becomes reduced. It is seen that inclusion of a hydrostatic fluid pressure condition in the models (corresponding to 5 MPa at 500 metres depth), significantly alters the split of freefall, kinematically unstable and kinematically stable blocks distribution. It is seen that the inclusion of the water pressure terms results in a reduction of kinematic stable block by approximately 50 % (90 % down to 50 % of all blocks formed). The reduction in stable blocks is similarly seen for both rock domains FFM01 and FFM06. In addition, a configuration where the fracture frictional properties have been greatly (uniformly) reduced indicates a similar significant increase in unstable blocks, with the percentage number reduction similar to the pore water cases (90 % down to 40 % of blocks showing high levels of stabilty).

In terms of proposals for further investigations, the following itemised points are considered important areas for further investigation:

- Investigation of the sensitivity of bigger variations and assignment impacts of fracture surface strength properties, as well as impacts of variable pore pressure conditions.
- Investigation and consideration of other locations (e.g. deformation zones), depths, tunnel geometries and multi-tunnel intersection locations in the repository.
- Investigation on the impact of geomechanical upscaling in terms of how the intact rock material properties are degraded by the presence on natural fracturing.
- Investigation of the role of variable in situ stress conditions and its inclusion into the stability models.

- Investigation of the role of shear induced fracture dilation on kinematic stability.
- Investigate the potential feasibility for using rockbolting or possibly shotcrete/netting for block instability mitigation; and
- Investigate the potential for recursive block stability assessment with evolving cavity growth.

5 References

SKB's (Svensk Kärnbränslehantering AB) publications can be found at www.skb.com/publications.

Barton N, Choubey V, 1977. The shear strength of rock joints in theory and practice. Rock Mechanics and Rock Engineering 10, 1–54.

Barton N, Stephansson O (eds), 1990. Rock joints: proceedings of the International Symposium on Rock Joints, Loen, Norway, 4–6 June 1990. Rotterdam: Balkema.

Chryssanthakis P, 2003. Forsmark site investigation. Borehole: KFM01A. Results of tilt testing. SKB P-03-108, Svensk Kärnbränslehantering AB.

Chryssanthakis P, 2004a. Forsmark site investigation. Borehole: KFM02A. Results of tilt testing. SKB P-04-08, Svensk Kärnbränslehantering AB.

Chryssanthakis P, 2004b. Forsmark site investigation. Borehole: KFM04A. Tilt testing. SKB P-04-179, Svensk Kärnbränslehantering AB.

Chryssanthakis P, 2004c. Forsmark site investigation. Borehole: KFM05A. Tilt testing. SKB P-04-205, Svensk Kärnbränslehantering AB.

Chryssanthakis P, 2004d. Forsmark site investigation. Drill hole: KFM01A. The normal stress and shear tests on joints. SKB P-04-175, Svensk Kärnbränslehantering AB.

Coulomb C A, 1776. Essai sur une application des règles de maximis et minimis à quelques problèmes de statique, relatifs à la architecture. Mémoires de mathématique et de physique 7, 343–382.

Follin S, 2008. Bedrock hydrogeology Forsmark. Site descriptive modelling, SDM-Site Forsmark. SKB R-08-95, Svensk Kärnbränslehantering AB.

Fox A, La Pointe P, Hermanson J, Öhman J, 2007. Statistical geological discrete fracture network model. Forsmark modelling stage 2.2. SKB R-07-46, Svensk Kärnbränslehantering AB.

Glamheden R, Fredriksson A, Röshoff K, Karlsson J, Hakami H, Christiansson R, 2007. Rock mechanics Forsmark. Site descriptive modelling Forsmark stage 2.2. SKB R-07-31, Svensk Kärnbränslehantering AB.

Goodman R E, Shi G-h, 1985. Block theory and its application to rock engineering. Englewood Cliffs, NJ: Prentice-Hall.

Hoek E, 2006. Practical rock engineering. Available at: https://www.rocscience.com/documents/hoek/corner/Practical-Rock-Engineering-Full-Text.pdf

Jacobsson L, 2005. Forsmark site investigation. Drill hole KFM01A. Normal loading and shear tests on joints. SKB P-05-08, Svensk Kärnbränslehantering AB.

Jacobsson L, Flansbjer M, 2005. Forsmark site investigation. Borehole KFM06A. Normal loading and shear tests on joints. SKB P-05-122, Svensk Kärnbränslehantering AB.

SKB, 2008. Site description of Forsmark at completion of the site investigation phase. SDM-Site Forsmark. SKB TR-08-05, Svensk Kärnbränslehantering AB.

SKB, 2010. Data report for the safety assessment SR-Site. SKB TR-10-52, Svensk Kärnbränslehantering AB.

6 Acronyms

A	Vector of Active Forces for rock wedge calculation, units Newtons.
B	Vector of Rock Bolt Forces for rock wedge calculation, units Newtons.
C	Vector of Shotcrete Forces for rock wedge calculation, units Newtons.
Cohesion	Mohr Coulomb cohesion, units of Pa or MPa.
Concentration	Parameter relating to the type of orientation distribution used.
Distribution	Relates to the type of orientation distribution used to describe the fracture set orientation, e.g. Fisher distribution.
E	Material Young's Modulus, typical units MPa or Pa.
E	Vector of Seismic Forces for rock wedge calculation, units Newtons.
F	Resultant vector of Forces for rock wedge calculation, units Newtons.
FOS	Factor of Safety parameter for rock wedge calculation.
H	Vector of Shotcrete resistive Forces for rock wedge calculation, units Newtons.
Kn	Normal fracture compliance, typical units GPa/metre.
Kt	Tangential fracture compliance, typical units GPa/metre.
P	Vector of Passive Forces for rock wedge calculation, units Newtons.
P_{21}	Areal fracture intensity measure, units m/m^2.
P_{32}	Volumetric fracture intensity measure, units m^2/m^3.
Phi	Mohr Coulomb friction angle, units of degrees;
Pole Trend	Azimuth of the vector normal to the fracture place, units degrees.
Pole Plunge	Plunge angle of the vector normal to the fracture place, units degrees.
r_0	Minimum fracture length size specified in Power Law distribution, units metres.
r_{max}	Maximum fracture length size specified in Power Law distribution, units metres.
RhoB	Bulk Density, typical units g/cc or kg/m^3.
Slope	Slope relating to Power Law size distribution.
TCM	Tectonic Continuum Model.
U	Vector of Water Pressure Forces for rock wedge calculation, units Newtons.
W	Vector of Self Weight Forces for rock wedge calculation, units Newtons.
v	Material Poisson Ratio, dimensionless units.
X	Vector of Pressure Forces for rock wedge calculation, units Newtons.
Y	Vector of Passive Pressure Forces for rock wedge calculation, units Newtons.

Arkitektkopia AB, Bromma, 2017

SKB is responsible for managing spent nuclear fuel and radioactive waste produced by the Swedish nuclear power plants such that man and the environment are protected in the near and distant future.

skb.se